HIV-1 Glycoprotein 120-Specific Exosome-Targeted $CD8^+$ T Cell Vaccine

A Thesis Submitted to the College of Graduate Studies and Research

In Partial Fulfillment of the Requirements

For the Degree of Master of Science

In Health Science Program, College of Medicine

University of Saskatchewan

Saskatoon

By

Roopa Hebbandi Nanjundappa

PERMISSION TO USE

In presenting this thesis in partial fulfillment of the requirements for a Master of Science degree from the University of Saskatchewan, I agree that the Libraries of this University may make it freely available for inspection. I further agree that permission for copying of the thesis in any manner, in whole or in part, for scholarly purposes may be granted by the supervisor of my thesis work or, in his absence, by the Head of the Department or the Dean of the College. It is understood that any copying or publication or use of this thesis or parts thereof for financial gain shall not be allowed without my written permission. It is also understood that due recognition shall be given to me and to the University of Saskatchewan in any scholarly use which may be made of any material in my thesis.

Requests for permission to copy or to make other use of material in this thesis in whole or part should be addressed to:

Health Science Program, College of Medicine

University of Saskatchewan

S7N 4H4 Canada

ACKNOWLEDGEMENTS

I would like to thank people those who helped me in successful completion of the research presented in this thesis. Firstly, I thank my supervisor Dr. Jim Xiang for providing excellent research objectives and guidance to finish my research work. My stay in this laboratory provided me a solid foundation in immunological research. I would like to thank my advisory committee members Dr. Lou Qualtiere, Dr. Lixin Liu and Prof. Mabood Qureshi for their continuous support and guidance in reaching my research goals. I sincerely thank Dr. Barry Ziola for providing valuable critiques and comments on my research work and written thesis. I am very fortunate to have his guidance, which allowed me to improve my scientific writing skills.

I would like to extend my sincere thanks to past and present members of my laboratory, particularly Dr. Umeshappa, who constantly helped my research that allowed me to learn fundamentals of immunology and various techniques required to carryout immunological research. As a husband, he also provided incredible support to shape my career path.

I also thank Canadian Institute for Health Research, Herb R. and Marian H. Clark Scholarship and College of Medicine for financial support during my program. I take this opportunity to thank all animal technicians at Laboratory Animal Service Unit (LASU) and members of Animal Research Ethics Board (AREB).

I like to thank all staffs in Health Science Program, particularly Angie Zoerb for setting up my committee meetings.

I always remember and thankful to Dr. Satish Kagale, Dr. Rajendra K Sharma, Dr. Sujatha Prasad and Nalina Shankar for their help during my difficult times in Saskatoon.

Finally, I take this opportunity to thank my parents for their unconditional love and support. Their strong hold in every unpleasant incident of my life made me stronger.

ABSTRACT

Immunosuppression is a hallmark of human immunodeficiency virus-1 (HIV-1) infection. Upon binding to cluster of differentiation (CD) 4 receptor via trimeric glycoprotein (Gp) 120, HIV-1 enters and multiplies in $CD4^+$ T cells, leading to the death of these cells. $CD4^+$ T helper (Th) cells are required for the generation and maintenance of $CD8^+$ T cells, which are crucial to control HIV-1 proliferation. The stimulation of HIV-1-specific $CD8^+$ T cell responses in CD4-deficient environment is a major scientific challenge. In addition, dendritic cells (DCs) expressing C-type lectin and dendritic cell-specific intercellular adhesion molecule-3-grabbing non-integrin (DC-SIGN) with high affinity for Gp120, appear to act as "Trojan horses", facilitating the spread of HIV-1 from mucosal surfaces to T cells in lymph nodes, and these HIV-1-infected T cells have been found to be impaired. Currently, highly active antiretroviral therapy (HAART) is the only means to halt progression of acquired immunodeficiency syndrome (AIDS). Although HAART suppresses viral replication and significantly improves prognosis, toxicity and cost of the treatment have become major limitations for its use. In addition, with long-term use, HAART also decreases HIV-1-specific $CD4^+$ Th1 and $CD8^+$ T cell responses, causing a functional decrease in capacity of HIV-1-capturing DCs in initiating adaptive immune responses. As a result, HIV patients are unable to eliminate infected cells and proviral latent reservoirs. Therefore, how to stimulate efficient $CD8^+$ T cell responses in AIDS patients is one of the major challenges in HIV-1 patient therapy.

Previously, it was demonstrated that novel ovalbumin (OVA)-specific exosome (EXO)-targeted $CD4^+$ T cell vaccine ($CD4^+$aTexo) was capable of stimulating $CD4^+$ T cell-independent $CD8^+$ T cell responses and antitumor immunity to a highly metastasizing tumor challenge in wild-type mice. Since $CD4^+$ T cells are killed by HIV-1, the present study proposed to use

active $CD8^+$ T cells rather than active $CD4^+$ T cells for vaccine development. First, OVA-specific $CD8^+$aTexo (OVA-aTexo) vaccine was prepared by pulsing concanavalin A (Con A)-stimulated $CD8^+$ T cells with OVA-pulsed DCs (DC_{OVA})-released exosomes (EXO_{OVA}). In wild-type mice, OVA-aTexo vaccine stimulated CD4-independent OVA-specific $CD8^+$ T cell responses via CD40L and interleukin (IL)-2 signaling, and exosomal peptide major histo-compatibility complex (pMHC)-I targeting. To further provide insight into whether $CD8^+$aTexo vaccine induces similar cellular immune response in the context of human immune system, transgenic A2-K^b mice expressing α1 and α2 domains of human leukocyte antigen (HLA)-A2 and α3 domain of mouse H2-K^b were used. Adenovirus (AdV_{Gp120}) expressing HIV-1 envelope protein Gp120 was used to transfect bone-marrow DCs to generate DC expressing Gp120 and DC_{Gp120}-released EXO were purified (EXO_{Gp120}). EXO_{Gp120} were also purified from the culture supernatant of $DC2.4_{Gp120}$-transfected cells. Next, Gp120-specific $CD8^+$aTexo (Gp120-aTexo) vaccine was prepared by pulsing ConA-stimulated $CD8^+$ T cells with EXO_{Gp120}. In wild-type and A2-K^b mice, Gp120-aTexo vaccine stimulated Gp120-specific effector and memory $CD8^+$ cytotoxic T lymphocyte (CTL) responses, and provided preventive immunity to BL610-Gp120 and BL6-10A2K^b/Gp120 tumor cells, respectively. Gp120-aTexo vaccine also provided therapeutic immunity against 3 and 6-day lung tumor metastasis in transgenic A2-K^b mice. Taken together, these results represent a novel approach to the induction of immunity for the treatment of AIDS patients with $CD4^+$ T cell deficiency or for use in AIDS patients on HAART to clear virus-infected cells.

TABLE OF CONTENTS

LIST OF TABLES

LIST OF FIGURES

ABBREVIATIONS

AIDS	Acquired immunodeficiency syndrome
Ab(s)	Antibody(ies)
AdV	Adenovirus
Ag	Antigen
APCs	Antigen presenting cells
aTexo	EXO targeted active T cell
BMDC	Bone marrow dendritic cells
C	Conserved
CAR	Coxsackie adenovirus receptor
CCR	C-C chemokine receptor
CD	Cluster of differentiation
$CD4^+$ aT	Active $CD4^+$ T
$CD4^+$aTexo	EXO targeted active $CD4^+$ T cell
$CD8^+$ aT	Active $CD8^+$ T
$CD8^+$aTexo	EXO targeted active $CD8^+$ T cell
CFSE	Carboxyfluorescein diacetate succinimidyl ester
ConA	Concanavalin A
CTL(s)	Cytotoxic T lymphocyte(s)
CVL	Crude viral lysate
CXCR4	C-X-C chemokine receptor
DC-SIGN	Dendritic cell-specific intercellular adhesion molecule-3-grabbing non-integrin
DC2.4	Dendritic cell line 2.4
DC_{OVA}	OVA-specific DCs
DCs	Dendritic cells
DMEM	Dulbecco's modified eagle's medium

ECD	Energy coupled dye
EDTA	Ethlenediamine tetracetic acid
EMEM	Eagle's minimum essential medium
EXO(s)	Exosome(s)
EXO_{Gp120}	Gp120-specific EXO
EXO_{OVA}	OVA-specific EXO
FBS	Fetal bovine serum
FITC	Fluorescein isothiocyanate
GFP	Green fluorescent protein
GM-CSF	Granulocyte-macrophage colony-stimulating factor
Gp	Glycoprotein
Gp120-aTexo	Gp120-specific $CD8^+$aTexo
HAART	Highly active antiretroviral therapy
HEK	Human embryonic kidney cells
HIV-1	Human immunodeficiency virus type-1
HLA	Human leukocyte antigen
IFN	Interferon
IL	Interleukin
IV	Intravenous
KO	Knockout
LAMP	Lysosomal associated membrane protein
LB	Luria-Bertani
MHC	Major histo-compatibility complex
MOI	Multiplicity of infection
NK cells	Natural killer cells
OVA	Ovalabumin
OVA-aTexo	OVA-specific $CD8^+$aTexo

PBS	Phosphate-buffered saline
PCR	Polymerase chain reaction
PE	Phycoerythrin
pMHC	Peptide major histo-compatibility complexes
RBCs	Red blood cells
RGD	Arginine-guanine-aspartate
RPMI	Roswell park memorial institute
RT-PCR	Reverse transcriptase-polymerase chain reaction
SDS	Sodium dodecyl sulfate
SIV	Simian immunodeficiency virus
Th-APCs	$CD4^+$ T helper Ag-presenting cells
TNF	Tumor necrosis factor
V	Variable
α-MEM	Alpha-minimum essential medium
FSC	Forward scatter
SSC	Side scatter

CHAPTER 1

REVIEW OF THE LITERATURE

1.1 Acquired immunodeficiency syndrome (AIDS) and limitations to current treatments

AIDS causes millions of deaths each year around the world (1). Human immunodeficiency virus type-1 (HIV-1) is the causative agent of this syndrome (2). The virus enters the body by crossing the mucosal barrier and infecting cells bearing cluster of differentiation (CD) 4 receptors (3). A strong immune response mounts against HIV-1 during the early stages of infection (see section 1.3.1 for details). However, the virus exhibits several protective mechanisms that prevent complete elimination. These protective mechanisms include integration of viral DNA into the host genome, extensive mutation of the viral DNA and depletion of crucial host immune cells (4). HIV-1 infection is mainly characterized by a gradual depletion of $CD4^+$ T cells (5), a key regulator of the adaptive immune response. HIV-1 also infects dendritic cells (DCs) via either the CD4 receptor and/or the DC specific intercellular adhesion molecule-3-grabbing non-integrin (DC-SIGN) receptor. Infection of these cells leads to development of tolerogenic DC (reviewed in (6)). Tolerogenic DCs are dysfunctional and unable to stimulate further immune responses. Consequently, infected individuals enter an immune-suppressive state and become susceptible to cancers and opportunistic secondary infections.

To date, highly active antiretroviral therapy (HAART), which suppresses virus replication, is the only treatment available to stop disease progression in HIV-1-infected individuals (7). However, HAART is very expensive and has several direct side effects,

such as mitochondrial toxicity, pancreatitis, liver toxicity, and predisposition to coronary heart disease. In addition, HAART is only effective during the early infection stage when the viral DNA is rapidly replicating. This therapy does control disease progression and increases HIV-1-specific $CD4^+$ Th1 responses. However, in later stages of the infection, the virus becomes integrated into the host genome, thereby reducing its rate of replication and developing resistance against the treatment. Therefore, HAART does not completely eliminate the pro-viral (latent) reservoir or residual viruses from patients. This in turn leads to a decline in virus-specific $CD4^+$ Th1 and $CD8^+$ cytotoxic T cell (CTL) responses (8, 9).

Current HIV-1 vaccine protocols, which use viral proteins, plasmid DNA or recombinant viruses in the vaccines, only stimulate $CD4^+$ T cell dependent $CD8^+$ T cell responses (10). The result is limited to humoral and cellular immune responses against the initial viral epitopes. HIV-1 targets and depletes $CD4^+$ T cells, and the virus is capable of rapid antigenic variation, as a result the host is unable to develop effective immune responses against subsequent epitopes. In addition, in the absence of a healthy $CD4^+$ T cell population, stimulation of an efficient $CD8^+$ T cell response becomes a major challenge. Due to these limitations, there is an immediate need to develop novel vaccine strategies (which enhance CTL responses and are able to rapidly respond to a broad range of viral recombinants) to control the progression of and/or prevent HIV-1 infection.

1.2 HIV-1 structure

HIV-1 belongs to the genus *Lentivirus*, which is a member of the *Retroviridae* family. The viral particle is spherical in shape. It consists of an inner core (the capsid) and an outer viral membrane (11). The inner core of HIV-1 consists of two copies of 9.7 kb single-stranded RNA as genetic material (12) and enzymes, such as protease, integrase and reverse transcriptase, that are essential for replication of the virus. The outer viral membrane, known as the viral envelope, is derived from the plasma membrane of human cells and forms around the capsid as it is released from the cell. The HIV-1 genome encodes nine genes. Three of these genes encode crucial structural gene products: gag, pol and env. '*Gag'* gene products are precursors for viral capsid proteins, and are involved in packaging of the viral genome (13). The '*pol'* gene products are precursors for several enzymes (reverse transcriptase and integrase), and are important for viral replication. The '*env'* gene product glycoprotein (Gp) 160 is the precursor for the viral envelope proteins, Gp41 and Gp120 (14). In addition, the HIV-1 genome also encodes other accessory gene products, such as tat, rev, vpu, vpr, nef and vif, which help in viral replication (15).

The viral membrane consists of a spherical lipid bilayer and contains about 14 spikes, called Gp160 complexes (16). The mature Gp160 complex consists of three Gp120 subunits and three Gp41 subunits (17). The Gp120 subunits are exposed on the surface of the viral envelope while the Gp41 subunits are embedded within the membrane. The Gp160 complex binds the CD4 receptor, thereby facilitating HIV-1 entry into target cells and subsequent release of the viral capsid into the host cytoplasm (18, 19). Specifically, Gp120 forms a complex with the CD4 receptor with a strong affinity.

This causes a conformational change in Gp120, leading to exposure of Gp120 to the chemokine-binding domain of either of two co-receptors (C-X-C chemokine receptor (CXCR4) or C-C chemokine receptor (CCR)-5), and results in viral penetration into the cell (20, 21). Macrophage/monocyte/DC-tropic viruses use CCR5 as the co-receptor, whereas $CD4^+$ T cell-tropic viruses use CXCR4 as the co-receptor. It has been reported that, in the process of HIV-1 transmission from mucosal surface to blood, the macrophage/monocyte/DC-tropic viruses can convert into CD4-tropic viruses (21, 22).

One of the peculiar features of HIV-1 is the reverse transcriptase enzyme. This enzyme is highly error-prone in nature and lacks proof-reading activity (23). This results in a high rate of non-specific mutations being introduced into the HIV-1 genome during viral replication. Mutations that arise in antigenic epitopes are often non-lethal and, as they present a novel epitope, these viruses are no longer recognized by the initial immune responses. Therefore, generation of these mutations is part of the viral mechanism for evading immune responses. When HIV-1 infects a host, the viral RNA is converted into double-stranded DNA via the virus-encoded reverse transcriptase enzyme (24). HIV-1 hijacks host nuclear import machinery to transport and integrate its double-stranded DNA into the genomic DNA. The integrated DNA or provirus template encodes virus structural, regulatory and other accessory proteins to generate new viral particles (25).

Based on the analysis of genomic sequences, HIV-1 variants are categorized into three major phylogenetic groups, M (main), O (outlier) and N (non M/O). Group M viruses, which infect widely around the world, have the greatest genetic diversity, and are classified into nine subtypes or clades called (A-D, F-H, J and K) (26-29); clade-C viruses alone cause more than 80% of all HIV-1 infections. Similar to group M, group O

viruses consist of diverse strains of viruses (forty-nine strains), but this group is not sub-divided by clades (30). Group N, some time referred as 'new' group, viruses are more distinctive compared to group M and O, and rare viruses. Group N viruses are more common in Cameroon; only a few group N viruses have been isolated and characterized (31).

1.3 HIV-1 pathogenesis

The pathogenesis of HIV-1 infection is distinct from other viral infections in that the virus selectively depletes $CD4^+$ T cells. HIV-1 infection also leads to the development of dysfunctional or tolerogenic DCs due to continuous exposure to viral proteins, particularly to Gp120. A stepwise progression of HIV-1 pathogenesis is discussed below.

1.3.1 Early infection stage

In most instances, the transmission of HIV-1 occurs through the mucosal barriers (32, 33). In the mucosa, HIV-1 multiplies in CD4, CCR5/CXCR4 and DC-SIGN receptor-expressing cells (34). Subsequently, within one week of exposure, HIV-1 enters into local draining lymph nodes (35-38) and later spreads throughout the body via the blood steam. Replication of HIV-1 peaks between 2 to 4 weeks after infection, just before the development of a virus-specific adaptive immune response (39). Strikingly, although all $CD4^+$ T cells are susceptible to the viral infection, HIV-1-specific $CD4^+$ T cells preferentially get infected when they interact with infected DCs (40). Thus, in HIV-1 infection, viral antigen (Ag) presentation by DCs has both advantages and disadvantages.

After 8-12 weeks, in addition to other organs, HIV-1 preferentially spreads to gut-associated lymphoid tissues, which are rich in $CD4^+$ memory T cells. HIV-1 infects

$CD4^+$/CXCR4 T cells and multiplies rapidly, which results in the death of >80% of gut-associated $CD4^+$ T cell population (41). Subsequently, virus particles enter into the blood stream and infect more and more target cells, reaching peak viremia. Consequent to viral multiplication and infection, the body responds promptly at the beginning of infection by developing both humoral and cellular immune responses, which lead to a drastic decrease in the viremia (42-44). During this early infection stage, the infected individuals gradually recover in 2 to 6 months (45). Nevertheless, the blood $CD4^+$ T cell counts continue to drop to <200-400 cells/μl.

1.3.2 Asymptomatic stage

A clinically asymptomatic stage, which follows the acute infectious stage, may extend up to 8-10 years, depending on the anti-viral immune status (HIV-1-specific CTLs, memory T cells and neutralizing antibodies (Abs)), host genetic composition, and virulence of the acquired HIV-1 strain (46, 47). All of these factors are known to contribute to the slower-progression of HIV-1 infection in infected individuals. In the asymptomatic stage, the number of viral RNA copies in the blood decreases due to the host's immune response and due to the presence of virus-specific Abs in the serum. However, the virus replicates continuously in $CD4^+$ T cells, leading to the generation of a multitude of HIV-1 mutants (48).

1.3.3 Symptomatic stage and AIDS

HIV-1 mutants produced in the asymptomatic stage are capable of escaping from previously generated immune responses, which enables continuous HIV-1 replication in $CD4^+$ T helper cells. $CD4^+$ T helper cells are regarded as master regulators of the adaptive immune system, and without functional T helper cells HIV-1 patients become

completely immune-compromised. Consequently, HIV-1-infected individuals are highly susceptible to many opportunistic microbial infections, such as *Mycobacterium tuberculosis* and *Candida* species and herpes viruses, and more susceptible to development of many cancers. The affected patients commonly show symptoms of weight loss, repeated respiratory tract infections and skin rashes. (49) (50, 51). Finally, patients exhibit complex symptoms and signs of many diseases. This condition is known as AIDS. AIDS patients usually die due to the secondary complications associated with the primary HIV-1 infection.

1.4 Immune responses to HIV-1 infection

Depending on the genetic composition and immune status of an individual, both innate and adaptive immune responses control viral replication and spread. Upon HIV-1 entry into the body, the innate immune response develops to control viral spread. Later, HIV-1-specific cell-mediated and humoral immune responses develop to kill virally infected cells and neutralize cell-free virus, respectively.

1.4.1 Innate immune responses

The innate immune response is non-specific and is the immediate line of defense against invading pathogens. A variety of innate immune cells, such as natural killer (NK) cells and NK T cells, macrophages and DCs, contribute to the innate response to HIV-1 infection. In acutely infected individuals, the innate response is characterized by increased levels of acute-phase proteins and cytokines, particularly interleukin-1 (IL-1) (52). As the infection progress, cytokines (IL-15, IL-18, IL-22, type-1 interferons (IFNs), IFN-γ and tumor necrosis factors (TNFα)) and chemokines (ligand-C X C motif ligand

10) levels also increase in the blood (53). Ironically, the magnitude of cytokine secretion, particularly IFNs, IL-15, IL-18, may support rather than control viral replication early after infection (54). NK and NK T cells have proven effective in reducing HIV-1 levels by killing virally infected cells and producing anti-viral chemokines (55). Macrophages have been shown to have less effect in controlling HIV-1 infection; instead they increase viral spread to T cells during Ag-presentation (56, 57). DCs play a multifaceted role during HIV-1 infection. DC numbers drastically decrease in the acute phase (58). Unlike with other viral infections, during HIV-1 infection, infected DCs show incomplete activation, and secrete lower levels of IL-12, although they retain the ability to secrete normal levels of IFNs (53). DCs also produce indoleamine 2,3 dioxygenase, which converts $CD4^+$ helper T cells into regulatory T cells, which suppress virus-specific immune responses (59, 60). Furthermore, DCs are known to spread HIV-1 to T cells. Several possible mechanisms were proposed to explain DC-mediated HIV transmission. DCs transfer viral particles binding to cell surface (to DC-SIGN) receptors to T cells during DC-T cell contact in Ag-presentation. In addition, DCs transfer infection by an exocytic pathway, where DCs release HIV-1 associated exosomes. These exosomes transfer HIV-1 particle to $CD4^+$ T cells by membrane binding and fusion (reviewed in (61, 62).Collectively, although the innate immune system responds strongly to HIV-1 infection, by targeting CD4 receptors on immuno-regulatory cells, the virus is able to capitalize on many strategies, such as modulating the response of different immune cells, and regulating cytokine- and chemokine-expression profiles, to escape from innate immune control.

1.4.2 Humoral immune responses

The humoral immune response in the form of Abs is crucial for neutralizing cell-free viruses and for activating the cell-mediated Ab-dependent cytotoxicity effect to kill infected cells, thereby preventing the spread of infection. Production of HIV-1-specific Abs is usually detectable within 4-6 weeks after infection. Non-neutralizing Abs are first produced against the structural proteins, such as p24, p17 and Gag (63, 64), followed by neutralizing Abs against the envelope protein, Gp120 and Gp41. The neutralizing Abs produced during HIV-1 infection are predominantly specific to epitopes present in the variable (V) 3 domain and CD4- and CCR5/CXCR4-binding sites on Gp120, and Gp41 trans-membrane domain. (65). During the early stage of infection, immunoglobulin (Ig) A, IgG and IgM Abs are produced (66). However, these Abs often exhibit narrow specificity. The Abs are only specific to the initial HIV-1 variant, and are not selected to recognize HIV-1 mutants, which are generated after each round of multiplication (67). One of the difficulties the immune system encounters, with respect to generating Abs against mutated forms of the initial HIV-1 strain is that the reduced $CD4^+$ T cell population prevents efficient helper activity for maturation of new B cell populations. HIV-1 replication in the lymph node germinal centers leads to apoptosis of more than 50% of B cells within first 10 weeks of infection (68). This also reduces generation of effective neutralizing Abs during the early infection stage. Continuous changes in the glycosylation sites and structure of Gp120 epitopes (69) prevent viral progeny from being recognized by existing neutralizing Abs (70). All these factors contribute to the humoral immune response to HIV-1 being inefficient at containing the infection.

1.4.3 Cell-mediated immune responses

The primary immune response is initiated upon exposure of the body to HIV-1. Ag-presenting cells engulf the viral particles, then internalize, process and present viral peptides on human leukocyte antigen (HLA) MHC (major histocompatibility complex) class-I and-II molecules. DCs activate both HIV-1-specific $CD4^+$ and $CD8^+$ T cells, resulting in the development of virus-specific cell-mediated immune response. The activated HIV-1-specific $CD8^+$ CTLs destroy virally infected cells, including infected $CD4^+$ T cells (71), (72). In addition, $CD8^+$ CTLs suppress HIV-1 replication and inhibit viral spread by secreting different types of cytokines (IFN-γ and TNF-α) and chemokines (73). This leads to a drastic decrease in the viral titer towards the end of acute infection stage. HIV-1 mainly infects and destroys $CD4^+$ T cells, both effector and memory $CD4^+$ T cells (74, 75). HIV-1 viral replication is highly efficient, using much of the host cell catabolic and metabolic resources, resulting in apoptosis of the host cell. HIV-1-specific $CD4^+$ T cells are particularly susceptible as they are in direct contact with the infected antigen presenting cells (APCs) during Ag presentation. Mutations in antigenic epitopes, generated during HIV-1 replication within the APCs, result in new epitopes being presented on major histo-compatibility complex (MHC)-I and MHC-II complexes. This prevents expansion and maturation of HIV-1-specific $CD4^+$ and $CD8^+$ T cells, as the appropriate epitope is no longer present on the APC (76-79). Continued T cell activation against newly generated HIV-1 mutant epitopes puts the patient's immune system under constant immunological pressure. High levels of microbial components and inflammatory cytokines present in the blood of HIV-1 infected subjects' increase the expression of programmed death-1 marker on monocytes, which is involved in apoptosis and negative

regulation of T cell activation, leading to $CD4^+$ T cells dysfunction or tolerance (80).

Nevertheless, strong virus-specific $CD8^+$ CTL responses are critical in controlling in HIV-1 infection and its progression (81, 82). The efficient $CD8^+$ CTL response to many conserved HIV-1 immuno-dominant epitopes results in decreased viremia and disease progression (82). Therefore, an effective vaccination strategy should aim to generate a strong $CD8^+$ T cell response against multiple highly conserved epitopes of HIV-1 (83, 84).

1.5 Immune responses to Gp120

As noted before, the trimeric Gp120 protein molecule is part of the spikes on the HIV-1 envelope (85). Key protein domains present on the Gp120 protein interact with specific regions present on CD4 and chemokine receptors. This interaction leads to conformational changes in both Gp120 and Gp41. These conformational changes lead to HIV-1 virus entry into target cells. Based on the results of comparative sequence analysis, Gp120 is divided into five conserved (C) (C1-C5) and five variable segments (V1-V5). The conserved regions of Gp120 protein, C1-C5, are responsible for the non-covalent interactions between the three Gp120 subunits of the trimeric complex and with Gp41, resulting in Gp160. It has been reported that neutralizing Abs can bind to these conserved regions only when Gp120 is in its monomeric form (86). This is likely because these epitopes are buried within the core of the complex. The variable regions of Gp120 protein, particularly V1, V2 and V3, are present on the exposed area of Gp120. The V2 region is a highly variable, whereas the V3 region consists of a few conserved sequences and is the target for most neutralizing Abs.

During HIV-1 infection, polyclonal Abs are generated to various viral proteins. Only a small percentage of these Abs are specific to Gp120 and have neutralizing capacity (87). Neutralizing Abs to Gp120 are defined as being able to control HIV-1 infection by binding cell-free HIV-1 (88) and/or being able to facilitate destruction of virally infected cells via Ab-dependent cell-mediated cytotoxicity or complement-mediated cell lysis (89, 90). Clinical studies, using various viral vectors, recombinant protein and adjuvant-enhanced Gp120 vaccines, have resulted in the generation of relatively effective cell-mediated immune responses as well as neutralizing Abs responses (reviewed in (91)).

There are intrinsic limitations to Gp120 antigenic properties. Although Gp120 consists of potential epitopes for neutralizing Abs and $CD8^+$ T cells, it has negative effects on activation of professional APCs, $CD4^+$ T cells and B cells. Studies have shown that HIV-1 adapts several strategies to evade binding of neutralizing Abs to Gp120. More than 50% of this envelope protein surface is covered by carbohydrates, which are known as the glycan shield. Due to the presence of this glycan shield, the neutralizing epitopes of Gp120 protein are often buried and not efficiently recognized by Abs (92). Gp120 is known to be a super Ag for B cell activation which results in T cell independent differentiation of B cells and spontaneous production of polyclonal non-specific Abs (93). Furthermore, Gp120 is known to interact with the C-type lectin or DC-SIGN receptors of DCs, inducing development of tolerogenic DCs incapable of presenting Ag (94). Therefore, new approaches to vaccine development, which eliminate these limitations, are needed to control HIV replication. Ideally these approaches should enhance virus-specific T cell responses.

1.6. HIV-1 vaccine development

It has been more than 20 years since the eradication of smallpox. Through vaccination numerous diseases, including polio, rabies, measles, hepatitis B and influenza, have been controlled successfully. HIV-1's unique properties, such as preferentially killing $CD4^+$ cells and the establishment of latency in infected cells, are preventing development of an effective vaccine. The traditional vaccine development approaches are ineffective for HIV-1 because these vaccination protocols rely on $CD4^+$ T cells to induce protective immunity. The lack of good experimental models to test the efficacy of vaccines generates additional challenges. In the following section, highlights of traditional and some unique vaccine approaches against HIV-1 are reviewed.

1.6.1 Traditional vaccine approaches

To date, many traditional vaccine strategies, such as live-attenuated viruses and inactivated viruses have shown their efficiency in controlling viral diseases such as small pox, polio and measles. Initially, the effectiveness of these approaches was evaluated in the development of HIV-1 vaccines.

Many safety concerns were raised against the use of live-attenuated vaccines for HIV-1 patients. In the few cases that have been studied, (e.g. chimpanzees with simian immunodeficiency virus (SIV)-live-attenuated vaccine and humans with non-pathogenic *Nef*-deleted HIV-1-live-attenuated vaccine) the reversion of non-pathogenic virus to the virulent form occurred during later stages of vaccination (95-97). Hence, no further investigations have been carried out using this approach of vaccine development for HIV-1. Inactivated or killed vaccines are safer than live-attenuated vaccines and are efficient in controlling disease, such as polio and influenza. However, one SIV-inactivated vaccine

study on primates (98) and another HIV-1-inactivated vaccine study on humans both failed to induce protective immunity (99).

A successful subunit vaccine has been developed for Hepatitis B virus, a chronic viral disease that causes T cell exhaustion similar to HIV-1 (100, 101). Therefore, significant efforts have been spent on the development of recombinant-HIV-1-subunit vaccine involving Gp120 epitopes (102). A monomeric recombinant envelope Gp120 subunit vaccine was produced and its efficacy was tested in clinical trials. Unfortunately, this vaccine approach again failed to confer protection as the induced immune response was unable to neutralize the broad range of HIV-1 isolates and/or mutants found within both the general populace and infected individuals (103).

1.6.2 Novel vaccine approaches

Novel vaccine approaches using live-vector-based and plasmid DNA vaccines are under intense study. In the live-vector-based vaccine approach, HIV-1 genes are inserted into the live vectors. These vector-based vaccines were administrated into humans and were found to simultaneously induce cellular and humoral immune responses to both the parental virus and inserted viral genes. Initially, vaccinia virus was used for the development of live-vector-based vaccines for HIV-1. When tested in small laboratory animals and primates the vaccine proved effective in stimulating HIV-1-specific immune responses (104-106). However, these vaccines were discontinued for further testing on humans, as they are replication competent and are therefore contraindicated for use in immuno-compromised individuals such as AIDS patients.

Subsequently, genetically modified and replication-deficient vaccinia vectors have been developed (107). Avian and canarypox viruses belong to the vaccinia virus

group. These two viruses were used in HIV-1 vaccine development, and have been shown to be effective against multiple strains of HIV-1 virus in primates (108). Currently, the efficiency of vaccinia virus vaccines is being testing in HIV-1 patients. In addition, adenovirus (AdV) recombinant serotype-5 and RNA alpha virus vectors have been used for HIV-1 vaccine development. These virus-based vaccines demonstrated a strong immuno-stimulatory capacity in both small animal and primate models, and are currently being assessed for safety and immunogenicity in human patients (109).

Currently, numerous vaccines are in clinical trials to identify the most effective vaccine for HIV-1 (110). Despite these many efforts, none have proven highly promising. This is likely due to the fact that HIV-1-infected individuals are deficient in CD4 T cell and DC function.

1.6.3 Therapeutic vaccine approaches

The limitations of HAART and the importance of the continuous presence of humoral and cell-mediated immune response in halting HIV-1 replication and disease progression have forced immunologists to explore novel therapeutic approaches, including novel vaccines. The goal of these vaccines is to be effective in controlling disease progression rather than curing disease. Many experimental studies have shown the therapeutic role of $CD8^+$ CTLs in controlling established HIV-1 infection. The administration of autologous monocyte-derived DCs loaded with immunogenic HIV-1 peptides to patients resulted in increased HIV-1-specific $CD8^+$ CTLs responses, and reduced viremia (111). Schmitz et al. (82) also confirmed the importance of $CD8^+$ T cells in controlling SIV infection in macaque monkeys. Similarly, Amara et al. (81) demonstrated the ability of recombinant-modified-Ankara-vaccinia vaccine to increase

Ag-specific immune response in monkeys using heterologous prime-boost regimens. Together, these results suggest the importance of therapeutic vaccines in increasing HIV-1-specific $CD8^+$ CTL responses, thereby preventing progression of disease by controlling viral replication.

1.7 Adenoviral vectors

AdV-based vectors are widely used in clinical and basic research studies worldwide. AdVs infect the upper respiratory tract. The associated symptoms are similar to those of the common cold (influenza infection) (112). In the laboratory, AdVs infect a broad range of cultured mammalian cells, both dividing and non-dividing cells, which enables expression of recombinant proteins of interest (113). Currently, AdVs are being used for a variety of applications, including vaccine development, gene therapy, and gene expression studies. To date, nearly 53 human AdV serotypes have been identified (114). A comprehensive knowledge of AdV biology and their unique infectious characteristics makes them excellent vectors for transgene expression studies. Human serotypes AdV-2 and -5 are the more commonly used laboratory recombinant adenoviral strains. These recombinant AdVs are highly antigenic in nature, similar to the parental strain (wild-type), and induce strong cell-mediated immune responses. This strong immune response is one of the major limitations of using AdVs for therapeutic purpose, as most people have been previously exposed to the virus and neutralize the administrated AdV quickly (115, 116). Hence, efforts are being made to develop vaccines using serotypes of non-human AdVs, such as bovine AdVs and porcine AdVs. Importantly, AdVs possess the

characteristic of efficient cell-infectivity and their capsid can be easily modified to target them to particular type of cells.

1.7.1 AdV structure

AdVs are non-enveloped icosahedral viruses containing a linear double-stranded DNA genome. They have a large (36 kb) genome that encodes three major and three minor structural proteins. AdVs contain inverted terminal repeats on both ends of the genomic DNA, which assist in initiation of viral replication. The AdV genome is encased by the icosahedral capsid proteins, which make up the exterior of the viral particle. The major proteins within the capsid are the hexon, penton and knob fiber proteins (117). Adenoviral transcripts are generally classified as early genes (E1, E2, E3 and E4), delayed early or intermediate genes (proteins IX and Iva2) and late genes (L1 to L5). The early gene products are crucial for replication, host immuno-suppression and inhibition of cell apoptosis. Delayed early gene products are involved in encapsidation, transactivation of major late promoter and virus packaging. And, the late gene products are important for assembly of virion particles before their release.

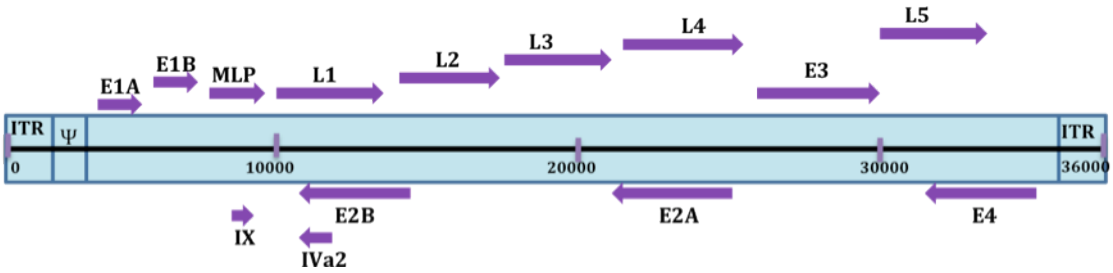

Figure 1.1 Schematic representation of the AdV genome. The AdV genome encodes early genes (E1A, E1B, E2A, E2B, E3 and E4), delayed early genes (IX and Iva2) and late genes (L1 to L5), which are flanked by inverted terminal repeats. The AdV genome also contains a major late promoter (MLP) and a packaging signal (Ψ).

1.7.2 AdV replication

Unlike retroviruses, which need to integrate into the genome for replication, AdV replication is epi-chromosomal. Infection is initiated by attachment of fiber proteins present in the capsid onto cell surface receptors. The coxsackie AdV receptor (CAR) is the primary cell surface receptor for AdVs (118) present on epithelial cells. DC and macrophage express CAR at low levels and secondary AdV receptors such as integrins at high levels (119, 120). After attachment, the AdV knob protein interacts with integrin molecules present on the cell surface facilitating the process of receptor-mediated endocytosis (121). AdV lyses endosomes and escapes into the cytoplasm. Adenoviral DNA is then transported into the nucleus (via nuclear pore transportation) for gene transcription. Transcription of the genome begins with early gene transcription of E1A, followed by transcription of other necessary genes, such as E1, E2, E3 and E4. Early gene products alter the cell's defensive mechanism and metabolism. E1 and E2 gene products are involved in arresting cell cycle to favor AdV replication, whereas E3 and E4 gene products are involved in viral-DNA replication (122). The delayed early and late gene products are involved in AdV packaging and they are important structural proteins. AdV uses host RNA polymerase for gene transcription, then mRNA is exported into cytoplasm for translation. During translation, synthesis of DNA polymerase for viral DNA replication, and structural proteins occur. Finally, viral particle assembly occurs by incorporating viral DNA into synthesized viral capsids (immature capsids). Capsids then undergo maturation and viral particles are released though cell lysis (123).

1.7.3 Amino acid sequence Arg-Gly-Asp (RGD)-modified AdVs

In the process of cell entry, the fiber proteins of the AdV attach to the CAR present on epithelium of upper respiratory tract. CAR is present on epithelial cells as an adhesion molecule, acting as a physical barrier to prevent viral infections. AdVs exploit adhesion molecules interaction by inhibiting CAR-CAR dimmer formation and forming a strong affinity bond between viral fiber protein and the host's CAR (124). Subsequently, the RGD domain of the penton protein is brought into proximity of the cell integrin molecule facilitating binding and internalization through receptor-mediated endocytosis. These integrin molecules are present on most cells. It is difficult to achieve efficient infection of typical laboratory cell lines since most cells do not express CARs. Specifically with respect to HIV-1 research, AdVs do not naturally infect DCs. To enable AdVs to infect different cell types, an RGD motif can be genetically introduced directly into the viral fiber knob protein. These RGD-modified AdVs are capable of infecting a broad range of cells. A similar study by Sas et al. (125) demonstrated that RGD-modified AdV can induce of transgene expression in more than 80% transduced murine bone marrow dendritic cells (BMDCs).

1.8 DC vaccines

1.8.1 DC

DCs are present throughout the body, lying in wait to identify foreign entities and potential pathogens. DCs identify pathogens/Ags and transport them from the periphery to lymphoid organs. They also are a key component required to enable transition from the innate to the adaptive immune responses. Therefore, DCs are often referred to as

"professional" APCs or "sentinels". DCs play a crucial role in identifying invading pathogens (danger signals) and sensitizing Ag-specific T cells. They have the capability to activate or inhibit Ag-specific immune responses. Immature DCs internalize invading pathogens, viruses, bacteria, and apoptotic bodies through receptor-mediated endocytosis and phagocytosis via toll like receptors or C-type lectins. Upon exposure to certain stimulatory microbial products (e.g. lipopolysaccharides, CpG oligonucleotides), and inflammatory cytokines (TNFα, IL-1), phagocytosis of the foreign entity occurs, followed by formation of lysosomes, maturation and presentation of the microbial peptides for T and B cell activation (126). Some pathogens, such as Dengue virus and HIV-1, are able to exist within the lysosomal compartment without being processed for Ag presentation. Transfer of these unprocessed form of virus to T cells during the process of Ag-presentation enhances transinfection (37, 127).

During Ag-presentation, DCs present antigenic peptides on MHC class-I and -II molecules through which (signal I) Ag-specific $CD8^+$ and $CD4^+$ T cells are activated, respectively. DCs also provide co-stimulatory (signal 2) and cytokine (signal 3) signals. In the early events of T or B cell stimulation, the activated DCs move to lymphoid tissues to stimulate the adaptive immune response (128). Apoptotic body proteins, such as heat shock proteins and beta defensins, are also known to induce DC maturation. Mature DCs express high levels of co-stimulatory molecules, such as CD80, CD86, peptide MHC class-I and -II complexes and adhesion molecules. In addition, mature DCs exhibit reduced expression of endocytic or phagocytic receptors, and increased secretion of IL-12 and IL-23 cytokines, which are crucial for T cell activation.

1.8.2 DCs in immunotherapy

At present, DCs, specifically monocyte-derived DCs, are being used in immunotherapy to stimulate tumor- or microbial Ag-specific $CD8^+$ CTL responses. A study on the treatment of melanoma in humans has demonstrated that adoptive transfer of *in vitro*-proliferated monocyte-derived DCs loaded with tumor peptides was able to induce strong tumor-specific immune responses (129). Similarly, in phase-I clinical trials of prostate cancer, DCs transfected with DNA encoding cancer-specific Ags were shown to stimulate tumor-specific T cell responses (130). In contrast, in the treatment of allergies and autoimmune disorders, tolerogenic DCs were able to induce tolerance by expanding specific regulatory T cells or inactivating already expanded T cells (131).

The whole-cell DC-based tumor vaccines have been used to treat cancer (132, 133) using tumor-specific Ag-expressing adenoviral vectors to transduce DCs. This helps to overcome the problem of natural long-lasting immunity to AdVs in previously sensitized patients that prevents AdV immunizations. Stimulation of DCs via AdV transduction could be more beneficial than stimulation using purified antigenic molecules, since AdV infection results in a strong signal to toll like receptors, which is required for maturation of DCs (133, 134). DC vaccines have been shown to be able to break disease-associated tolerance and have subsequently proven beneficial to patients with cancer or chronic diseases. Compared to other available cancer vaccines, initial clinical trials show that DC vaccines are safer to use (135). However, many other factors need to be evaluated, such as dose, route of administration, and method of maturation, activation, and Ag-loading. Understanding these factors may result in further improvement. With respect to HIV treatment, DC-based vaccines may not be as

promising as they will need to overcome the requirement of CD4-help for $CD8^+$ T cell activation.

1.9 Exosome (EXO)-derived vaccines

1.9.1 EXOs

EXOs are one of many examples of small secretory vesicles present in cell culture medium. EXOs are present in endosomes and are released into the culture medium when the endosome fuses with the cell membrane.

To date, different types of secretory membrane vesicles have been isolated and characterized from the mammalian cell-culture supernatants. Based on physiochemical characteristics, such as size, density, appearance under electron microscope, intracellular origin or protein composition, secretory membrane vesicles are classified into many types. The most biologically important secretory vesicles studied include EXOs, EXO-like vesicles, microvesicles, ectosomes, membrane particles and apoptotic bodies (136). EXOs have been extensively studied and characterized especially in the immunological context due to their immuno-stimulatory property (137).

EXOs are small lipid bilayer vesicles of 50 to 100 nm in diameter and can be isolated from cell-culture supernatants. EXOs are spherical in shape, however, they often appear “cup” or “saucer” shaped in electron micrographs (138). EXOs play a major role in transferring membrane-associated molecules from one cell to other. Many studies have demonstrated the presence of multiple receptors and ligands on the surface of EXOs, which allow them to interact with different cells (139).

The protein composition of EXOs provides information regarding their pathway of origin. Many studies have confirmed that proteins related to mitochondria, golgi complex, endoplasmic reticulum or nucleus are not observed in EXO. However, most of the proteins existing in EXOs are found to be present in the cytoplasm and plasma membrane. Flow cytometry and western blot analysis showed that EXOs contain important trans-membrane proteins, where these proteins are not necessarily derived from plasma membrane (140), and cytosolic proteins, such as annexin II, and TSG101. EXOs contain proteins mainly present in endocytic pathways, indicating that they are endocytic in origin (141). Lysosomal or endosomal proteins, such as lysosomal-associated membrane proteins (LAMPs), are observed in EXOs and are often found in DC- and B cell-released EXOs (138, 142). Enzymes involved in metabolism and various proteins involved in cell signaling are present in EXOs. In addition, tetraspanin family proteins, such as CD63, CD81 and CD82, are also abundant in EXOs.

1.9.2 DC-released EXOs in vaccination

Among the different types of EXOs, DC-released EXOs have attracted greater attention from immunologists since they possess immuno-stimulatory functions. Unlike B cell-released EXOs, DC-released EXOs are heterogeneous in size (143). One of the remarkable features of DC-secreted EXOs is their composition; they consists of Ag-presenting machinery such as MHC-I and -II molecules, co-stimulatory molecules such as CD80 and CD86, and adhesion molecules such as CD11c and CD54, which are collectively required to induce immune responses (144, 145).

Numerous studies have shown the functional importance of EXOs derived from different cell types such as DCs, T cells, B cells, platelets, mastocytes, fibroblasts and

tumor cells, both *in vitro* and *in vivo* in different animal models. *In vitro* studies confirmed that EXOs alone, unlike DCs, are unable to stimulate T cell responses (138). EXOs released from DCs or tumor cells are involved in transferring Ag-specific MHC complexes and immuno-stimulatory molecules to mature DCs, which in turn gain the ability to stimulate Ag-specific T cell responses. For the first time, Zitvgel et al. (138) showed that immunization with DC-released EXOs completely eradicated well-established tumors in murine model. Raposo et al. (143) showed that EXOs derived from B cells transduced with Epstein-Barr virus were able to stimulate Ag-specific $CD4^+$ T cells *in vivo* in humans. In addition, EXOs secreted by tumor cells have been shown to play a major role in cross presentation of tumor Ags to mature DCs (142, 146). EXOs released from tumor cells are known to express tumor-specific Ags on MHC-I molecules. These molecules can be used as an Ag source in cancer immunotherapy by loading them onto DCs to induce strong tumor-specific $CD8^+$ CTLs and memory response (138). Many studies have also shown that tumor-specific EXOs can successfully cause regression of tumors in skin and lymph nodes (147, 148). As part of a phase-I clinical trial in Institute Gustave Roussy and institute Curie, France, DC-derived EXOs are being used to treat different metastatic malignancies in humans (147).

Recently, the concept of using EXO-loaded T cell vaccines in immunotherapy has gained more attention. It has been demonstrated that EXO-based T cell vaccines can stimulate strong Ag-specific $CD8^+$ CTL responses and provide anti-tumor immunity (149). Hao et al. (150, 151) also demonstrated that $CD4^+$ T cells, which have acquired exosomal molecules, are more efficient than mature DCs in stimulating Ag-specific effector CTLs, memory response, and anti-tumor immunity.

Regardless of whether EXOs have *in vivo* or *in vitro* immuno-stimulatory effects, a full understanding of EXO function and physiological relevance is still elusive. Furthermore, the mechanisms by which EXOs induce immune stimulation are not well understood.

1.10 EXO-targeted active $CD4^+$ T cell ($CD4^+$aTexo) vaccine

Transfer of membrane molecules has been reported to occur between different types of immune cells including DCs (10), T cells (152), B cells, NK cells (153), basophiles (10) and macrophages (153, 154). Several possible mechanisms have been proposed to explain intercellular membrane molecular transfer. Among these, the two most important mechanisms of relevance to immunology are: 1) immunological synapse formation - between DCs and T cells facilitating T cell stimulation (155); and 2) DC-released EXOs. DC-released EXOs, expressing MHC-I & -II, and co-stimulatory molecules, modulate immune responses when they transfer to other immune cells (156, 157).

The formation of an immunological synapse between APCs and Ag-specific $CD4^+$ T cell is a key event for activation of T cells (158, 159). It has been reported that, during formation of the immunological synapse, APC surface molecules get transferred to T helper cells through the process of internalization and recycling pathways (160, 161). Based on this principle, Xiang et al. (162) proposed a new dynamic model of Ag-presentation. According to this model, $CD4^+$ T cells stimulated with ovalbumin (OVA)-specific DCs (DC_{OVA}) acquire Ag-presenting machinery, such as peptide major histo-compatibility complex (pMHC)-I and –II complexes, and co-stimulatory molecules,

CD80 or CD86, and behave like APCs (called $CD4^+$ T helper Ag-presenting cells (Th-APCs)) (163). These Th-APCs are known to stimulate naïve Ag-specific $CD8^+$ T cells to become effector and memory $CD8^+$ T cells, thereby providing anti-tumor immunity to the host (162). Subsequently, Umeshappa et al. (164) demonstrated that Th-APCs have fewer pMHC-I complexes compared to DC_{OVA}. The Th-APCs were able to induce central memory CTL development whereas DC_{OVA} were able to stimulate effector memory CTL development. In addition, it was shown that the Th-APCs' stimulatory effect is mainly mediated through acquired pMHC-I complex (signal-1), CD40L-co-stimulation (signal-2) and IL-2 cytokine secretion (signal-3) (165).

Based upon this new concept of Th-APCs, which induce immune responses via acquired pMHC-I and co-stimulatory molecules (162, 165), Hao et al. (150) demonstrated the development of a novel EXO-targeted T cell vaccine using polyclonally actived $CD4^+$ T cells co-cultured with EXOs derived from Ag-stimulated DC. In this test case, the Ag OVA was used. The $CD4^+$aTexo cells/vaccine efficiently stimulated an OVA-specific $CD8^+$ T cell response and elicited immunity to tumor lines bearing the OVA Ag. It has been shown that $CD4^+$aTexo vaccines can induce stronger immune responses than OVA-specific EXO (EXO_{OVA}) and DC_{OVA} alone (150). Interestingly, the stimulation of OVA-specific $CD8^+$ T cells by $CD4^+$aTexo vaccine was found to be CD4-independent, but relied on acquired pMHC-I complex and co-stimulatory molecules (150). Furthermore, it has been found that $CD4^+$aTexo vaccine has the ability to stimulate $CD8^+$ central memory CTL responses in the absence of $CD4^+$ Th cells, but in the presence of $CD25^+$ T regulatory cells (151), suggesting their potential application in HIV-1 vaccine development. Unfortunately, $CD4^+$ T cells are targets for HIV-1, and it is likely

that this vaccine will fail to induce efficacious results upon vaccination in HIV-1 patients. Therefore, this thesis focuses on whether a similar result can be achieved through activating $CD8^+$ T cells using EXO_{OVA} and HIV-1-specific EXOs.

CHAPTER 2

HYPOTHESIS

$CD4^+$ T cell deficiency is the hallmark of HIV-1 infection and stimulation of HIV-1-specific $CD8^+$ T cell responses in this CD4-deficient environment is a major scientific challenge. Existing vaccination approaches, using subunit, recombinant or killed strategies, rely on functional $CD4^+$ T cells to induce protective immune responses. Anti-retroviral therapies targeting DNA replication decrease HIV-1-related morbidity and mortality (7). However, these treatments are associated with many disadvantages including long-term toxicity, high cost, development of drug resistance, and failure to clear residual virus completely. Hence, there is a great need to develop alternate methods to stimulate immune response. Ideally these alternate methods would stimulate CD4-independent $CD8^+$ T cell responses.

Previously, it was demonstrated that non-specific $CD4^+$ aT cells take up OVA-specific EXOs. These cells are the basis behind what has been termed the $CD4^+$aTexo vaccine (150). This vaccine was able to stimulate Ag-specific CTL responses independent of $CD4^+$ T cell help and able to induce both effector and memory $CD8^+$ T cells. The vaccine was also able to protect mice exposed to lethal doses of Ag-specific tumor cells. It was reported that $CD4^+$aTexo vaccine's stimulatory effect occurs independent of $CD4^+$ T cell help and was mediated through acquired pMHC-I complex, CD40L and CD80 co-stimulations, and IL-2 secretion (150, 151). This type of immuno-stimulation, independent of $CD4^+$ T cell, would appear to have promise in the development of a HIV-1 vaccine.

$CD8^+$ T cells share many features of $CD4^+$ T cells. If EXO targeted active $CD8^+$ T cells ($CD8^+$aTexo) were able to induce an immune response in a similar manner as the $CD4^+$aTexo vaccine, then this technique could be an ideal approach in the control of HIV/AIDS. This thesis first tests the hypothesis that $CD8^+$ T cells can be stimulated in an Ag-specific manner using OVA-activated DC-derived EXOs in $CD8^+$aTexo vaccine preparation. Secondly, it was hypothesized that the use of $CD8^+$aTexo could induce HIV-1-Gp120-specific $CD8^+$ T cell responses. Gp120 contains many conserved epitopes for $CD8^+$ T cells to induce effective $CD8^+$ CTL responses. CTLs specific to an epitope of Gp120 are cross-reactive with some of other Gp120-specific CTL epitopes slightly modified in their amino acid sequence. Therefore, if proven efficacious, Gp120-specific $CD8^+$aTexo (Gp120-aTexo) vaccine could induce efficient cross-reactive $CD8^+$ T cell responses that can target a broad-range of HIV-1 isolates.

CHAPTER 3

OBJECTIVES

The proposed research objectives were as follows.

My first objective was to develop an OVA-specific $CD8^{+}$aTexo (OVA-aTexo) vaccine and test its stimulatory capacity. This involved development of an OVA-aTexo vaccine and testing its immuno-stimulatory potential in wild-type mice. OVA-aTexo vaccine was also developed, which was selectively deficient in pMHC-1 and CD40L molecules. Testing specific molecule deficient OVA-aTexo vaccine stimulatory function in wild-type mice was performed to understand molecular mechanism of immuno-stimulation. OVA-aTexo vaccine immuno-stimulation was also tested in IL-2R$\alpha^{-/-}$ mice to analyze the involvement of IL-2 signaling.

My second objective was development of a Gp120-aTexo vaccine and testing its stimulatory capacity in wild-type and transgenic A2-K^b mice. Here, I first transfected dendritic cell 2.4 (DC2.4) and BL6-10 cell lines with *Gp120* or/and *A2-K^b,* and constructed an AdV vector to express Gp120 protein. I then developed Gp120-aTexo vaccine and tested its immuno-stimulatory capacity in wild-type and A2-K^b mice using a tumor challenge study.

My third objective was to assess Gp120-aTexo vaccine's immunotherapeutic efficacy in A2-K^b mice by employing a tumor challenge study.

CHAPTER 4

MATERIALS AND METHODS

The source of chemicals, reagents and media used in this study are given in **Table 4.1.** Composition of solutions, buffers and media used are given in **Table 4.2.** Abs used for the study are listed in **Table 4.3.**

Table 4.1 List of chemicals and reagents

Reagents	Suppliers
1 kb ladder	Invitrogen
Acrylamide:bisacrylamide	Bio-Rad
Agar	Invitrogen
Agarose	Invitrogen
Alkaline phosphatase	New England Biolab
Ammonium Chloride	EM Sciences
Ammonium persulfate	Gibco
Ampicillin	Sigma
Bacto-tryptone	BD Pharmingen
Blocking buffer	LI-COR Odyssey
Bovine serum albumin	Sigma
Calcium chloride	Sigma
Cesium chloride	Sigma
Carboxyfluorescein diacetate succinimidyl ester (CFSE)	Molecular Probes
Chloroform	EM Sciences
Dulbecco's modified eagle's medium (DMEM)	Gibco
Dimethyl sulfoxide	Sigma
dNTP mix (dATP, dCTP, dGTP, dTTP)	Invitrogen
Eagle's minimum essential medium (EMEM)	Gibco
Ethanol	EM Sciences
Ethidium bromide	Sigma

Reagents	Suppliers
Ethylenediamine tetra acetic acid (EDTA)	Sigma
Fetal bovine serum (FBS)	Cyclone
Histopaque-1077	Sigma
Formalin	EM Sciences
Gentamicin reagent	Gibco
Glutaraldehyde	Sigma
Glycerol	BDH Inc
Glycine	EM Sciences
Granulocyte macrophage-colony stimulating factor (GM-CSF)	R & D Systems
Hydrochloric acid	EM Sciences
IL-2	Peprotech
IL-4	R & D Systems
Isopropanol	Gibco
Kanamycin	EM Sciences
LS column	Miltenyi Biotec
Magnesium chloride	Sigma
Methanol	EM Sciences
Mouse CD8 (Ly-2) paramagnetic beads	Miltenyi Biotec
Phenol	EM Sciences
Pre-stain molecular weight protein marker	Bio-Rad
Proteinase-K	Invitrogen
RNAse	Amersham Biosciences
Roswell park memorial institute (RPMI)-1640	Gibco
Sodium dodecyl sulfate (SDS)	Sigma/ Bio-Rad
Sodium acetate	BDH Inc
Sodium azide	Sigma
Sodium hydroxide	EM Sciences
Streptomycin	Sigma
Sucrose	BDH Inc
Sulfuric Acid	BDN Inc

Reagents	**Suppliers**
T4 DNA ligase	New England Biolabs
Taq DNA polymerase	Invitrogen
Tetramethylethylenediamine	Gibco
Tris	EM Science
Trypan blue stain	Gibco
Trypsin/EDTA	Gibco
Tween-20	Bio-Rad
Yeast extract	Gibco
Alpha-minimum essential medium	Gibco
β-mercaptoethanol	Bio-Rad
λDNA/*Hind*III marker	Invitrogen
φX174/*Hae*III fragment marker	Invitrogen

Table 4.2 Compositions of the solutions, buffers and media

Solutions, Buffers and Medium	Composition
1M $CaCl_2$	7.35 g of $CaCl_2$ in 50 ml of water
6X DNA loading buffer	0.25% (w/v) bromophenol blue, 0.25% (v/v) xylene cyanol, 40% (w/v) sucrose in 10 ml of water.
Citric saline	10% (w/v) KCl and 4.4% (w/v) sodium citrate
Luria-Bertani (LB) agar	1% (w/v) bacto-tryptone, 0.5% (w/v) bacto-yeast extract, 1% (w/v) NaCl and 1% (w/v) agar
LB broth	1% (w/v) bacto-tryptone, 0.5% (w/v) bacto-yeast extract, 1% (w/v) NaCl, pH 7.0
Lysis buffer solution	0.2 M NaOH, 1% (w/v) SDS in 100 ml of water
Phosphate-buffered saline (PBS)	140 mM NaCl, 2.7 mM KCl, 10 mM Na_2HPO_4, 1.8 mM KH_2PO_4, pH 7.2
Tween-PBS	0.05% (v/v) Tween-20 in PBS
Precipitate solution	3 M CH_3CO_2K, 11.5% (v/v) glacial acetic acid in 100 ml of water.
Protein sample buffer	125 mM tris pH 6.8, 4% (w/v) SDS, 10% (v/v) glycerol, 0.006% (w/v) bromophenol blue, 1.8% (v/v) β-mercaptoethanol
Resuspension buffer	Glucose 50 mM, EDTA 10 mM, tris 25 mM in 100 ml of water
1X Running Buffer	3.5 g Tris, 14.45 g glycine, 0.5 g SDS and water to 1 L
SOC medium	2% (w/v) Bactro-tryptone, 0.5% (w/v) Bacto-yeast extract, 0.05% (w/v) NaCl, 20 mM glucose, 2.5 mM KCl, 10 mM $MgCl_2$, pH 7.0
Tris-acetate EDTA buffer	24% (w/v) tris, 5.7% (v/v) glacial acetic acid, 10% (w/v) EDTA, pH 8.0
Transfer buffer	Tris 3.03 g, Glycine 14.4 g, methanol 200 ml and water to 1 L
Tri-ammonium Chloride lysis buffer	8.26 g of NH_4Cl, 1 g of $KHCO_3$, 0.037 g EDTA in 1 L of water. Mix well and autoclave before use.

Table 4.3 List of fluorescein isothiocyanate (FITC), phycoerythrin (PE), energy coupled dye (ECD) or biotin-conjugated Abs used in the study

Antibodies	Clone number	Suppliers
Anti-H2-K^b/OVA1 (pMHC-I)		eBiosciences
Anti-mouse CD11c-FITC	HL3	BD Pharmingen
Anti-mouse CD25-FITC	7D4	BD Pharmingen
Anti-mouse CD40-FITC	HM40-3	BD Pharmingen
Anti-mouse CD54-FITC	3E2	BD Pharmingen
Anti-mouse CD80-FITC	16-10A1	BD Pharmingen
Anti-mouse CD86-FITC	GL-1	BD Pharmingen
Anti-mouse CD8-FITC	CT-CD8α	Beckman Coulter
Anti-mouse H2-K^b -FITC	AF6-88.5	BD Pharmingen
Anti-mouse Ia^b -FITC	AF6-120.1	BD Pharmingen
Anti HLA-A2	BB7.2	Santa Cruz Biotechnology
Anti-mouse CD40L	MR1	Biolegend
Anti-mouse CD62L	MEL-14	BD Pharmingen
Anti-mouse CD69	H1.2F3	BD Pharmingen
Anti-mouse CD44	IM7	BD Pharmingen
Anti-mouse CCR7	4B12	eBiosciences
Anti-mouse IL-7Rα	A7R34	eBiosciences
Avidin-IRDye700CW		LI-COR Odyssey
Anti-rat IRDyeRCW800		LI-COR Odyssey
Anti-mose-IRDyeRCW700		LI-COR Odyssey
Anti-Calnexin		Cell-Signaling technology
Biotinylated goat anti-HIV-Gp120		Cederlane
Anti-LAMP-1		Santa-Cruz Biotechnology
Streptavidin-FITC		BD Pharmingen
Streptavidin-PE texas Red		BD Pharmingen

4.1 Cell lines

BL6-10 cells are skin melanoma tumor cells of C57BL/6 mouse origin. BL6-10 and BL6-10_{OVA} tumor cells were cultured in alpha-minimum essential medium. DC2.4 is a DC cell line of C57BL/6 mouse origin, and was kindly provided by Dr. K L Rock, Dana Farber Cancer Research unit, Boston, MA. DC2.4 cells were cultured in DMEM.

Human embryonic kidney cells (HEK-293) express early region-1 (E1) product of AdV, which helps the growth and amplification of replication deficient AdV. These cells were purchased from the Microbix, Toronto, ON, and cultured in EMEM. All culture media were supplemented with 10% (v/v) FBS and 30 μg/ml gentamicin reagent. Trypsin/EDTA solution and 1X citric saline solution were used for BL610 and HEK-293 cell passage, respectively. Cells were cultured in a humidified incubator at 37^{o}C with 5% CO_2 saturation. Viable cells were counted using Trypan blue stain using a haemocytometer.

4.2 Bacterial cells

Escherichia coli, DH5α strain (New England Biolabs), was routinely used for expression-vector propagation. *E. coli,* BJ5183 strain (Stratagene), was used for the homologous recombination in AdV vector construction. Both cells were grown in LB a broth at 37^{o}C on a shaker. Medium was supplemented with selective antibiotic, ampicillin (100 μg/ml) or kanamycin (50 μg/ml), depending on the expression vector's resistance gene. After transformation, transformed bacterial cells were selected by plating them on selective LB-agar plates containing appropriate selective antibiotics, and plates were incubated overnight at 37^{o}C.

4.3 Animals

Wild-type (C57BL/6) female mice with H2-K^b background, and transgenic A2-K^b mice were obtained from the Animal Resource Centre, University of Saskatchewan and Charles River Laboratories, Canada, respectively. CD40L, K^b and IL-2Rα gene knockout (KO) mice on C57BL/6 background were purchased from Jackson Laboratory, USA. Mice were 4-6 weeks old at initiation of the experiments and were housed in the animal facility at Saskatoon Cancer Center or in the Health Science Building, Laboratory Animal Service Unit. Animal protocols and procedures used in this study were approved by the University Committee on Animal Care and Supply in accordance with the guidelines of the Canadian Council for Animal Care.

4.4 Peptides

OVA-I peptide, SIINFEKL, was obtained from the Peptide Core Synthesis Facility, University of Calgary, AB, Canada. This peptide spans between 257-264 of the OVA protein (166). Gp120 peptide, KLTPLCVTL, was obtained from the GenScript, USA Inc, Custom service peptide facility and the peptide spans between 121-129 of the Gp120 protein (167, 168). Both peptides were purified by high-performance liquid chromatography (HPLC), which yielded >95% purity.

4.5 General molecular biology techniques

General molecular biology techniques used in this study were based on the protocols described in Molecular Cloning, a Laboratory Manual by Sambrook et al. (215) and Sambrook and Russel (216) with few modifications.

4.5.1 Restriction enzyme digestion

The restriction enzymes used in this study were purchased from New England Biolabs. DNA digestions were performed according to the manufacturer guidelines. Briefly, around 1 μg of DNA was digested using at least 1 unit of specific restriction enzyme in 1X recommended optimal buffer in the presence or absence of bovine serum albumin for 1 hr at 37^{o}C.

4.5.2 Agarose gel electrophoresis

Agarose gels were prepared in varying concentration, from 0.7% (w/v) to 2% (w/v), in tris-acetate EDTA buffer, depending on the size of the DNA band to be visualized. Concentration of 1 μg/ml Ethidium bromide was used in the gel to stain DNA. Samples were mixed with loading buffer and loaded on the gel along with DNA markers, λDNA/*Hind* III, φX174/*Hae* III or a 1 kb ladder from New England Biolabs. For optimal resolution, gels were run between 90 to 110 volts in tris-acetate EDTA buffer for varying times, and then bands were visualized under UV trans-illuminator gel documentation system (Bio-Rad).

4.5.3 Purification of linear DNA fragments

For further downstream applications, such as cloning and transfection, linear DNA fragments were purified from agarose gel using a Min-gel elution kit (Qiagen). The method was followed as per the procedure provided by manufacturer. Typically, DNA was eluted in 20 μl of sterile water to facilitate the subsequent ligation or transfection procedures.

4.5.4 Competent cell preparation and transformation

4.5.4.1 Chemical competent cell preparation and transformation

Chemical competent cells of *E coli* strain DH5α, recombination-deficient bacteria, were prepared according to the method in Sambrook et al. (215) with few modifications. In brief, 100 ml of 16 hr cultured bacterial cells of OD between 0.4-0.6 at 600 nm were pelleted. Cell were washed twice with 10 ml of chilled 50 mM $CaCl_2$ and re-suspended in 1 ml of $CaCl_2$ solution containing 15% (v/v) glycerol.

For transformation, 100 µl of competent cells were incubated with 10-20 ng of plasmid DNA on ice for 30 min. Cells were heat-shocked by quickly placing into a 42^{o}C water bath for 40 sec without shaking. The samples were then placed on ice for 2 min. Pre-warmed super optimal broth (SOC) was added to the samples and incubated for 2 hr at 37^{o}C to allow cell recovery. Finally, the cells were plated on selective antibiotic LB agar plates and incubated overnight at 37^{o}C.

4.5.4.2 Electrocompetent cell preparation and transformation

This method was adopted from Sambrook and Russell et al. (216). For electrocompetent cells preparation, *E coli,* BJ5183 bacterial cells were grown for 16 hr in LB broth containing selective antibiotic. The cells were then sub-cultured into fresh medium and grown to reach mid log phase (OD_{600} 0.4-0.6). The culture was chilled on ice for 30 min, then spun at 1000 X *g* in a JA-20 rotor (Beckman Coulter). Finally, the cells were washed 2-3 times in cold water, re-suspended in 10% (v/v) glycerol in water, then stored at -80^{o}C until use.

Electrotransformation was performed to transfer AdV vector into bacteria, BJ5183, which contained of pAdEasy-1 AdV backbone vector. Briefly, electrocompetent

cells were transferred into pre-chilled electroporation cuvettes (Bio-Rad) and incubated with linearized plasmid DNA for 5 min. Electroporation was achieved by applying a 200Ω (ohms), 2.5 kV and 25 μFD electric field in a Gene Pulser (Bio-Rad). Immediately after electric shock, pre-warmed SOC medium was added to the samples, which were then incubated for 1 hr at 37^{o}C to allow cell recovery. Finally, the cells were plated on selective antibiotic LB agar plates and incubated overnight at 37^{o}C.

4.5.5 Isolation of plasmid DNA

4.5.5.1 Small scale purification

To isolate plasmids in small scale, the Mini-prep (Qiagen) purification kit was used. Generally, bacterial colonies were selected from overnight-incubated plates and cultured for 12-14 hr in 2 ml LB medium containing selective antibiotic. Purification was performed according to the manufacturer's protocol. Finally, purified plasmid DNA was quantified in a Nanodrop (Thermo-Scientific) instrument.

4.5.5.2 Large scale purification

Transfection of HEK-293 cells to generate AdV requires an AdV vector in large quantity. In addition, the recombinant AdV vectors are large in size, more than 38 kb, hence, they can shear in miniprep column purification. Therefore, plasmids were isolated by a traditional alkaline lysis method. In brief, 10 ml of overnight grown cultures were pelleted and cells were re-suspended in 1 ml of Resuspension Buffer by vortexing for 3 min. One ml of freshly prepared Lysis Buffer was added, mixed gently and kept at room temperature for 5 min. One ml of precipitate solution was added to the mixture and the tubes were inverted 5-6 times to mix. The samples were centrifuged at 12,000 rpm (17418 X *g*) for 20 min in a JA-20 rotor (Beckman Coulter) at 4^{o} C and the supernatant

was transferred into fresh tubes. Plasmid DNA was precipitated using phenol:chloroform:water and iso-propanol. The DNA pellet was washed twice in 70% ethanol, finally dissolved in sterile water.

4.5.6 RNA isolation

RNA was isolated from transfected and non-transfected cells using a RNeasy mini kit (Qiagen) by following the manufacturer's guidelines. Sample concentration and purity was determined using a Nanodrop instrument. After purification, samples were used immediately for cDNA preparation (see Section 4.5.9).

4.5.7 DNA ligation

DNA ligation was performed using T4 DNA ligase in supplied ligation buffer. Typically, a 20 µl ligation reaction consists of 50 ng of vector DNA, at least 150 ng of purified insert DNA with 1-5 units of T4 DNA ligase in 1X ligation buffer. Ligation reactions were performed overnight at room temperature.

4.5.8 DNA sequencing

Automated dideoxy sequencing was performed at the sequencing facilities located in Plant Biotechnology Institute of the National Research Council of Canada in Saskatoon, Canada.

4.5.9 cDNA synthesis

Approximately 2 to 5 µg of isolated total RNA of each sample was used to prepare cDNA using a Superscript-II Reverse transcriptase kit (Invitrogen) by following manufacture's instructions. Briefly, in 12 µl reaction volume, 2 to 5 µg of total RNA and oligo (dt) primers were boiled at 65^{o}C for 5 min and then chilled on ice. To this reaction

mixture, first-strand enzyme buffer was added and incubated at 42^{o}C for 2 min. SuperScript-Reverse transcriptase enzyme and water were added to obtain a final volume of 20 µl. The reaction mixture was incubated at 42^{o}C for 50 min, then incubated at 70^{o}C for 15 min to terminate the reaction. Prepared cDNA samples were stored at -80^{o}C until further use.

4.5.10 Polymerase chain reaction (PCR)

PCR was carried out using a thermal cycler (Perkin Elmer Gene Amp-PCR system) and the New England Biolabs high fidelity PCR kit. A typical 50 µl reaction mixture consisted of 0.5 ng of template DNA, 10 mM each of dNTP, 5 µM of each primer, 10X PCR buffer, high fidelity polymerase and ultra pure water. PCR was performed by initial denaturation of samples at 98.4^{o}C for 45 sec, followed by 30 cycles of 10 sec denaturation at 98^{o}C, 30 sec annealing at 62^{o}C, 40 sec extension, and 10 min of final extension at 72^{o}C. An aliquot of each sample were subjected to electrophoresis on 1% (w/v) agarose gel for visualization of the PCR product. For gene amplification, the Gp120-Forward, 5' ATCTATGGTACCTCTAGAGCCCCTCCATG 3' and GP120-Reverse, 5'- AGCTGTAAGCTTGGATCCTTAGCGCTTCTC 3' primers, which include *Kpn I* and *Hind III* restriction sites, respectively, were used to facilitate directional cloning of PCR product into the pShuttleCMV AdV entry vector.

4.5.11 Quantitative reverse transcriptase-polymerase chain reaction (RT-PCR)

Isolated RNA samples were subjected to quantitative RT-PCR using a SYBR green Q-PCR master mix (Applied-Biosystems) according to the manufacturer's instructions. Briefly, 25 µl reaction mixture was consisting of 20 ng of cDNA, 50 nM of each primer and 1X PCR master mix. To quantify Gp120 transcripts, a series of samples

containing 0.2 ng to 0.2 μg of pConBGp120-opt were used to develop a standard curve. To determine relative expression of Gp120, the concentration of Gp120 transcripts in each sample was normalized to relative expression of β-actin as cycle threshold. The samples were amplified in a real time thermo cycler (Applied Biosystems) and data were analyzed in the thermo cycler-associated software. The sequences of primers used in this analysis include: β-actin F; TTCGTTGCCGGTCCACA, β-actin R; ACCAGCGCAGCGATATCG, Gp120 F: TGATGCACTCCTTCAACTGC, and Gp120 R: TCCTGCCACATGTTGATGAT.

4.6 Expression vectors

4.6.1 pConBGp120-opt

pConBGp120-opt expression vector was originally obtained from the National Institute of Health. This expression vector has the full-length gene of HIV-I envelope protein Gp120. Gene-Gp120 is present between *Xba I* and *BamH I* restriction sites. pConBGp120 has a neomycin gene, which enables selection of transfected cells.

4.6.2 pcDNA3.1Hygro-Gp120

Vector pConBGp120-opt was digested with *Xba I* and *BamH I* restriction enzymes, which liberated the 1.5 kb full-length Gp120 gene. This liberated DNA fragment was ligated into the pcDNA3.1Hygro (Invitrogen) expression vector on same restriction sites to get pcDNA3.1Hygro-Gp120 expression vector. This vector has a hygromycin drug resistance gene to facilitate selection of stable cell transfectants.

4.6.3 pmax-green fluorescent protein (GFP)

The pmax-GFP expression vector provided with the Amaxon cell line Nucleofector-V transfection kit was used as a positive control to monitor transfection efficiency. This vector encodes GFP; therefore, GFP-expressing cells after transfection can be easily identified by fluorescence microscopy or flow cytometry analysis.

4.7 AdV-Gp120 production

AdV was generated using an AdEasy-1 adenoviral vector system that utilizes *E. coli* homologous recombination. Parental vectors used in AdV construction, pShuttleCMV and pAdEasy-1, were obtained from Dr. Lixin Zhang, John Hopkins and Stratagene, respectively.

4.7.1 Generation of pAdEasy vector expressing Gp120

Gp120 gene was amplified from expression vector, pConBGp120-opt, by PCR using full-length gene-specific primers, which include *Kpn I* and *Hind III* restriction sites to facilitate directional cloning. Amplified fragments were purified, digested using *Kpn-I* and *Hind-III* restriction enzymes, and cloned into pShuttleCMV to get pShuttleCMV-Gp120 vector. Orientation of the gene insertion was confirmed by restriction digestion analysis, and sequenced for mutations. pShuttleCMV-Gp120 vector was linearized using *Pme-I* restriction enzyme, then treated with alkaline phosphatase. Approximately, 1 μg of *Pme-I* linearized pShuttleCMV-Gp120 was used to transform electrocompetent AdEasier cells, *E coli* BJ5183, which contain the RGD-motif modified AdV backbone plasmid, pAdEasy-RGD. Recombination between AdV backbone vector (pAdEasy-RGD) and entry vector (pShuttleCMV-Gp120) leads to the generation of recombinant adenoviral

vector (pAdEasy-Gp120), which is used to generate AdV in HEK-293 cells. Electro-transformed cells were plated on selective kanamycin (100 μg/ml) LB agar plates and incubated overnight at 37^{o}C. Around 40 very small colonies were picked up to perform Mini-preps. The recombinants were screened using *Pac-I* restriction enzyme digestion analysis. Selected recombinant vectors were called pAdEasy-Gp120 and were then transformed into *E. coli* DH5α bacteria to amplify in large amount for HEK-293 cells transfection (to generate AdV)

Digestion of pAdEasy-Gp120 with *Pac-I* liberated a 3.5 or 4 kb fragment. Completely digested pAdEasy-Gp120 was purified in phenol:chloroform:isoamyl alcohol (25:24:1) followed by ethanol precipitation. The resultant digested product was dissolved in sterile water for transfection.

4.7.2 Transfection of HEK-293 cells for AdV production

AdV propagation and amplification was performed as described previously (169), (170). After purification and confirmation of recombinant adenoviral vector (pAdEasy-Gp120), HEK-293-39 cells were transfected with the *Pac-I* digested pAdEasy-Gp120 to generate AdV using lipofectamine-2000 (Invitrogen-11668-019) reagent. pmax-GFP-transfected 293-39 cells were used to assess the transfection efficiency. After transfectoin, flasks were maintained for 10 to 12 days for virus plaque formation. Cells were harvested in EMEM serum-free medium when extensive cytopathic effect observed. Then cells were subjected to five rounds of freeze and thaw cycles by placing them at -80^{o}C and 37^{o}C temperatures, respectively, to obtain crude-viral-lysate (CVL). This was used to infect fresh HEK-293-26 cells to amplify AdV for further infection. HEK-293-26 lysates were used to confirm Gp120 mRNA and protein expression by RT-PCR and

western blotting, respectively. For final AdV_{Gp120} amplification, CVL was used to infect HEK-293-26 cells (35 T-175 cm^2 culture flasks at 85% cell confluence).

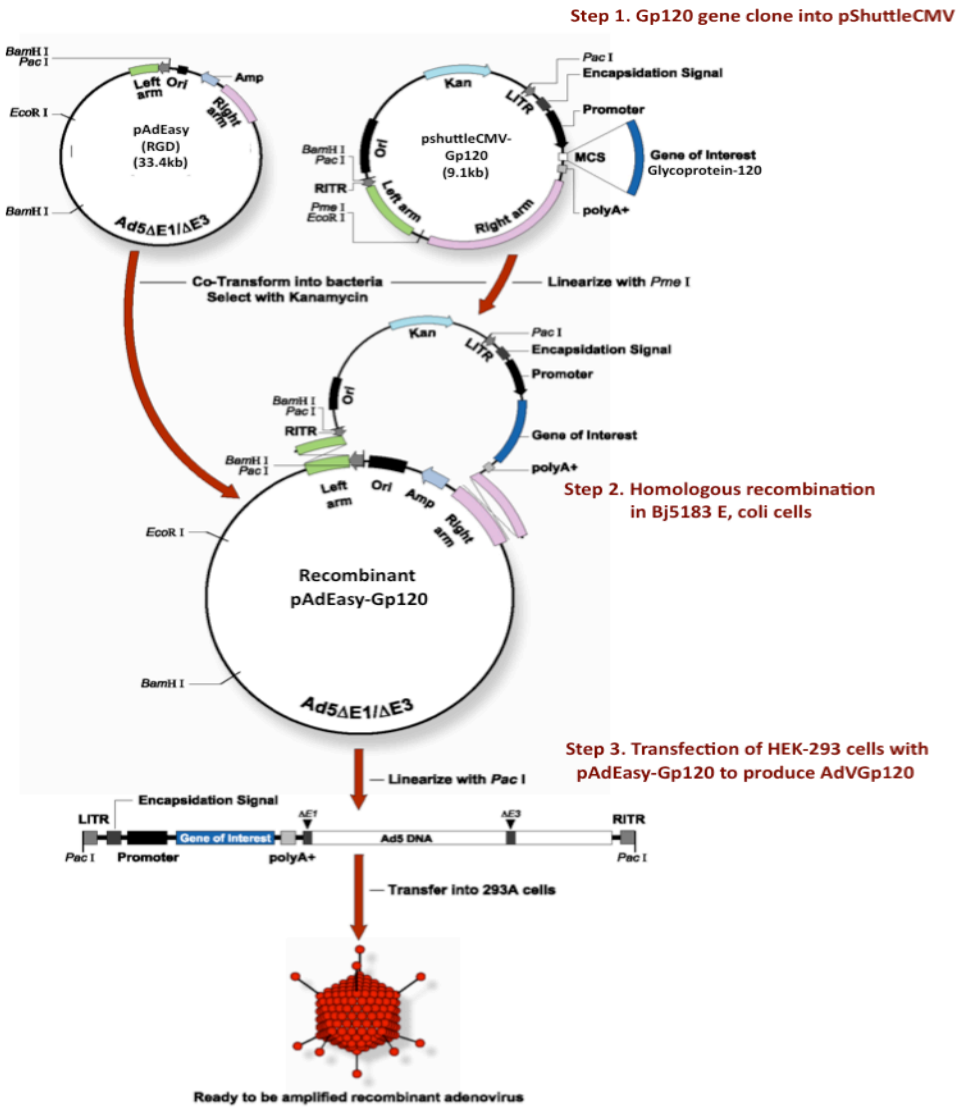

Figure 4.1 Schematic representation of AdEasy system and AdV production (adopted from Qbiogene, Inc).

Gp120 gene was cloned into pShuttleCMV, AdV entry vector, and it was linearized by *Pme-I* digestion. pShuttleCMV-Gp120 vector was transformed into electrocompetent *E coli* BJ5183 cells with pAdEasy-RGD for homologous recombination. Resulting recombinant pAdEasy-Gp120 adenovector was linearized by *PacI* digestion and transfected into HEK-293 cells for replication-deficient AdV_{Gp120} production.

4.7.3 Purification of AdV

When more than a 50% cytopathic-effect was observed in the last step of amplification, entire cells were harvested in PBS or serum-free EMEM and subjected to four rounds of freeze and thaw cycles as mentioned above. Subsequently, the samples were centrifuged at 10,000 rpm for 30 min in a JA-20 rotor (Beckman Coulter) at 4^{o}C to remove as much cell debris and proteins as possible, which otherwise may interfere with virus purification. After centrifugation, supernatants were collected for discontinuous CsCl density-gradient ultracentrifugation.

CsCl density-gradient ultracentrifugation was performed using quick seal centrifuge tubes layered with 1.25g/ml CsCl and 1.40g/ml CsCl gradient solutions. CVL was layered slowly above the density gradient solutions and subjected to ultracentrifugation for 2 hr at 45,000 rpm (145,000 X *g*) in a 80Ti rotor (Beckman Coulter) at 20^{o} C. The opalescent viral band was collected and layered on a 1.34 g/ml CsCl gradient solution and centrifuged again at 145,000 X *g* for about 18 hr at 20^{o}C to separate infectious AdV particles from defective particles. After centrifugation, the lower viral band was collected. Salts present in the purified AdV samples were removed by dialysis using Slide-A-lyzer dialysis cassettes (Pierce) by following the manufacturer's instructions. Finally, the concentration of the AdV was determined in spectrophotometry at A_{260} as described in Xiang and Wu et al. (171). Optical density of 1 is equivalent to 1 X 10^{10} plaque forming unit/ml. The virus was stored in sterile 10% (v/v) glycerol at -80^{o}C until use.

4.7.4 AdV_{Gp120} characterization

After AdV_{Gp120} purification, Gp120-gene insertion and protein expression was confirmed by PCR and western blot, respectively.

4.7.4.1 PCR

To verify the presence of the Gp120 gene in purified AdV_{Gp120}, samples were treated with proteinase-K (20 mg/ml) for 1 hr at 56^{o}C followed by enzyme inactivation at 95^{o}C for 5 min. For gene amplification, gene-specific primers Gp120-Forward, 5' ATCTATGGTACCTCTAGAGCCCCTCCATG 3' and GP120-Reverse, 5'-AGCTGTAAGCTTGGATCCTTAGCGCTTCTC 3' were used. PCR was performed along with positive controls, cDNA of Gp120-transfected 293 cells or recombinant pAdEasy-Gp120 vector, as described in section 4.5.10.

4.7.4.2 Western blot

Purified AdV_{Gp120} samples were subjected to western blot along with the positive control, transfected HEK-293 cell lysate, to test for Gp120 protein expression. First, samples were run on 7.5% (v/v) SDS-polyacrylamide gel electrophoresis, and protein bands were transferred onto nitrocellulose membranes (Millipore). Membranes were blocked (LI-COR Odyssey blocking buffer- LI-COR Biosciences) and stained with primary Ab-specific for Gp120 (Cederlane; biotinylated goat anti-Gp120). After thoroughly washing with Tween-PBS, membranes were incubated with avidin-IRDyeR700 and scanned in a LI-COR Odyssey scanner.

4.8 Transfection

4.8.1 Liposome-mediated transfection

Lipofectamine-2000 (Invitrogen) is a liposome-based transfection reagent used to transfect HEK-293 cells with pAdEasy-Gp120 (recombinant AdV vector) to produce AdV. The day before transfection, 2 X 10^6 HEK-293-39 cells were seeded in T25cm^2 flasks. Transfection was performed following the manufacturer's guidelines. Briefly, 5 µg of *pac-I* digested pAdEasy-Gp120 was mixed with lipofectamine (20 µl) reagent in serum free EMEM. The mixture was incubated at room temperature for 30 min, which leads to the formation of DNA-liposome complexes, then added to the flasks. The flasks were incubated for 4 hr then medium was replaced with fresh EMEM with 10% FBS.

4.8.2 Nucleofector–V electroporation

Nucleofector-V transfection (Amaxon, VCA-1003) kit was used to transfect BL6-10 and DC2.4 cells to achieve stable expression of Gp120 protein. BL6-10 and DC2.4 cells in log phase growth were used for the transfection to increase transfection efficiency. Transfection was carried out following the manufacturer's instructions using 2 µg of pcDNA3.1HygroGp120 per reaction. The positive transfection control, pmax-GFP, was used to monitor transfection efficiency in a fluorescent microscopy or flow cytometry. Briefly, cells were centrifuged and supernatant was decanted completely. The cells were resuspended in Nucleofector-V solution at 2 X 10^6 cells per 100 µl and 2 µg of pcDNA3.1hygroGp120 or pmax-GFP was added. The required electric field was applied using the L-103 program on the machine as per the manufacturer's specifications. Immediately after electroporation, 1 ml of warm medium was added, and cells were transferred to a 6-well plate containing 1 ml of pre-warmed medium.

After 24-36 hr were allowed for expression of the transfected gene. Then hygromycin drug was added to transfected cells at the concentration of 3 to 3.5 mg/ml to select stable transfectants. On day 3, the medium was replaced with fresh medium containing 0.5 mg/ml hygromycin and the plates were maintained for 7-8 days. New clones growing in the presence of the drug were selected and maintained further under 0.5 mg/ml hygromycin drug pressure. After assessing mRNA expression by RT-PCR, high Gp120-expressing clones were selected. To obtain stable transfectants, the clones were serially diluted and plated in 96 well (1 to 2 cell(s)/well), and maintained for 10-12 days. Then, two to three new clones were selected to confirm Gp120 mRNA and protein expression.

4.9 Western blotting

4.9.1 Transfected cells

To determine the expression of Gp120 protein in the BL6-10 and DC2.4 transfected cell lines, cell lysates were prepared using a mammalian cell lysis kit (Sigma). Protein concentration of samples was determined by the Bradford method (Bio-Rad). Protein samples for western blot were prepared by adding equal amounts of 2X sample buffer to cell lysates and boiling at 95^{o}C for 5 min. About 30 μg of prepared protein samples were subjected to SDS-polyacrylamide gel electrophoresis and protein bands were transferred onto nitrocellulose membranes (Millipore). Membranes were blocked overnight in blocking buffer (LI-COR Odyssey). To detect the protein of interest, membranes were stained with biotin-conjugated anti-Gp120 Abs, then with avidin-

IRDyeR700CW-conjugated Abs. The florescence intensity of the membranes was read with a LI-COR Odyssey scanner at 680 nm according to the manufacturer's instructions.

4.9.2 EXOs

EXOs were also subjected to western blot to analyze DC- and EXO-specific marker expression. Approximately, 20 μg of EXOs were dissolved in 2X sample buffer. Similarly, as described above (section 4.9.1), proteins were separated by SDS-polyacrylamide gel electrophoresis, and transferred onto nitrocellulose membranes (Millipore) for western blotting. Membranes were stained with marker-specific Abs to detect the protein of interest. To detect CD54, LAMP-1, CD86 and calnexins molecules, marker-specific Abs were used to stain the membranes, followed by staining with anti-rat-IRDyeRCW800 or anti-mouse-IRDyeRCW700 secondary Abs. Finally, membranes were scanned at 680 or 800 nm in a LI-COR Odyssey instrument following the manufacturer's instructions.

4.10 Immunological techniques

4.10.1 Purification of lymphocytes

4.10.1.1 Nylon wool column separation

Prior to spleen harvest, nylon wool columns were saturated with complete medium and incubated for 40-50 min at 37^{o}C. Spleens were harvested aseptically from naïve mice, and single cell suspensions were prepared. Red blood cells (RBCs) were depleted using 0.85% (w/v) Tris-ammonium chloride lysis buffer; splenocytes were washed twice in PBS and incubated in pre-warmed nylon columns for 1 hr. After incubation, columns were washed with 10-15 ml of RPMI medium (with 10% (v/v) FBS) to obtain an

enriched T cell population.

4.10.1.2 Magnetic bead separation (positive selection)

Specific T lymphocyte subtypes were purified using para-magnetic microbeads following the manufacturer's instructions. Briefly, for $CD8^+$ T cell purification, enriched T cells or concanavalin A (ConA)-activated splenocytes were incubated with anti-CD8α(Ly-2) para-magnetic microbeads for 20 min at 4°C in 0.5% (v/v) bovine serum albumin buffer, and washed in buffer by centrifuging at 1200 rpm for 10 min in a JA-10 rotor (Beckman Coulter). Positive selection was performed using LS column (Miltenyi Biotec) following the manufacturer's guidelines to separate the magnetically bound cells from unbound cells.

4.10.2 Preparation of BMDCs

BMDCs were generated from C57BL/6, different gene KO or A2-K^b mice as described previously (164). First, bone marrow from the femors and tibia were collected and homogeneous single cell suspensions were prepared. RBCs were depleted using 0.85% (v/v) tris-NH_4Cl_2 lysis buffer. Bone marrow cells were washed and cultured in DMEM medium supplemented with 10% (v/v) FBS, GM-CSF (20 ng/ml) and IL-4 (20 ng/ml). On day 2, floating cells, consisting of granulocytes, and T and B lymphocytes, were removed and the remaining cells were cultured with fresh medium. On day 4, proliferating aggregates of DCs were observed; the old medium was replaced with fresh medium. On day 6, cells slightly adherent to the plate were observed and these cells were pulsed with 0.4 mg/ml OVA in the presence of lipopolysaccharide for 8 to 16 hr. The resultant DCs are referred to as DC_{OVA}. DC_{OVA} generated from $Kb^{-/-}$ and $CD40L^{-/-}$ gene-KO mice were called $(Kb^{-/-})DC_{OVA}$ and $(CD40L^{-/-})DC_{OVA}$, respectively. BMDCs

generated from the A2-K^b mice were transduced with AdV_{Gp120} at multiplicity of infection (MOI) 150 to get DC_{Gp120}. DC culture supernatants were collected for EXO preparation by ultracentrifugation.

4.10.3 ConA activated $CD8^+$ T ($CD8^+$ aT) cell preparation

Naïve C57BL/6 or A2-K^b mice spleens were collected aseptically and single cell suspensions were prepared. RBCs were depleted using 0.85% (v/v) tris NH_4Cl_2 lysis buffer, and the splenocytes were cultured in RPMI-1640 medium containing 10% FBS (v/v), IL-2 (20 U/ml) and ConA (1 mg/ml) for 3 days. Finally, $CD8^+$ aT cells were enriched using Histopaque-1077 (Sigma).

4.10.4 OVA-aTexo or Gp120-aTexo vaccine preparation

Previously, a protocol was established for optimal exosomal molecule acquisition by activated T cells (150). Briefly, ConA $CD8^+$ aT cells were co-cultured with EXO_{OVA} or Gp120-specific EXOs (EXO_{Gp120}) (10 μg EXOs/1 X 10^6 T cells) in serum-free medium containing IL-2 (20 U/ml) for 4-5 hr at 37°C. These cells were termed as OVA-aTexo or Gp120-aTexo cells. $CD8^+$aT cells incubated with $EXO_{OVA}(Kb^{-/-})$ were termed as ($Kb^{-/-}$)aTexo. Similarly, $CD8^+$aT($CD40L^{-/-}$) incubated with $EXO_{OVA}(CD40L^{-/-})$ were termed as ($CD40L^{-/-}$)aTexo. These different OVA-aTexo are similar to the normal OVA-aTexo, but deficient in designated molecular expression. Both OVA-aTexo and Gp120-aTexo cells were analyzed by flow cytometry to detect the presence of exosomal molecules on the cell surface after staining with Abs specific for EXO markers.

4.10.5 DC2.4$_{Gp120}$ maturation

DC2.4$_{Gp120}$ cell maturation was achieved by culturing overnight in AIM-V serum free medium containing IFN-γ (20 ng/ml) and GM-CSF (1 ng/ml). After 8-16 hr, the mature DC2.4$_{Gp120}$ cells were analyzed by flow cytometry with a panel of Abs specific for DC maturation and activation markers. The culture supernatant was collected and stored at -80^{o}C for EXO purification.

4.10.6 Transduction of BMDCs with AdV$_{Gp120}$

AdV$_{Gp120}$ produced in this study contains a RGD-modified fiber domain, which enhances virus infection and transgene expression in BMDCs. DCs were transduced with AdV$_{Gp120}$ as described previously (125). Briefly, A2-K^{b} BMDCs were infected with AdV$_{Gp120}$ for 1 hr at 37^{o}C in DC culture medium at a MOI of 150, then the medium was replaced. DCs were cultured for another 24 hr to achieve optimal transgene expression. These DCs are called as DC$_{Gp120}$. DC culture supernatants were collected and stored at -80^{o}C for EXO purification.

4.10.7 Flow cytometry staining

4.10.7.1 Cell staining

Cells (DCs, T cells or tumor cells) (1 X 10^{6}) were pelleted at 3100 rpm for 3 min using a SEROFUGE-II centrifuge and re-suspended in 100 µl of PBS. About 1 to 5 µg/ml of FITC, PE or biotin-conjugated Abs were added and cells were incubated on ice for 30 min in the dark and then washed twice with cold PBS. Cells were re-suspended in 100 µl PBS if secondary Ab staining was necessary. Finally, cells were washed in cold PBS and re-suspended in 400 µl of PBS for flow cytometry analysis (Beckman Coulter) and were

analyzed fresh. Cells were stained with irrelevant isotype-matched Abs were used as controls. Expression profiles are presented in histograms of fluorescence intensity (log_{10}) of FITC on X-axis and the number of DC, CD8+ aT, OVA/Gp120-aTexo or tumor cells on the Y-axis. A total of 30,000 events were analyzed by flow cytometry for each marker.

4.10.7.2 EXO staining

Abs conjugated with FITC were used for the EXOs staining. About 1 µl of 50 µg/ml of FITC-conjugated Abs were added to the 20-40 µg EXOs re-suspended in 100 µl PBS and incubated for 30 min on ice. The samples were further diluted with PBS (final volume 300-400 µl) and analyzed by flow cytometry. Expression profiles are presented in histograms of fluorescence intensity (log_{10}) of FITC on X-axis (analyzed for K^b/HLA-A2, Ia^b, CD11c, CD54, CD80, CD86 and pMHC-1 expression) and the number of EXOs on the Y-axis. A total of 30,000 events were analyzed by flow cytometry for each marker.

4.10.8 *In vivo* cytotoxicity assay

In vivo cytotoxicity was assessed as described previously (164). Briefly, splenocytes collected from naïve mice were labeled differentially with high (3.0 µM) and low (0.6 µM) concentration of CFSE dye. High CFSE-labeled cells, pulsed with OVA-I peptide, (SIINFEKL) or Gp120 peptide, (KLTPLCVTL), act as target cells; and low CFSE-labeled cells, pulsed with non-specific peptide, act as control cells. Both target and control cells (1 X 10^6 of each) were then adoptively transferred at a 1:1 ratio into immunized and control mice on day 7 of immunization. After 16 hr of adoptive transfer, spleens were removed from the mice and analyzed to determine the proportion of target cell lysis ($CFSE^{high}$) in comparison to control cells ($CFSE^{low}$) by flow cytometry. Profiles presented are histograms of fluorescence intensity (log_{10}) of $CFSE^{low}$ and $CFSE^{high}$ on X-

axis and number of splenocytes on the Y-axis. An average of 1000 labelled targets remaining in the spleen were analyzed by flow cytometry for each sample. The number of residual $CFSE^{high}$ and $CFSE^{low}$ cells in spleen is presented in each figure.

4.10.9 *In vivo* tetramer proliferation assay

On day 6 of vaccination or immunization, 60 µl of peripheral blood was collected in 40 µl of heparin. Blood samples were incubated with PE-conjugated H2-K^b/$OVA_{257-264}$ (Beckman Coulter) or HLA-2/$Gp120_{121-129}$ (National Institute of Health) tetramer and FITC-CD8 Ab for 30-40 min at room temperature. The samples were fixed and treated with lysis buffer (Beckman Coulter) to remove RBCs, washed twice and finally resuspended in 400 µl PBS. In flow cytometric analysis of each sample, lymphocyte population was gated based on their size (FSC; forward scatter) and granularity (SSC; side scatter) and used in the analysis. A total of 0.2 X 10^6 cells (events) were used for analysis in each sample. Flow cytometry profiles are presented as dot-scatter plots. In each dot-scatter plot, X-axis represents fluorescence intensity of FITC (CD8 molecule expression) and Y-axis represents fluorescence intensity of PE (OVA-specific TCR). The value in each plot represents percentage of $tetramer^+CD8^+$ T cells in total $CD8^+$ population.

4.10.10 Intracellular IFN-γ cytokine secretion assay

4.10.10.1 Peptide stimulation

This assay was performed as described (172) using a Cell Fixative/Permeabilization intracellular cytokine analysis kit (BD Bioscience). Briefly, the blood samples were collected and RBCs were depleted using Tris-NH_4Cl_2 lysis buffer. Peripheral blood mononuclear cells were harvested in 500 µl RPMI-1640 with 10% (v/v)

FBS and stimulated with 2 μM of Gp120 peptide (KLTPLCVTL) for 5 hr in the presence of 2 μM GolgiStop (BD Biosciences) in U-bottom culture plates. Stimulated cells were washed with PBS, stained with anti-CD8-FITC Abs and fixed using cytofix/cytoperm solution (BD Biosciences). The samples were washed twice in 1X wash buffer (BD Bioscience) and stained with anti-IFN-γ-PE Abs for 30 min. Finally, samples were washed twice and resuspended in 400 μl of 1X wash buffer. The samples were analyzed in lymphocyte-gated population by flow cytometry to see the percent Gp120-specific CTLs that secrete IFN-γ cytokine. A total of 0.2 X 10^6 cells (events) were used for analysis in each sample. Flow cytometry profiles are presented as dot-scatter plots. In each dot-scatter plot, X-axis represents fluorescence intensity of FITC (CD8 molecule expression) and Y-axis represents fluorescence intensity of PE (IFN-γ^+ lymphocytes). The value in each plot represents percentage of IFN-γ^+CD8+ T cells in total CD8+ population.

4.10.10.2 Cell activator or mitogen stimulation

Whole blood samples (around 200 μl) were collected from immunized or control mice in heparin and diluted with equal volume of RPMI-1640 medium. Samples were incubated with cell activators, phorbol myristate acetate (50 ng/ml), calcium ionophore (1 μg/ml), and transport inhibitor GolgiStop (BD Biosciences) for 4 hr at 37^{o}C. Then samples were washed twice with serum-free medium or PBS. Intracellular IFN-γ staining and flow cytometry analysis was performed as described in section 4.10.10.1.

4.11 EXO purification

EXOs were purified from DC_{OVA}, $DC2.4_{Gp120}$ or DC_{Gp120} culture supernatants as described previously (150). Briefly, EXOs were isolated by differential centrifugations; initial centrifugation at 300 X *g* to remove cells, cellular debris and protein aggregates, and final centrifugation (in quick seal centrifuge tubes) at 100,000 X *g* in a 80Ti rotor (Beckman Coulter) for 1 hr to pellet out the EXOs. EXOs were washed twice with PBS and quantified with the Bradford method (Bio-Rad). EXOs derived from DC_{OVA}, ($Kb^{-/-}$)DC_{OVA}, and ($CD40L^{-/-}$)DC_{OVA} were termed as EXO_{OVA}, $EXO_{OVA}(Kb^{-/-})$ and $EXO_{OVA}(CD40L^{-/-})$, respectively. EXOs purified from $DC2.4_{Gp120}$ and DC_{Gp120} were called EXO_{Gp120}. An average of 10 μg EXO_{OVA} or EXO_{Gp120} was recovered from an overnight-cultured 1 X 10^6 DCs.

4.12 Electron microscopic analysis of EXOs

Purified EXOs were fixed in 4% (w/v) Para-formaldehyde. They were loaded on carbon-coated formvar grids and incubated for 20 min in a moist chamber. Later, the samples were washed twice with PBS and fixed in 1% (w/v) glutaraldehyde for 5 min. The samples were then washed three times with PBS and stained with aqueous uranyl for 10 min. The EXOs were finally examined with a JEOL 1200EX electron microscope at 60KV.

4.13 Histopathological analyses

Lung tissues were collected on day 24 of tumor challenge from immunized or un-immunized groups. These lung samples were fixed in 10% (w/v) formaldehyde,

embedded in paraffin, sliced into 6-7 μm sections and stained with hematoxylin-eosin dye according to standard protocols.

4.14 Mouse immunization

Four- to six-week-old C57BL/6 and A2-K^b mice were used for the experiment. Mice were immunized intravenously (IV) with 2 X 10^6 DC_{OVA}, $DC2.4_{Gp120}$ or DC_{Gp120} and 4 X 10^6 OVA-aTexo or Gp120-aTexo cells per mouse. PBS- and $CD8^+$ aT (4 X 10^6/mouse)-injected mice were used as controls. On day 6, the peripheral blood samples were analyzed in tetramer assay for proliferating Ag-specific $CD8^+$ T cells.

4.15 Tumor protection study

C57BL/6 mice and A2-K^b transgenic mice were immunized with DC_{Gp120} and Gp120-aTexo cells. On day 6 and day 30 post immunization, mice were challenged with the BL6-10_{Gp120} or BL6-10_{Gp120}/A2-K^b tumor cells (0.5 X 10^6 cells/mouse). Mice injected with PBS or $CD8^+$ aT cells were used as controls. All mice were sacrificed on day 24 of tumor challenge, and visible tumor colonies in lungs were counted. Tumors appear as black-pigmented colonies and are easily distinguished from the surrounding healthy tissue. If the tumor colonies are too many and difficult to count, an arbitrary value of >100 was assigned.

4.16 Statistical analysis

Statistical analysis was performed using Graphpad Prism Software. The results are presented as mean ± standard deviation (SD) unless specified. The statistical

significance between two or more groups was analyzed by Student's *t*-test or one-way analysis of variance (Tukey's post hoc test), respectively. *P* value less than 0.05 was considered significant.

CHAPTER 5

RESULTS

PART A

5.1 OVA-specific $CD8^+$aTexo vaccine stimulates primary and memory $CD8^+$ CTL responses

5.1.1 DC_{OVA} and EXO_{OVA} express immuno-stimulatory molecules

DCs play a crucial role in activation of T cells to induce Ag-specific immune responses. DCs convert protein Ags to peptides and display them on MHC molecules for T cell recognition and provide additional stimuli (co-stimulators) to T cells for complete activation. Therefore, cultured DC_{OVA} cells were characterized phenotypically with flow cytometry by staining with a panel of Abs specific for DC maturation, co-stimulatory molecules, and Ag presentation. DC_{OVA} showed higher expression of co-stimulatory molecules, CD54, CD80 and CD86; MHC molecules, K^b and Ia^b; and the DC-specific marker, CD11c, suggesting Ag-presenting ability of mature DC_{OVA} **(Figure 5.1).**

Many studies have shown that membrane-associated proteins are major components of DC-derived EXOs (138, 146). In this study, EXOs were analyzed in flow cytometry to examine the expression of membrane proteins. EXOs purified from DC_{OVA} culture supernatant by ultracentrifugation were termed as EXO_{OVA}. For phenotypic characterization, EXO_{OVA} were stained with a panel of Abs specific for co-stimulatory molecules, MHC class I and II molecules and a DC-specific marker and analyzed by flow cytometry. As expected, expression of CD80 and CD86 co-stimulatory molecules, CD54, CD11c, and MHC class I and II activation markers was observed in EXO, but the levels were appeared to be ~10 times less compared to expression levels of DC_{OVA}. Since the

size EXO (~100nm) is much lesser than a DC (15-20μm) and immunostimulatory molecules expression levels of the EXO is lesser when compared to DC, a high concentration (10 μg per 1 X 10^6 ConA $CD8^+$ T cells) of EXOs was used to prepare OVA-aTexo cells, and a high dose of 4 X 10^6 OVA-aTexo cells, which is twice the number of DCs, were used for the immunization. In flow cytometry analysis, DC population was gated based on FSC and SSC dot plots and used to obtain histogram fluorescence (FITC) on FL1 channel. A total of 8000 events of DC or EXOs, respectively, were analyzed for each marker. DC_{OVA} and EXO_{OVA} were analyzed in flow cytometry every time they were prepared (at least 3-4 times) to verify the quality of purification.

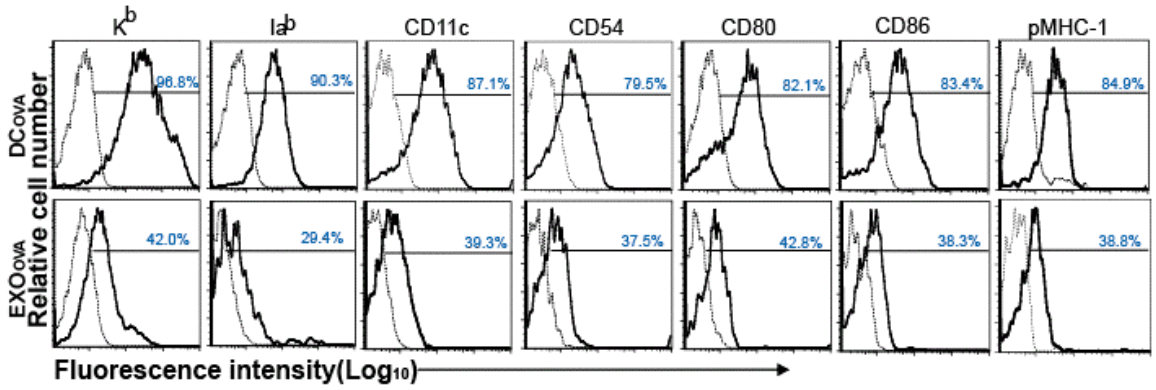

Figure 5.1 Phenotypic characterization of mature DC_{OVA} and EXO_{OVA}. Mature DC_{OVA} and EXO_{OVA} were stained with a panel of FITC-conjugated Abs specific for DC maturation markers, MHC class I and II molecules, and other DC-specific markers (solid thick line) or with irrelevant isotype-matched Ab controls (dotted thin line), and analyzed by flow cytometry. In each figure, X-axis represents histograms of fluorescence intensity (log_{10}) of FITC (analyzed for K^b, Ia^b, CD11c, CD54, CD80, CD86 and pMHC-1 expression) and Y-axis represents the relative number of DCs or EXOs. Data presented are from a single analysis of an independent experiment.

5.1.2 Acquisition of exosomal molecules by ConA $CD8^+$ aT cells

ConA $CD8^+$ aT cells were purified to >90% purity by positive selection using anti-mouse $CD8^+$ paramagnetic beads **(Figure 5.2A)**. Purified $CD8^+$ aT cells were co-cultured with EXO_{OVA} in the presence of IL-2 for 5 hr, which allowed up take of exosomal molecules. After exosomal molecule acquisition, $CD8^+$ aT cells are called OVA-aTexo cells. Both $CD8^+$ aT and OVA-aTexo cells were stained with a panel Abs specific for activation markers (CD25), co-stimulatory molecules (CD80) and pMHC-I molecules, and analyzed by flow cytometry **(Figure 5.2B)**. In comparison with ConA $CD8^+$ aT cells, increased CD80, and pMHC-I molecules on OVA-aTexo cells clearly suggest the transfer of exosomal proteins, immunostimulatory molecules, on to active $CD8^+$ T cells. In flow cytometric analysis, lymphocyte population was gated based on forward versus side scatter dot plot and used to obtain histogram of fluorescence of FITC on FL1. A total of 30,000 events of $CD8^+$ aT or OVA-aTexo were used for analysis for each marker. OVA-aTexo cells were analyzed in flow cytometry at least 3 times in independent experiemnts, and data presented below are from a single analysis of an independent experiment.

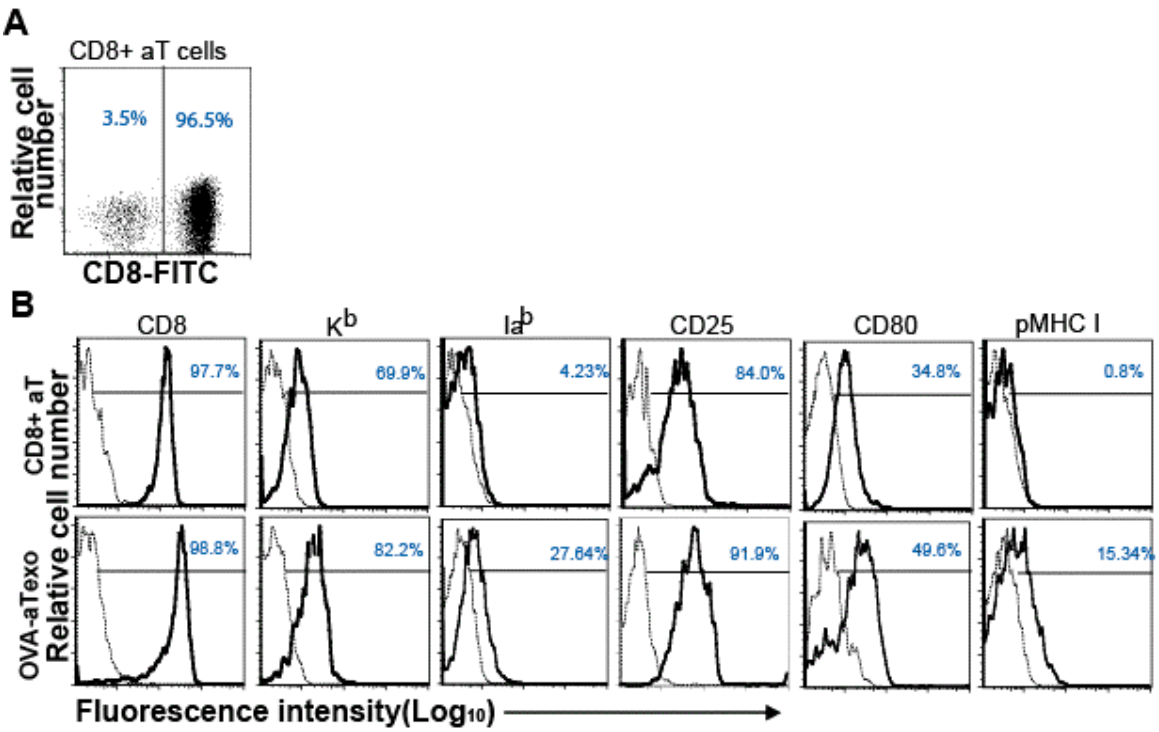

Figure 5.2 Acquisition of exosomal markers specific for mature DC_{OVA} on OVA-aTexo cells. A) Purity of the $CD8^+$ aT cells after magnetic bead separation. B) The $CD8^+$ aT and OVA-aTexo cells were incubated with a panel of Abs specific for T cell activation and DC-specific markers (solid thick lines) and analyzed by flow cytometry. Irrelevant isotype-matched Abs (dotted thin lines) were used as controls. In each figure, X-axis represents histograms of fluorescence intensity (log_{10}) of FITC (analyzed for CD8, K^b, Ia^b, CD25, CD80 and pMHC-1 expression) and Y-axis represents the relative number of $CD8^+$ aT or OVA-aTexo cells. A total of 30,000 events of $CD8^+$ aT or OVA-aTexo were used for analysis for each marker. OVA-aTexo cells were analyzed in flow cytometry at least 3 times in independent experiments, and data presented below are from a single analysis of an independent experiment.

5.1.3 OVA-aTexo vaccine stimulates proliferation of OVA-specific $CD8^+$ T cells *in vivo*

Following immunization of C57BL/6 mice with 4 X 10^6 OVA-aTexo cells, or 2 X 10^6 DC_{OVA}, the proliferated OVA-specific $CD8^+$ T cells in peripheral blood was monitored by H2-K^b/$OVA_{257-264}$ tetramer staining on day 3, 4, 5, 6, 7, 9 and 30 after immunization,. In whole blood samples, the lymphocyte population was gated based on forward and side scatter properties and used for the analysis by flow cytometry. A total of 0.2 X 10^6 cells (events) were used for analysis in each sample. Flow cytometry profiles are presented as dot-scatter plots. Experiment was performed twice, each of which contained 4 mice per test group. For statistical analysis, the values from both first and second experiments were used. Mean% ± 1 S.D (n=8) of OVA-specific $CD8^+$ T cells out of the total $CD8^+$ T cell population in DC_{OVA}- and OVA-aTexo-immunized groups was indicated: ** $p<0.01$ when compared with PBS or $CD8^+$ aT-injected groups.

. The results indicate the kinetics and magnitude of $CD8^+$ T-cell generation by OVA-aTexo cells are similar to those of $DC_{OVA,}$ where peak tetramer-positive $CD8^+$ T cells were observed on day 6 and 7 post-immunization **(Figure 5.3A).**

OVA-aTexo cells and DC_{OVA} induced an average of 1.12% $\pm^1$ 0.1 and 1.42% $\pm^1$ 0.15 OVA-specific $CD8^+$ T cells out of total $CD8^+$ T cells on day 6 after immunization **(Figure 5.3B)**. However, there was no response in control mice that were injected with PBS or $CD8^+$ aT cells (negative controls), suggesting that OVA-aTexo cells can induce a $CD8^+$ T-cell response similar to DC_{OVA} in an Ag-specific manner.

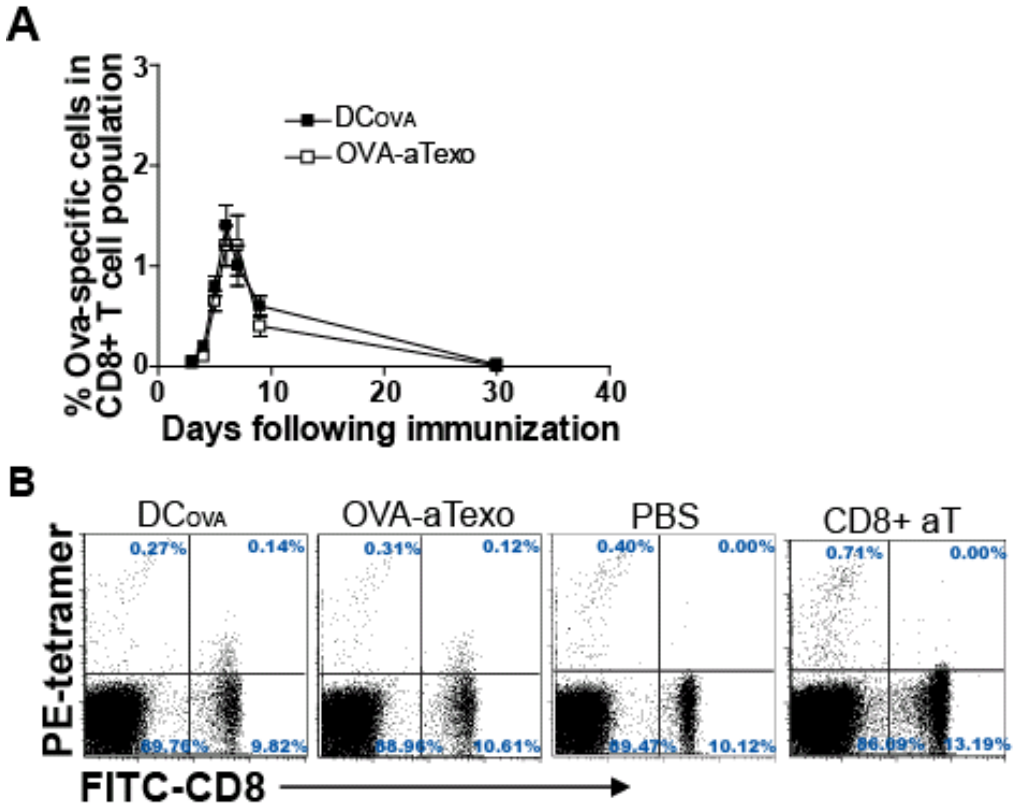

Figure 5.3 OVA-aTexo vaccine induces primary CD8$^+$ T-cell response *in vivo*. Wild-type mice were injected IV with DC_{OVA}, OVA-aTexo, CD8$^+$ aT or PBS. A) Tail blood samples were collected from injected mice on day 3, 4, 5, 6, 7, 9 and 30, stained with PE-H2-K^b/OVA1 tetramer and FITC-anti-CD8 Ab, and analyzed by flow cytometry. Values in line diagram represent the Mean% ± 1 S.D of OVA-specific CD8$^+$ T cells in total CD8$^+$ T cells and are cumulative of two independent experiments with 4 mice per group B) The scatter-dot plots are derived from a representative mouse in each group on day 6 post-immunization. In flow cytometric analysis, a total of 0.2 X 10^6 cells in lymphocyte-gated population were used for analysis in each sample. In each dot-scatter plot, X-axis represents fluorescence intensity of FITC (CD8 molecule expression) and Y-axis represents fluorescence intensity of PE (OVA-specific TCR). The net percentage of

labelled cells within the gated analysis region is presented in each figure. Data presented is from a single analysis of an independent experiment.

5.1.4 OVA-aTexo vaccine stimulates cytotoxic $CD8^+$ T cells

Whether OVA-specific $CD8^+$ T cells exhibit cytotoxic function was assessed by an *in vivo* cytotoxicity assay. Wild-type mice were injected with OVA-aTexo, $DC_{OVA,}$ $CD8^+$ aT or PBS, and monitored for $CD8^+$ T cells proliferation by tetramer assay as described above on day 6 after immunization. The data is presented as mean% ± 1 S.D (n=8) of OVA-specific $CD8^+$ T cells out of the total $CD8^+$ T cell population in DC_{OVA} and OVA-aTexo groups: * $p<0.05$ when compared with PBS or $CD8^+$ aT-injected groups. In *in vivo* cytotoxicity assay, on day 7, the above-immunized mice were adoptively transferred with equal number of target ($CFSE_{high}$-labeled, OVA1-pulsed splenocytes) and control ($CFSE_{low}$-labeled, irrelevant Mut1-peptide-pulsed splenocytes) cells. After 16 hr of adoptive transfer, spleens were removed and analyzed by flow cytometry to determine the proportion of target cell lysis ($CFSE_{high}$) in comparison to control cells ($CFSE_{low}$). An average of 1000 CFSE-labelled cells remaining in the spleen were analyzed by flow cytometry for each sample, and data is presented as mean% ± 1 S.D (n=8) of target ($CFSE^{high}$) and control ($CFSE^{low}$) cells remaining in the spleens of mice injected with $DC_{OVA,}$ OVA-aTexo, $CD8^+$ aT or PBS groups was indicated: ** $p<0.01$ when compared with PBS or $CD8^+$ aT-injected groups. For statistical analysis, the values of both first and second experiments with four mice per group were used.

OVA-aTexo, $DC_{OVA,}$ $CD8^+$ aT or PBS groups respectively showed an average of 1.15% $\pm^1$ 0.2, 1.65% $\pm^1$ 0.3, 0.05% $\pm^1$ 0.02 and 0.02% $\pm^1$ 0.01 $CD8^+$ T cells by tetramer analysis **(Figure 5.4A)**. Similarly, the vaccine-stimulated CTLs were able to lyse the target cells efficiently. Mice immunized with OVA-aTexo, DC_{OVA} or $CD8^+$ aT cells showed an average lysis of 70% $\pm^1$ 1.2, 71% $\pm^1$ 1.1 or 4% $\pm^1$ 3.1 $CFSE_{high}$-labeled target

cells, respectively **(Figure 5.4B),** suggesting OVA-aTexo vaccination-induced CTLs exhibit cytotoxic activity similar to those of DC_{OVA}-induced ones.

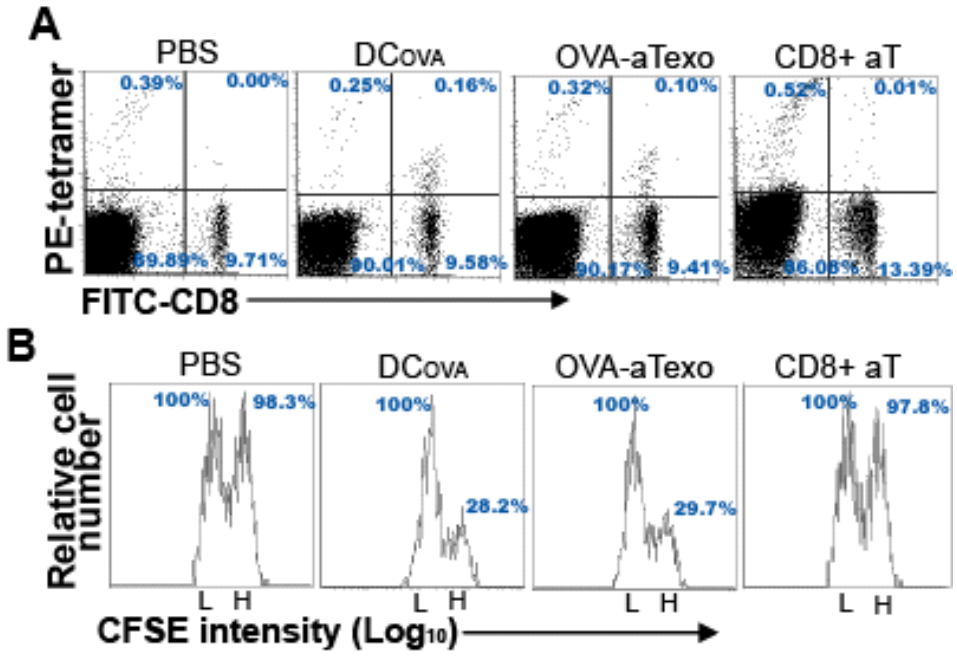

Figure 5.4 OVA-aTexo vaccine activates functional cytotoxic CD8$^+$ T cells. Wild-type mice (n=4/group) were IV immunized with PBS, DC_{OVA}, OVA-aTexo or $CD8^+$ aT. A) On day 6, tail blood samples were collected and stained with PE-H2-K^b/OVA1 tetramer and FITC-anti-CD8 Ab to analyze tetramer-positive $CD8^+$ CTLs by flow cytometry. The scatter-dot plots are derived from a representative mouse in each group on day 6 post immunization. In flow cytometric analysis, a total of 0.2 X 10^6 cells in lymphocyte-gated population were used for analysis in each sample. In each dot-scatter plot, X-axis represents fluorescence intensity of FITC (CD8 molecule expression) and Y-axis represents fluorescence intensity of PE (OVA-specific TCR). The net percentage of labeled cells within the gated analysis region is presented in each figure. Data presented is from a single analysis of an independent experiment. B) On day 7, the above immunized and control mice were injected IV with target and control labeled cells at 1:1 ratio. After 16 hr of target cell delivery, the percentage of residual $CFSE_{high}$ target cells remaining in the spleen in comparison to control $CFSE_{low}$ cells was determined using

flow cytometry. In each figure, X-axis represents histograms of fluorescence intensity (log_{10}) of $CFSE^{low}$ and $CFSE^{high}$ and Y-axis represents the relative number of labeled cells. An average of 1,000 labeled cells were analyzed by flow cytometry for each sample. The values in each figure represent the residual $CFSE^{high}$ and $CFSE^{low}$ cells remaining in the spleen. Data presented is from a single analysis of an independent experiment.

5.1.5 OVA-aTexo vaccine induces Ag-specific memory response

To determine whether $CD8^+$ memory T cells are induced by the OVA-aTexo vaccine, mice were immunized with OVA-aTexo, DC_{OVA} or PBS. All groups were boosted with DC_{OVA} on day 30 post-immunization. The blood samples were analyzed on day 4 of DC_{OVA} boost in the tetramer assay to assess expansion of memory cells. In whole blood samples, the lymphocyte population was gated and used for the analysis by flow cytometry. A total of 0.2 X 10^6 cells (events) were used for analysis in each sample. Flow cytometry profiles are presented as dot-scatter plots. Mice used for the kinetics and primary immune response study (section 5.1.3) were used for the memory response study, and statistical analysis was performed similarly as described in this section. The mean percentage (n=8) and 1 S.D values of tetramer positive cells in total $CD8^+$ T cells population on day 30 post-immunization and 4 days after DC_{OVA} boost was calculated for each group. Mean% ± 1 S.D (n=8) of OVA-specific $CD8^+$ T cells out of the total $CD8^+$ T cell population in DC_{OVA} and OVA-aTexo groups was indicated: ** $p<0.01$ when compared with PBS group.

On the 30^{th} day after primary immunization, the immunized groups had mean average of 0.09% $\pm^1$ 0.03 and 0.07% $\pm^1$ 0.02 response in DC_{OVA}- and OVA-aTexo-immunized mice, respectively **(Figure 5.5)**. Interestingly, OVA-aTexo cells also induced memory cells that were able to expand (up to 1.2% $\pm^1$ 0.15) as that induced by DC_{OVA} (up to 1.55% $\pm^1$ 0.2), suggesting OVA-aTexo cells have ability to induce a memory T cells response.

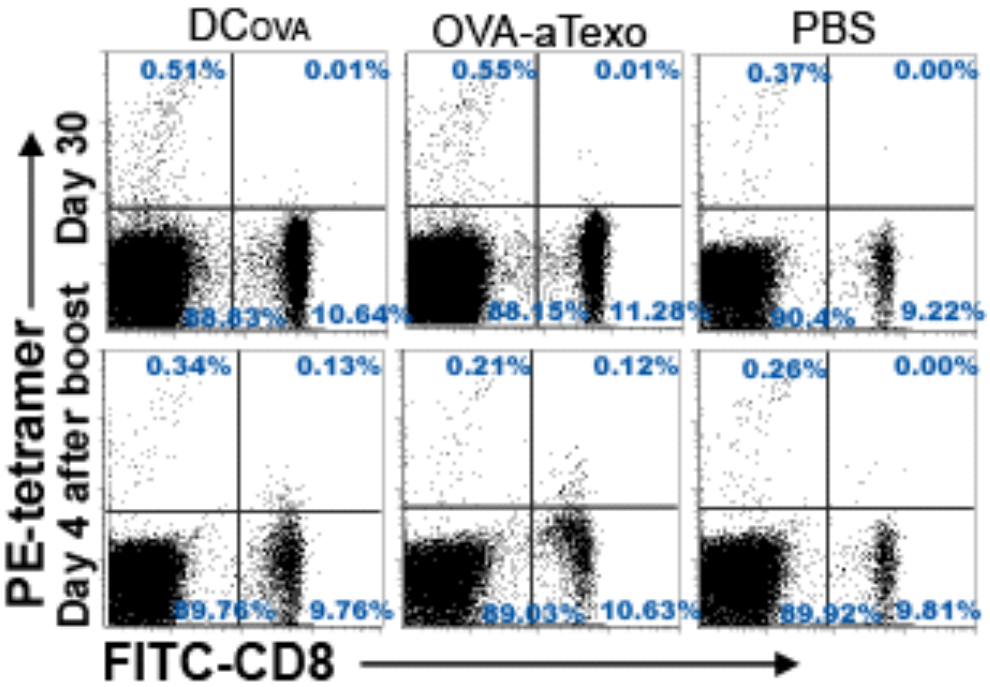

Figure 5.5 OVA-aTexo vaccine induces memory CD8$^+$ T cells. Wild-type mice were injected IV with DC_{OVA}, OVA-aTexo or PBS. After 30 days, blood samples were collected and stained in the tetramer assay to assess presence of OVA-specific CD8 T cells. All mice were boosted with DC_{OVA}, and expansion of memory T cells was examined 4 days later by the tetramer assay. The scatter-dot plots presented are derived from a representative mouse in each group. In flow cytometric analysis, a total of 0.2 X 10^6 cells in lymphocyte-gated population were used for analysis in each sample. In each dot-scatter plot, X-axis represents fluorescence intensity of FITC (CD8 molecule expression) and Y-axis represents fluorescence intensity of PE (OVA-specific TCR). The net percentage of labeled cells within the gated analysis region is presented in each figure. Data presented is from a single analysis of an independent experiment.

5.1.6 OVA-aTexo vaccine activation of $CD8^+$ T cells is mediated through CD40L signaling, IL-2 secretion and acquired pMHC-I complex

It has been shown previously that $CD4^+$aTexo vaccine is able to stimulate a strong $CD8^+$ CTL response and anti-tumor immunity through CD40L-signaling, CD80 co-stimulation and acquired pMHC-I complexes. Both the OVA-aTexo and $CD4^+$aTexo vaccine showed similar immuno-stimulatory capacity. This experiment investigated the OVA-aTexo vaccine mechanism of immuno-stimulation. OVA-aTexo cells with or without specific molecular deficiencies were injected into wild-type or gene-deficient mouse ($IL\text{-}2R^{-/-}$) as shown in **Table 5.1**. Immune response was measured by both *in vivo* $CD8^+$ T cell proliferation and cytotoxicity assays as described in section 5.4. In tetramer study, mean% ± 1 S.D (n=8) of OVA-specific $CD8^+$ T cells out of the total $CD8^+$ T cell population in wild-type groups immunized with OVA-aTexo, ($CD40L^{-/-}$)aTexo or ($Kb^{-/-}$)aTexo cells and $IL\text{-}2R^{-/-}$ mice immunized with OVA-aTexo cells were indicated: *$p<0.05$ when compared to OVA-aTexo-injected wild-type mice. In *in vivo* cytotoxicity assay, the data is presented as mean% ± 1 S.D (n=8) of target ($CFSE^{high}$) cells remaining in the spleens of wild-type groups immunized with OVA-aTexo, ($CD40L^{-/-}$)aTexo or ($Kb^{-/-}$)aTexo cells, and $IL\text{-}2R^{-/-}$ mice immunized with OVA-aTexo cells was indicated: * $p<0.05$ when compared with PBS or $CD8^+$ aT-injected groups. For statistical analysis, the values of both first and second experiments with four mice per group were used in the above experiments.

Mice immunized with ($CD40L^{-/-}$)aTexo showed significantly less proliferation of tetramer-positive $CD8^+$ T cells (0.65% $\pm^1$ 0.1) compared to the OVA-aTexo-injected mice **(Figure 5.6A).** Similarly, ($Kb^{-/-}$)aTexo-immunized mice failed to show any

proliferation of OVA-specific $CD8^+$ T cells (0.05% $\pm^1$ 0.01) compare to mice immunized with OVA-aTexo cells (1.1% $\pm^1$ 0.2). Furthermore, IL-2R$\alpha^{-/-}$ mice immunized with OVA-aTexo showed very little $CD8^+$ T cells (0.15% $\pm^1$ 0.05) proliferation. In contrast, wild-type mice immunized with OVA-aTexo showed an increase in proliferation of $CD8^+$ T cells. Similarly, an efficient $CD8^+$ CTL response capable of lysing target cells was observed by *in vivo* cytotoxicity assays in OVA-aTexo-immunized mice **(Figure 5.6B)**. These results suggest that the OVA-aTexo stimulatory effect is mediated through CD40L signaling, IL-2 secretion and acquired pMHC-I molecules.

Table 5.1 Preparation of specific molecule-deficient OVA-aTexo vaccines

OVA-aTexo vaccine types	Source of $CD8^+$ T cells	Source of DC-derived EXOs
OVA-aTexo	C57BL/6 mice (spleen)	C57BL/6 mice (bone marrow)
($CD40L^{-/-}$)aTexo	$CD40L^{-/-}$ mice (spleen)	$CD40L^{-/-}$ mice (bone marrow)
($K^{b-/-}$)aTexo	$K^{b-/-}$ mice (spleen)	$K^{b-/-}$ mice (bone marrow)

Note: OVA-aTexo cells were injected into IL-2R$\alpha^{-/-}$ mice to test the involvement of IL-2 signaling in the activation of OVA-specific $CD8^+$ T cells.

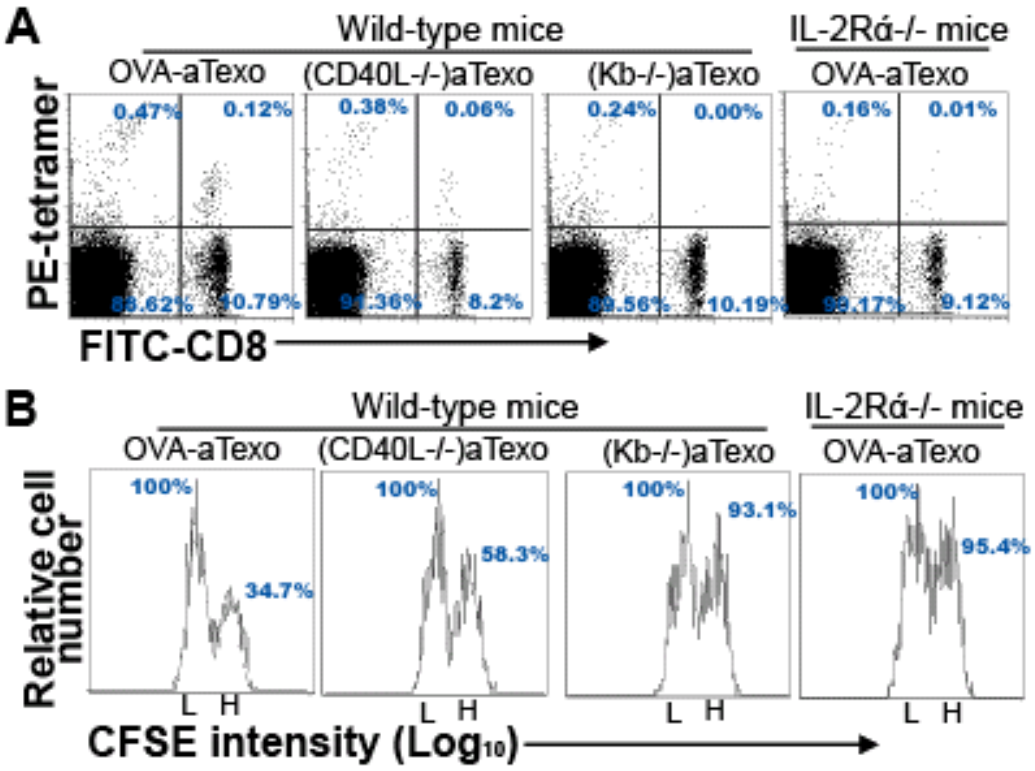

Figure 5.6 The mechanism of immuno-stimulation by OVA-aTexo vaccine. OVA-aTexo cells deficient in designated molecules were injected into wild-type mice, and OVA-aTexo cells were injected into IL2R$^{-/-}$ mice. A) On day 6, peripheral blood samples were analyzed using the tetramer assay to quantify OVA-specific CD8^{+} T cells by flow cytometry. The scatter-dot plots presented are derived from a representative mouse in each group on day 6 post immunization. In flow cytometric analysis, a total of 0.2 X 10^{6} cells in lymphocyte-gated population were used for analysis in each sample. In each dot-scatter plot, X-axis represents fluorescence intensity of FITC (CD8 molecule expression) and Y-axis represents fluorescence intensity of PE (OVA-specific TCR). The net percentage of labeled cells within the gated analysis region is presented in each figure. Data presented is from a single analysis of an independent experiment. B) In the *in vivo* cytotoxicity assay, on day 7, the above-immunized and -control mice were injected IV

with target and control labeled cells at 1:1 ratio. After 16 hr of target cell delivery, the percentage of residual $CFSE_{high}$ target cells remaining in the spleen in comparison to control $CFSE_{low}$ cells was determined by flow cytometry. In each figure, X-axis represents histograms of fluorescence intensity (log_{10}) of $CFSE^{low}$ and $CFSE^{high}$ and Y-axis represents the relative number of labeled cells. An average of 1,000 labeled cells were analyzed by flow cytometry for each sample. The values in each figure represent the residual $CFSE^{high}$ and $CFSE^{low}$ cells remaining in the spleen. Data presented is from a single analysis of an independent experiment.

PART B

5.2 Gp120-aTexo vaccine activates naïve and memory $CD8^+$ CTL responses and anti-tumor immunity in wild-type mice

5.2.1 Characterization of DC2.4 cells transfected with *Gp120*

DC2.4 cells are a type of DC cell lines. In this study, we transfected these cell lines with *Gp120* so that the EXOs secreted from them might express Gp120-specific epitopes on MHC-I and -II molecules. DC2.4 cells were transfected with pcDNAGp-120-Hygro expression vector while using pmax-GFP as a positive transfection control **(Figure 5.7A)**. After selecting transfected clones under hygromycin drug pressure, the cells were analyzed for Gp120 mRNA and protein expression in PCR and western blot, respectively. The positive colonies with confirmed Gp120 mRNA **(Figure 5.7B**) and protein **(Figure 5.7C)** expression were chosen for EXO purification.

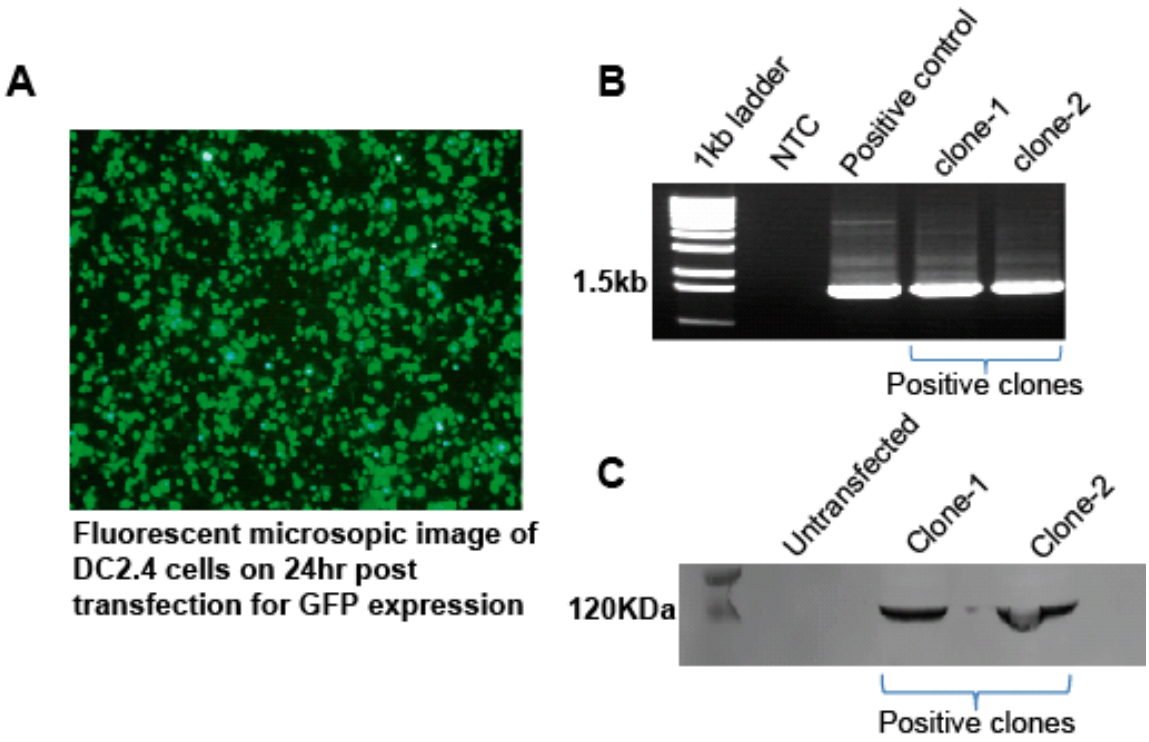

Figure 5.7 Characterization of DC2.4 cells transfected with *Gp120*. A) DC2.4 cells transfected with pmax-GFP were used as positive control to monitor transfection efficiency. Fluorescent microscopic image of cells to show the number of transfected cells on 24 hr post-transfection. B) and C) Potential positive clones were selected based on their growth with hygromycin selection. Selected clones were analyzed for Gp120 mRNA expression by RT-PCR (B) and protein expression by western blot (C).

5.2.2 Characterization of BL6-10 melanoma cells transfected with *Gp120*

At present, well-established murine models are unavailable for HIV-1 vaccine efficacy studies. Therefore, I employed a tumor challenge approach to evaluate the immunotherapeutic effect of the Gp120-aTexo vaccine. To do this, BL6-10 cells were transfected with pcDNAGp-120-Hygro expression vector while using pmax-GFP as a positive transfection control **(Figure 5.8A)**. Gene expression was confirmed by PCR and western blot. BL6-10 tumor cells are highly metastasizing skin melanoma tumor cells and upon injection IV cause black-pigmented tumor nodules in lungs. The PCR and western blot analysis confirmed that selected BL6-10 transfected-clones express Gp120 transcripts **(Figure 5.8B)** and protein **(Figure 5.8C)**, respectively.

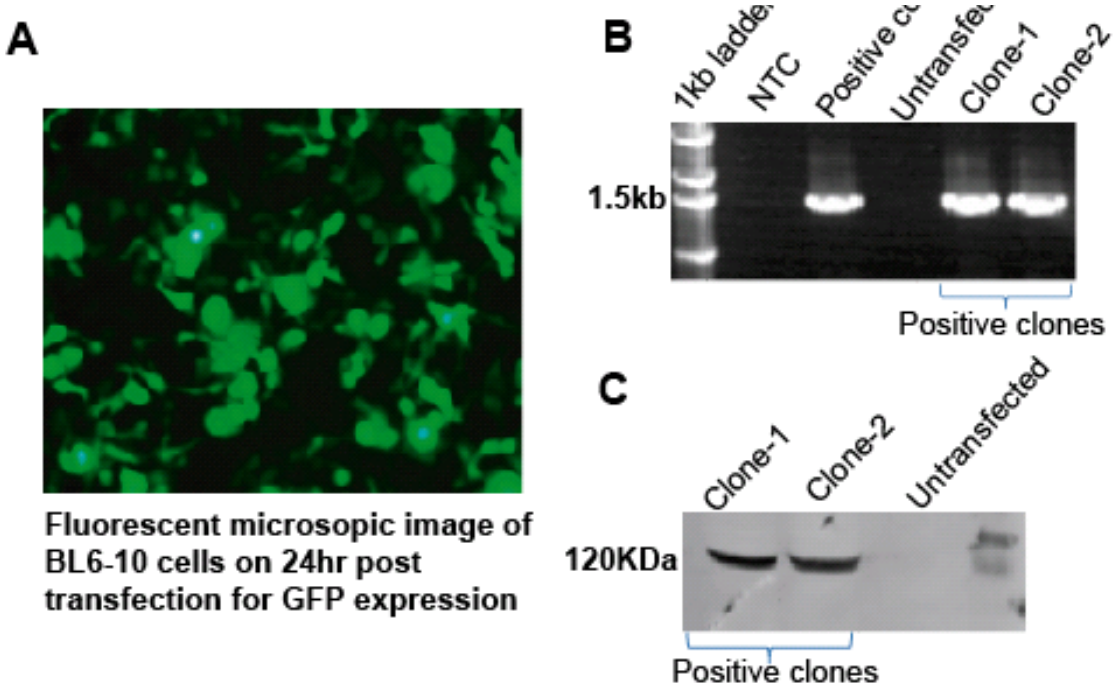

Figure 5.8 Characterization of BL6-10 melanoma cells transfected with *Gp120*. A) BL6-10 tumor cells were transfected with pmax-GFP to monitor transfection efficiency using the Nucleofector V kit. Fluorescent microscopic image of cells to show the number of transfected cells on 24 hr post-transfection. B) and C) Potential positive clones of BL6-10 were selected based on growth in the presence of hygromycin. Selected clones were analyzed for Gp120 mRNA by RT-PCR (B) and protein expression by western blot (C).

5.2.3 Mature DC2.4$_{Gp120}$ and their EXOs express immuno-stimulatory molecules

As a part of the current study, *Gp120*-transfected DC2.4 cells were used as a substitute for BMDCs. DC2.4 cells were successfully transfected with an expression vector containing the full-length Gp120 gene sequence. DC2.4$_{Gp120}$ cells were made to mature by culturing overnight in the presence of IFN-γ. An average of 10 μg of EXOs were recovered from cultures of 1 X 10^6 mature DC2.4$_{Gp120}$ cells. By flow cytometry, a total of 8000 events of DC EXOs were analyzed for each marker. The purified EXOs and mature DC2.4$_{Gp120}$ showed the expression of maturation, co-stimulatory and activation markers, such as CD11c, CD54, CD80, CD86, K^b and Ia^b, (solid thick lines) **(Figure 5.9A).** Irrelevant isotype-matched Abs (dotted thin lines) were used as controls. The expression profiles indicated that mature DC2.4$_{Gp120}$ express activation and maturation markers similar to that of mature BM DC$_{OVA}$. The EXO$_{Gp120}$ showed similar expression of all the markers, but likely at 10-fold reduced levels. As expected, expression of CD80 and CD86 co-stimulatory molecules, CD54, CD11c, and MHC class I and II activation markers was observed in EXO, but the levels were appeared to be 10 times less compared to expression levels of DC$_{OVA}$. DC$_{OVA}$ and EXO$_{OVA}$ were analyzed in flow cytometry every time when they were prepared (at least 3-4 times) to verify the quality of purification.

EXOs were further characterized in western blot to see the expression of LAMP-1, CD54, CD86 and calnexin. In line with previous results (164), EXOs showed the expression of CD54, CD86, and additionally LAMP-1, but not calnexin, which is an endoplasmic reticulum-specific marker **(Figure 5.9B)**. These results are similar to positive control EXO$_{OVA}$, suggesting that EXO$_{Gp120}$ are derived from endosomal

pathways (173). EXO_{Gp120} were also processed for electron microscopic visualization, which showed a characteristic “saucer” or “cup” like morphology similar to EXO_{OVA} **(Figure 5.9C).**

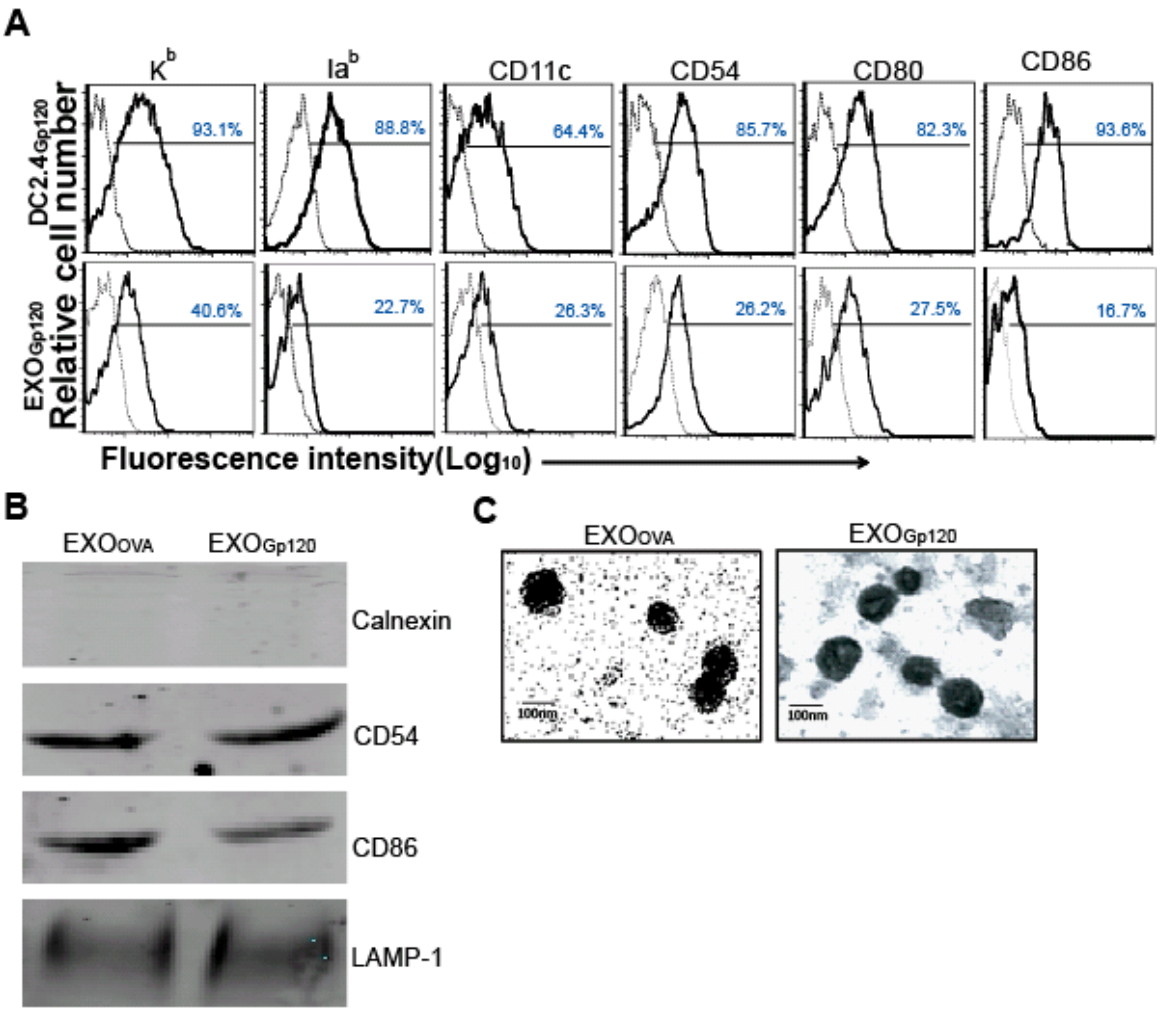

Figure 5.9 Phenotypic characterization of DC2.4$_{Gp120}$ and EXO$_{Gp120}$. A) DC2.4$_{Gp120}$ and EXO$_{Gp120}$ were stained with a panel of Abs specific for activation, co-stimulatory and maturation markers (solid thick lines) or with irrelevant isotype-matched control Abs (dotted thin lines), and analyzed by flow cytometry. In each figure, X-axis represents histograms of fluorescence intensity (log_{10}) of FITC (analyzed for K^b, Ia^b, CD11c, CD54, CD80, CD86 and pMHC-1 expression) and Y-axis represents the relative number of DCs or EXOs. A total of 30,000 events of DC2.4$_{Gp120}$ or EXO$_{Gp120}$ were used for analysis for each marker. Data presented are from a single analysis of an independent experiment. B) The expression of LAMP-1, CD54, CD86 and calnexin were analyzed in EXO$_{Gp120}$ by

western blot using EXO_{OVA} as a positive control. C. Electron microscopic visualization of EXO_{Gp120} and EXO_{OVA}.

5.2.4 Gp120-aTexo vaccine stimulates a primary immune response *in vivo*

Gp120-aTexo vaccine was prepared by co-culturing $CD8^+$ aT cells with EXO_{Gp120} as described previously (150). Gp120-aTexo cells were injected IV into wild-type mice to assess their immunostimulatory capacity. $CD8^+$ aT cell- or PBS-injected mice were used as negative controls. As no H2-K^b epitope of Gp120 has been characterized, Gp120-specific tetramer testing is not currently available to detect proliferated Gp120-specific $CD8^+$ T cells in wild-type mice. Hence, immune response was analyzed in peripheral blood on day 6 by analyzing the expression of activation marker CD44 or Gp-120-specific IFN-γ-expressing $CD8^+$ T cells out of total $CD8^+$ T cell population as described by Shedlock et al. (174). The IFN-γ assay was performed by stimulating whole blood sample with cell activators, phorbol myristate acetate and calcium ionophore, and then cells were stained for intracellular IFN-γ cytokine expression. Stimulation with cell activators helped to assess the degree of vaccine-induced IFN-γ-secreting cells in comparison to the PBS or $CD8^+$ aT control groups. In whole blood samples, the lymphocyte population was gated based on forward and side scatter properties and used for the analysis by flow cytometry. A total of 0.2 X 10^6 cells (events) were used for analysis in each sample in CD44 activation marker and IFN-γ interacellular assay,. Flow cytometry profiles are presented as dot-scatter plots. Experiment was performed twice, each of which contained 4 mice per test group. For statistical analysis, the values of both first and second experiments were used. Mean% ± 1 S.D (n=8) of $CD44^+$ $CD8^+$ T cells out of total T cells or IFN-γ^+ $CD8^+$ T cells out of the total $CD8^+$ T-cell population in DC_{GP120} and Gp120-aTexo groups was indicated: ** $p<0.05$ when compared with PBS or $CD8^+$ aT-injected groups.

Gp120-aTexo-vaccinated mice showed a significantly increased $CD44^{high}$ $CD8^{+}$ T cells (5.23 $\pm^{1}$ 0.36) compared to $CD8^{+}$ aT cell- (2.65 $\pm^{1}$ 0.14) or PBS-injected (2.51 $\pm^{1}$ 0.2) mice **(Figure 5.10A)** out of total T cells**.** $DC2.4_{Gp120}$ cells-injected mice also showed an increased $CD44^{high}$ $CD8^{+}$ (4.9 $\pm^{1}$ 0.29) T cells similar to the Gp120-aTexo vaccine. Similarly, IFN-γ^{-}secreting $CD8^{+}$ T cells were significantly elevated in Gp120-aTexo- (3.04 $\pm^{1}$ 0.47) and $DC2.4_{Gp120}$ (2.82 $\pm^{1}$ 0.43)-immunized mice compared to $CD8^{+}$ aT- (1.7 $\pm^{1}$ 0.31) or PBS-injected (1.51 $\pm^{1}$ 0.26) mice **(Figure 5.10B)**, indicating that the Gp120-aTexo vaccine effectively induced primary Ag-specific $CD8^{+}$ T-cell responses *in vivo*.

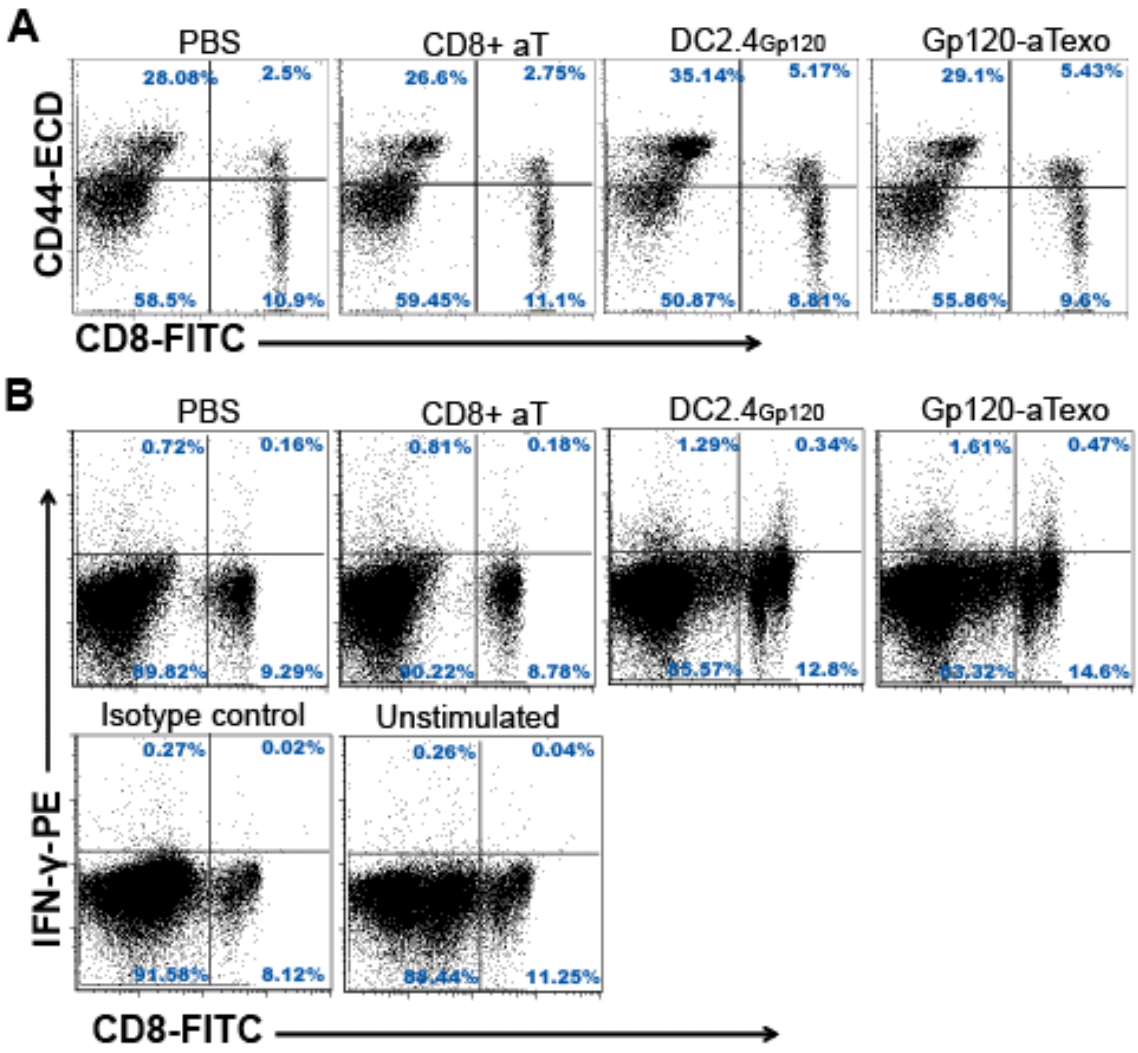

Figure 5.10 Gp120-aTexo vaccine activate naïve CD8$^+$ T cell stimulation *in vivo*. Wild-type mice were injected IV with DC2.4$_{Gp120}$ or Gp120-aTexo vaccine. On day 6, peripheral blood samples of immunized mice were stained with FITC-anti-CD8 Ab and ECD-anti-CD44$^+$ or PE-anti-IFN-γ Abs (intracellularly), and analyzed by flow cytometry. The scatter-dot plots are derived from a representative mouse in each group. In flow cytometric analysis, a total of 0.2 X 10^6 in lymphocyte-gated population were used for analysis in each sample in CD44 activation marker (A) and IFN-γ secretion analysis (B),. In each dot-scatter plot, X-axis represents fluorescence intensity of FITC (CD8 molecule expression) and Y-axis represents fluorescence intensity of ECD (CD44) or PE (IFN-γ).

The net percentage of labeled cells within the gated analysis region is presented in each figure. Data presented is from a single analysis of an independent experiment.

5.2.5 Gp120-aTexo vaccine induces efficient short- and long-term anti-tumor immunity

Both short- and long-term anti-tumor immunity following Gp120-aTexo vaccination was assessed in wild-type mice. First, C57BL/6 mice were injected IV with Gp120-aTexo 4 X 10^6 of cells per mouse and challenged with Gp120-expressing BL6-10 tumor cells (0.5 X 10^6 BL6-10_{Gp120} /mouse) on day 6 in experiment I or on day 30 in experiment II subsequent to the vaccination as shown in **Table 5.2**. Before tumor challenge, BL6-10_{Gp120} cells were cultured overnight in the presence of an IFN-γ to increase pMHC-I expression **(Figure 5.11A).** This approach increases the chances of efficient peptide presentation, enabling rapid recognition and killing of target cells by $CD8^+$ CTLs (175, 176). BL6-10 cells form lung tumor colonies, which are prominently seen as black-pigmented foci/nodules of variable size and can be easily distinguished from surrounding lung healthy tissue. Lung tumor colonies were counted randomly, and if tumor colonies were too many to count, an arbitrary value of >100 was given as described previously (162).

Following tumor challenge, all mice were sacrificed on day 24 to analyze lungs for tumor colonies. Mice immunized with Gp120-aTexo or DC2.4_{Gp120} cells (0/8) were completely protected against tumor challenge **(Figure 5.11B)** in both Experiment-I and -II **(Table 5.2),** further suggesting that the Gp120-aTexo vaccine can stimulate $CD8^+$ CTL responses efficiently, including both effector and memory stage anti-tumor immunity. Histopathological analysis of lung tissue sections was showed numerous tumor nodules in PBS-injected mice, but not in Gp120-aTexo-injected mice. **(Figure 5.11C**

Table 5.2 Gp120-aTexo protects C57BL/6 mice against lung tumor metastases

Immunization	Tumor challenge	Visible tumor growth incidence	Median number of lung tumor colonies
Experiment I.			
Gp120-aTexo	BL6-10_{Gp120}	0/8 (0)[a]	0
$DC2.4_{Gp120}$	BL6-10_{Gp120}	0/8 (0)[a]	0
$CD8^+$ aT	BL6-10_{Gp120}	8/8 (100)[b]	>100
PBS	BL6-10_{Gp120}	8/8 (100)[b]	>100
Experiment II			
Gp120-aTexo	BL6-10_{Gp120}	0/8 (0)[a]	0
$DC2.4_{Gp120}$	BL6-10_{Gp120}	0/8 (0)[a]	0
PBS	BL6-10_{Gp120}	8/8 (100)[b]	>100

[a]: Immunized group, [b]: control group

In experiment I, C57BL/6 mice were injected IV with the $DC2.4_{Gp120}$ (2 X 10^6/mouse), Gp120-aTexo vaccine (4 X 10^6/mouse), $CD8^+$ aT cells (4 X 10^6/mouse) or PBS, and challenged with BL6-10_{Gp120} (0.5 X 10^6/mouse) tumor cells on day 6 after immunization. In experiment II, challenge with BL6-10_{Gp120} tumor cells was done on day 30 after immunization. All mice were sacrificed on day 24 after tumor challenge, and the lungs were examined for the number of black tumor colonies.

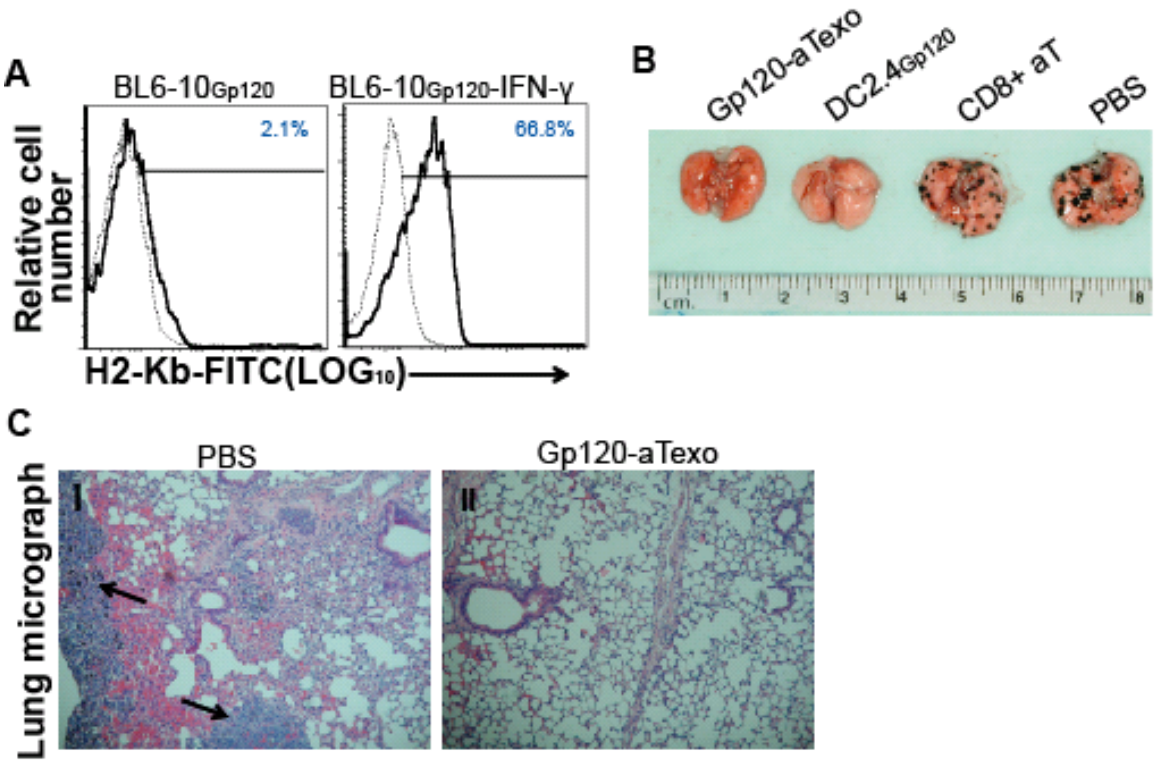

Figure 5.11 Gp120-aTexo vaccine induces short- & long-term anti-tumor immunity. A) BL6-10_{Gp120} cells were cultured in the presence of IFN-γ (20 ng/ml) to augment the expression of pMHC-I. (B and C). In the tumor protection study, Gp120-aTexo- and $DC2.4_{Gp120}$-immunized mice showed complete protection against lung metastasis as confirmed by both gross analysis (B) and histopathological studies (C), PBS-injected mice developed numerous tumor nodules (arrows) whereas the Gp120-aTexo-injected mice lungs were devoid of visible tumor nodules.

PART C

5.3 Gp120-aTexo vaccine induces primary and memory $CD8^+$ CTL responses and anti-tumor immunity in A2-K^b transgenic mice.

5.3.1 Characterization of recombinant AdV_{Gp120}

After successful AdV_{Gp120} construction and amplification, samples were analyzed to determine the expression of the gene of interest and protein synthesis by PCR and western blot, respectively. Both PCR and western blot analysis confirmed Gp120 gene insertion **(Figure 5.12C)** and efficient protein expression **(Figure 5.12D)** by the purified Adv_{Gp120} stock.

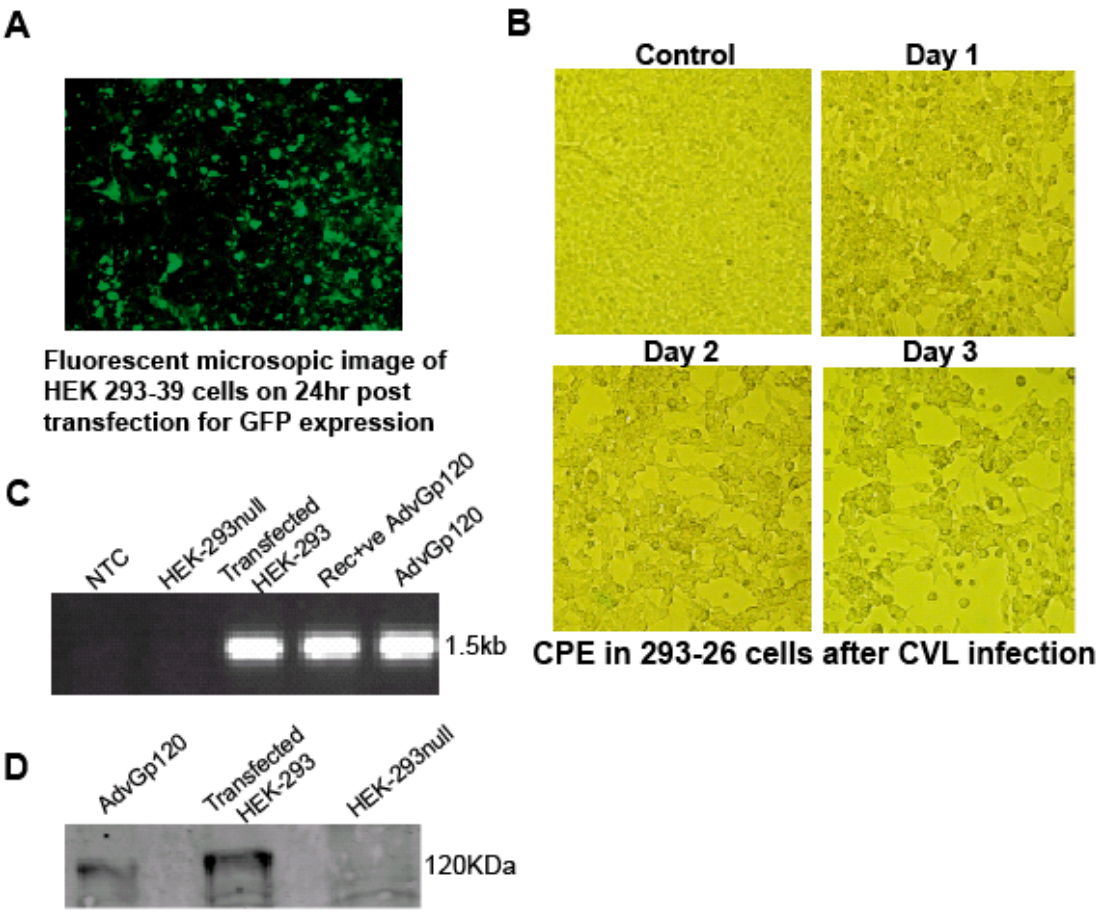

Figure 5.12 Characterization of the recombinant AdV vector. Adv_{Gp120} recombinant plasmid was generated using pShuttleCMV and pAdEasy AdV vector systems, and the virus particles were produced and amplified in HEK-293 cells. A) Transfection efficiency of the lipofectamine-2000 method in HEK-293 cells was checked using pmax-GFP as a transfection control. B) Cytopathic-effect in HEK-293 cells induced by AdV multiplication. C) PCR and D) western blot analysis for the characterization of *Gp120* insertion and Gp120 expression by the purified AdVGp120, respectively.

5.3.2 Characterization of BL6-10_{Gp120} tumor cells transfected with *A2-K^b*

A2-K^b transgenic mouse model is a well-recognized murine model used to investigate recognition of Ag epitopes in the context of HLA-A2 (177, 178). This is because A2-K^b transgenic mice contain MHC class-I molecules composed of α_1 and α_2 domains of HLA-A2, and ß-microglobulin, trans-membrane and cytoplasmic domains derived from H2-K^b mice (179-181). Many studies have shown that the α_1 and α_2 domains of MHC-I have a decisive role in MHC-I-specific $CD8^+$ T cell repertoire selection. Upon immunization, these transgenic mice develop A2-K^b-restricted CTL responses to the antigenic epitope which is also an immuno-dominent epitope in a HLA-A2-restricted environment (181). Therefore, the A2-K^b transgenic mouse model serves as an excellent model system for HLA-restricted immune response studies.

Hence, in the present study, the Gp120-aTexo vaccine immunotherapeutic effect was evaluated using a tumor protection study in A2-K^b transgenic mice. BL6-10_{Gp120} tumor cells were transfected with the *A2-K^b*. In this way, BL6-10 tumor cells were able to express Gp120 epitopes on HLA-A2 molecules as required to test the efficacy of the Gp120-aTexo vaccine in A2-K^b transgenic mice. The potential positive transfected clones were analyzed by flow cytometry where they showed HLA-A2 expression on cell surface **(Figure 5.13B).**

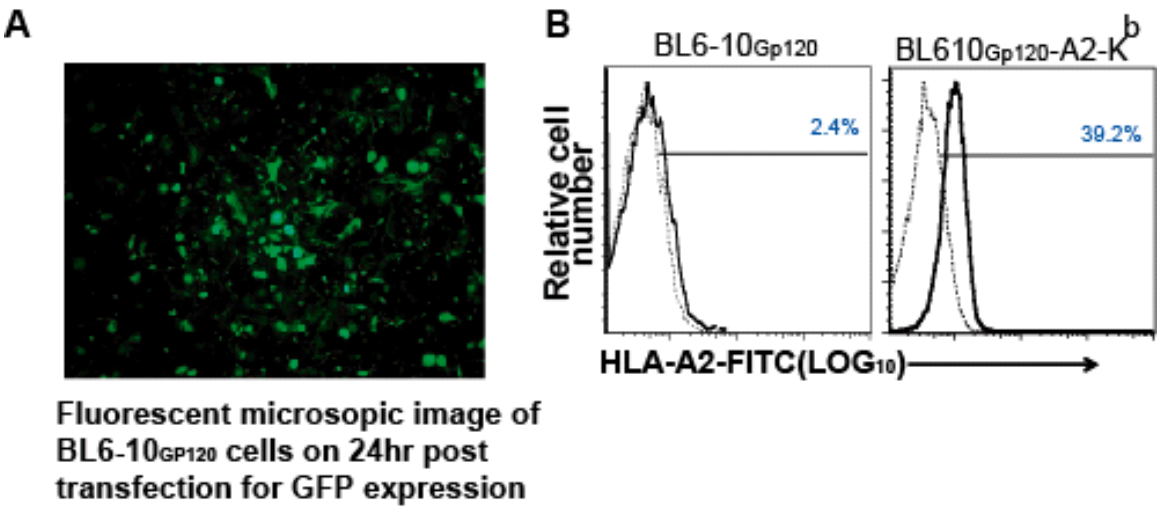

Figure 5.13 Characterization of BL6-10$_{Gp120}$ tumor cells transfected with *A2-K^b*. BL6-10$_{Gp120}$ tumor cells were transfected with pcDNA-A2-K^b vector. A) pmax-GFP-transfected BL6-10$_{Gp120}$ cells were used as transfection controls to monitor transfection efficiency. B) Clones grown under selective drug pressure were confirmed for the expression of HLA-A2 protein by flow cytometry by staining with HLA-A2 Abs (solid thick lines). An irrelevant isotype-matched Ab was used as a control (dotted thin lines). In figure, X-axis represents histograms of fluorescence intensity (log_{10}) of FITC (HLA-A2 expression) and Y-axis represents the relative number of tumor cells. A total of 5000 events were used for analysis for each marker. Data presented are from a single analysis of an independent experiment.

5.3.3 AdV_{Gp120}-transduced BMDCs and released EXOs express maturation and immune-stimulatory molecules

Adv_{Gp120} contains a RGD-modified fiber domain, which enhances AdV infection and transgene expression in BMDCs. The RGD-fiber-modified AdV shows of transgene expression in >80% BMDCs at a MOI of 150 (125). DCs transduced with AdV_{Gp120} to achieve transgene expression were termed as DC_{Gp120}. EXOs released from these cells were called EXO_{Gp120}. Mature Adv_{Gp120}-infected DCs derived from A2-K^b mice and their EXOs were characterized by flow cytometry for different surface marker expression with a panel of Abs. The results indicated that A2-K^b-derived DC_{Gp120} express both maturation and activation markers (HLA-2, Ia^b, CD11c, CD54, CD80 & CD86) **(Figure 5.14),** suggesting a potent Ag-presenting and immuno-stimulatory capacity. EXO_{Gp120} also showed the expression of maturation and activation markers, which is consistent with previous results (150, 151).

In flow cytometry analysis, DC population was gated based on FSC and SSC dot plots and used to obtain histogram fluorescence (FITC) on FL1 channel. A total of 30,000 and events of DC or EXO, respectively, were analyzed for each marker. DC_{OVA} and EXO_{OVA} were analyzed in flow cytometry every time when they were prepared (at least 3 times) to verify the quality of purification.

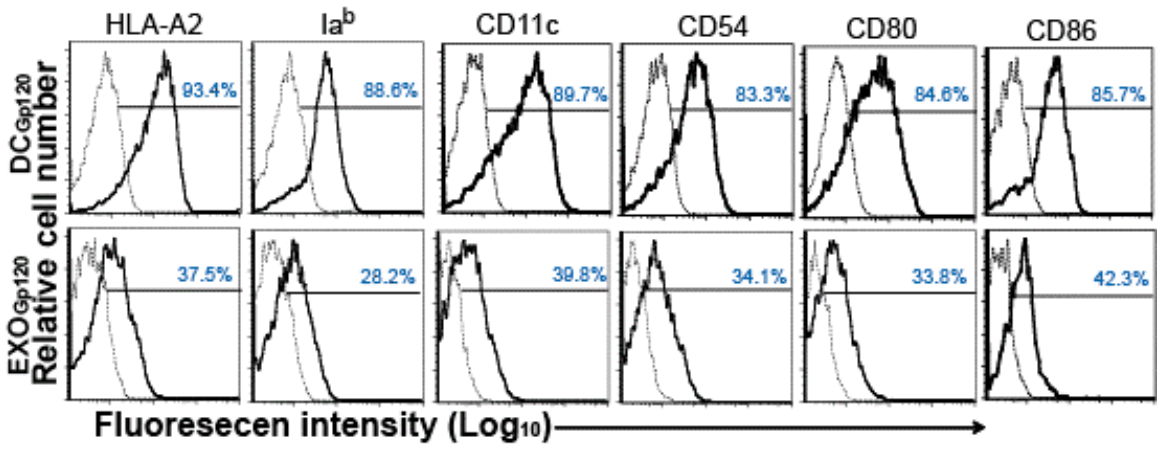

Figure 5.14 Phenotypic characterization of DC_{Gp120} and EXO_{Gp120}. Mature DC_{Gp120} or EXO_{Gp120} were stained with a panel of FITC-conjugated Abs specific for DC maturation markers, MHC class I and II molecules, and other DC-specific markers (solid thick line) with irrelevant isotype-matched Ab controls (dotted thin line), and analyzed by flow cytometry. In each figure, X-axis represents histograms of fluorescence intensity (log_{10}) of FITC (analyzed for HLA-A2, Ia^b, CD11c, CD54, CD80 and CD86 expression) and Y-axis represents the relative number of DCs or EXOs. A total of events were used for analysis for each marker. Data presented are from a single analysis of an independent experiment.

5.3.4 ConA $CD8^+$ aT cells acquire and express exosomal molecules

ConA $CD8^+$ aT cells were purified using anti-mouse $CD8^+$ paramagnetic micro-beads (Miltenyi Biotec) by positive selection, which gave >90% purity **(Figure 5.15A)**. Previously, a protocol has been established for optimal exosomal molecule acquisition by activated T cells (151). To produce Gp120-aTexo cells, $CD8^+$ aTcells were co-cultured with EXO_{Gp120} in the presence of IL-2 for 5 hr. Unstimulated $CD8^+$ T cells, $CD8^+$ aT cells and Gp120-aTexo cells were stained with a panel of Abs specific for $CD8^+$ T cell activation and DC maturation markers and analyzed by flow cytometry. The results indicate that $CD8^+$ aT cells acquired the exosomal molecules and present them on their surface **(Figure 5.15B)**. In comparison with ConA $CD8^+$ aT cells, increased CD80 molecules on Gp120-aTexo cells clearly suggest the transfer of exosomal proteins, such as immunostimulatory molecules, on to active $CD8^+$ T cells. In flow cytometric analysis, lymphocyte population was gated and used to obtain histogram of fluorescence of FITC on FL1. A total of 30,000 events of unstimulated $CD8^+$ T, $CD8^+$ aT or Gp120-aTexo were used for analysis for each marker. Gp120-aTexo cells were analyzed in flow cytometry at least 3 times, and data presented below are from a single analysis of an independent experiment.

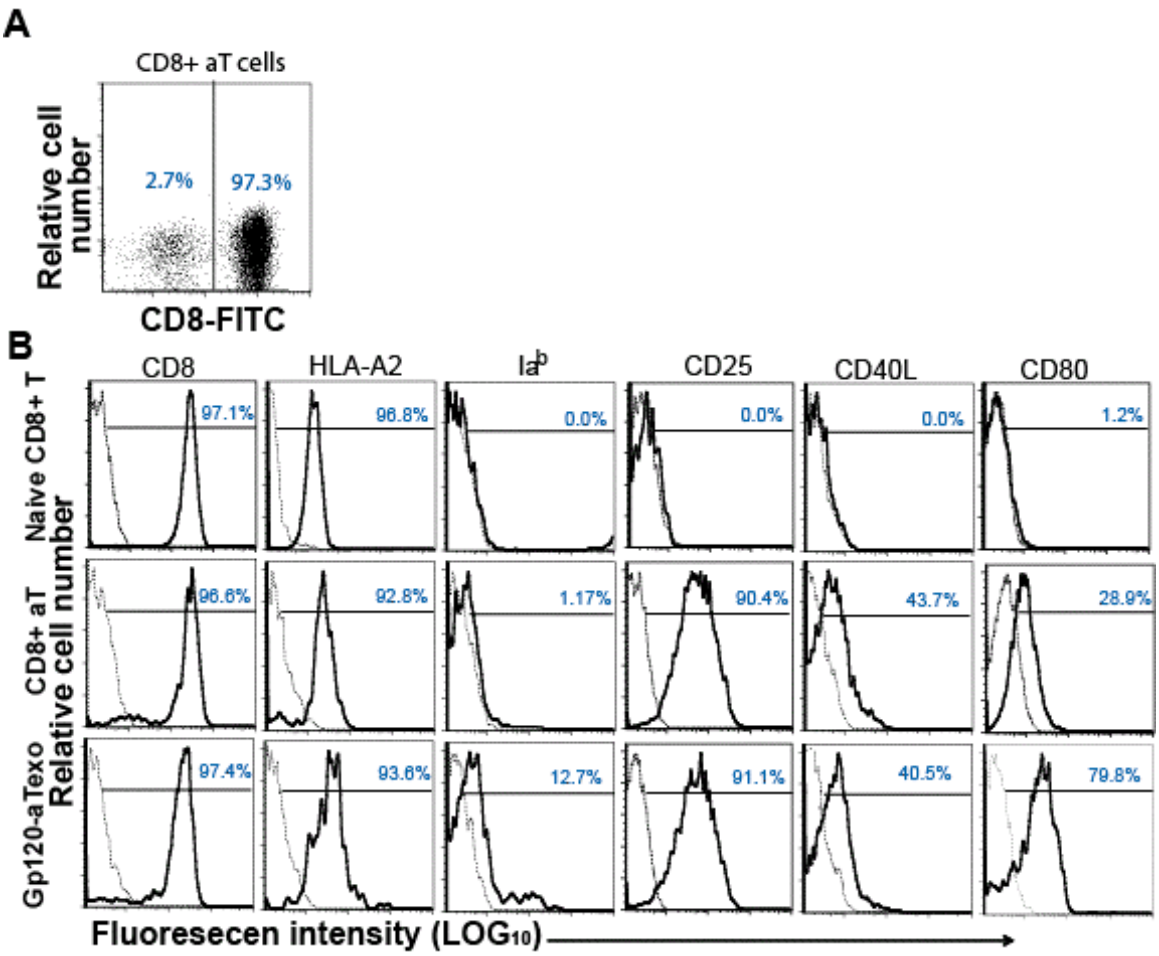

Figure 5.15 ConA CD8$^+$ aT cells up-take and express exosomal molecules. A) CD8$^+$ T cells purified from ConA-activated T cells by positive selection show >90% purity. The net percentage of labeled cells within the gated analysis region is presented in the figure. B) Naïve CD8$^+$ T, CD8$^+$ aT, and Gp120-aTexo cells were stained with a panel of Abs specific for mature DC and CD8$^+$ aT cell (solid thick lines) markers, and compared with irrelevant Ab isotype-matched controls (dotted thin lines) by flow-cytometry. In each figure, X-axis represents histograms of fluorescence intensity (log_{10}) of FITC (analyzed for CD8, HLA-A2, Ia^b, CD25, CD40L and CD80 expression) and Y-axis represents the relative number of CD8$^+$ aT or OVA-aTexo cells. A total of 30,000 events of CD8$^+$ aT or Gp120-aTexo were used for analysis for each marker. Gp120-aTexo cells were analyzed

in flow cytometry at least 3 times, and data presented above are from a single analysis of an independent experiment.

5.3.5 Gp120-aTexo vaccine stimulates proliferation of Ag-specific $CD8^+$ T cells

To assess the immuo-stimulatory effect of Gp120-aTexo vaccine in A2-K^b transgenic mice, blood samples were collected on day 6 after immunization. Blood samples were subjected to CD44 marker expression analysis and intracellular IFN-γ cytokine assay to detect vaccine-stimulated Gp120-specific $CD8^+$ T cells as described in Bolesta et al. (182). The tetramer assay was performed as described previously using PE-conjugated HLA-A2/$Gp120_{121-129}$ (KLTPLCVTL) (167, 168) reagent, which is specific for the T cell receptor of Gp120-specific $CD8^+$ T cells in A2-K^b mice.

Following immunization of A2-K^b mice with 4 X 10^6 Gp120-aTexo cells, or 2 X 10^6 DC_{GP120}, the proliferated $CD44^{high}$, $tetramer^+$ and IFN-γ^+ $CD8^+$ T cells in peripheral blood were monitored on day 6. In whole blood samples, the lymphocyte population was gated and used for the analysis by flow cytometry. A total of 0.2 X 10^6 cells (events) were used for analysis in each sample. Flow cytometry profiles are presented as dot-scatter plots. Experiment was performed twice, each of which contained 4 mice per test group. For statistical analysis, the values of both first and second experiments were used. Mean% ± 1 S.D (n=8) of $CD44^{high}$ $CD8^+$ T cells, Gp120-specific $tetramer^+$,or IFN-γ^+ $CD8^+$ T cells out of the total $CD8^+$ T cell population in DC_{OVA} or OVA-aTexo groups was indicated: ** $p<0.05$ when compared with PBS or $CD8^+$ aT-injected groups.

Gp120-aTexo- and DC_{Gp120}-immunized groups contained an average of 4.71% $\pm^1$ 0.48 and 5.85% $\pm^1$ 0.53 $CD44^+CD8^+$ cells out of total T cells, 3.55% $\pm^1$ 0.38 and 4.89% $\pm^1$ 0.41 of Gp120-specific $tetramer^+$ $CD8^+$ T cells out of total $CD8^+$ T cells, and 3.12% $\pm^1$ 0.31 and 3.77% $\pm^1$ 0.55 of IFN-γ^+ Gp120-specific $CD8^+$ T cells out of total $CD8^+$ T cells, respectively **(Figure 5.16).** These results strongly suggest that Gp120-aTexo vaccine is

capable to induce Gp120-specific $CD8^+$ T-cell proliferation *in vivo* similar to that induced by DC_{Gp120}.

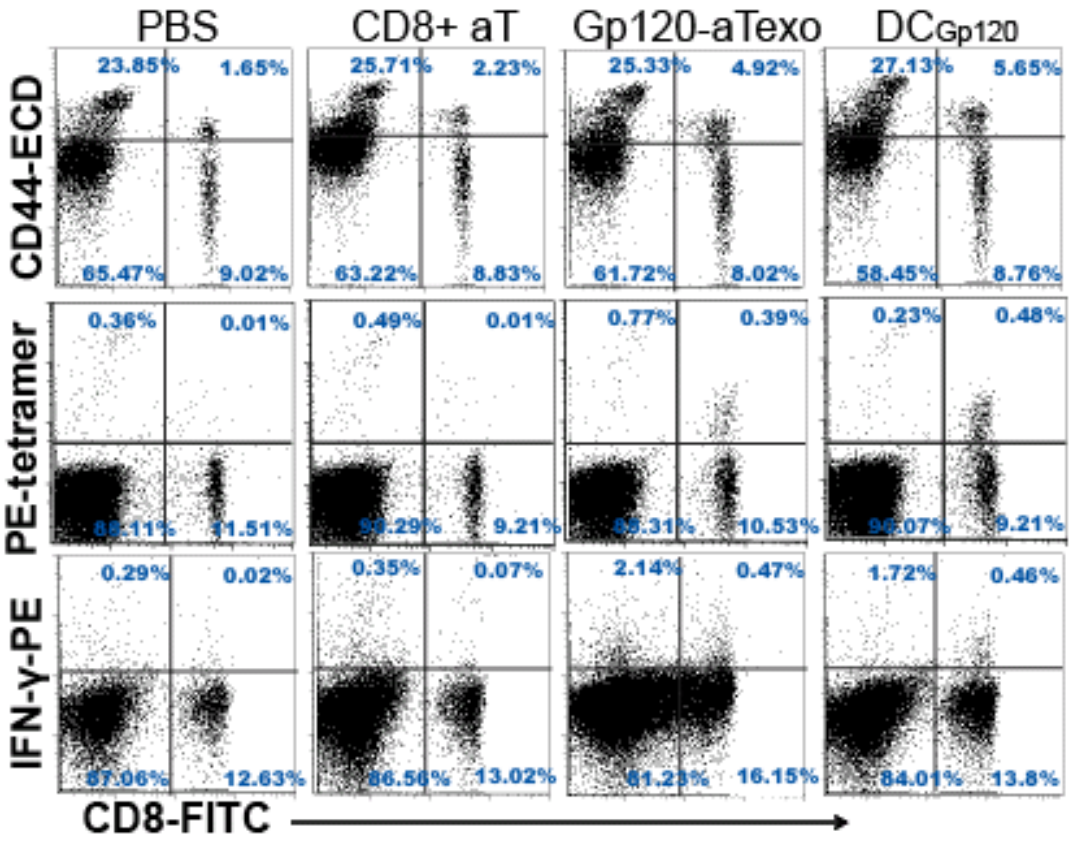

Figure 5.16 Gp120-aTexo vaccine induces efficient Ag-specific CD8$^+$ T-cell proliferation *in vivo*. A2-K^b transgenic mice were injected IV with PBS, CD8$^+$ aT, Gp120-aTexo or DC$_{Gp120}$. On day 6 post immunization, peripheral blood was collected and stained with PE-HLA-A2/Gp120$_{(121\text{-}129)}$, PE anti-CD44 or PE anti-IFN-γ, and FITC-anti-CD8$^+$ Abs, and analyzed by flow cytometry. The scatter-dot plots are derived from a representative mouse in each group on day 6 post immunization. In flow cytometric analysis, a total of 0.2 X 10^6 cells in lymphocyte-gated population were used for analysis in each sample. In each dot-scatter plot, X-axis represents fluorescence intensity of FITC (CD8 molecule expression) and Y-axis represents fluorescence intensity of PE (IFN-γ or Gp120-specific tetramer) or ECD (CD44). The net percentage of labeled cells within the gated analysis region is presented in each figure. Data presented is from a single analysis of an independent experiment.

5.3.6 Phenotypic characterization of Gp120-aTexo-stimulated $CD8^+$ effector CTLs

To further characterize the phenotype of Gp120-specific $CD8^+$ T cells, peripheral blood was collected from Gp120-aTexo- or DC_{Gp120}-immunized mice on day 7 and processed for triple staining. Ag-specific $CD8^+$ T cells in both groups immunized with Gp120-aTexo and DC_{Gp120} showed expression of activation markers such as CD44 and CD69, but not memory markers, such as CD62L, IL-7Rα and CCR-7, suggesting effector CTL phenotype **(Figure 5.17)**.

In whole blood samples, the lymphocyte population was gated based on forward and side scatter properties and used for the analysis by flow cytometry. A total of 0.5 X 10^6 cells (events) were used for analysis in each sample of primary immune response study (Results 5.3.5). To see the expression of specific markers on proliferated Gp120-specific $CD8^+$ T cells, tetramer and CD8 double positive cells were gated to obtain histogram fluroscence on FL3 (ECD). Experiment was performed twice wherein blood from different animals of each group was pooled, stained for different markers and analyzed.

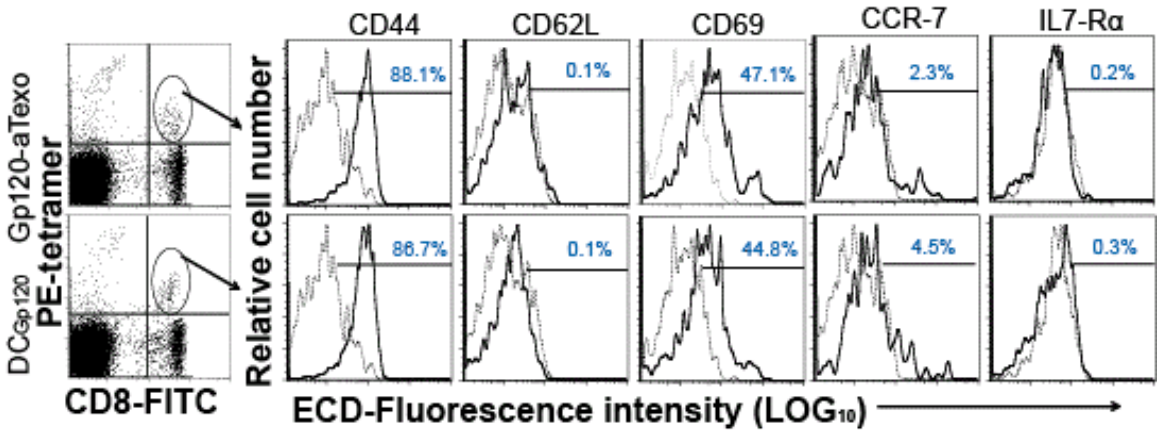

Figure 5.17 Phenotypic characterization of Gp120-specific CD8$^+$ CTLs. On day 7, peripheral blood samples from immunized mice were stained with PE-HLA-A2/Gp120$_{121\text{-}129}$ tetramer and FITC-CD8 Ab along with a panel of biotin-labeled Abs specific for effector or memory T cells markers, and streptavidin-PE-Texas Red (ECD), and then analyzed by flow cytometry. In each histogram figure, X-axis represents histograms of fluorescence intensity ($\log_{10}$) of ECD (conjugated to CD44, CD62L, CD69, CCR7, or IL-7Rα expression) and Y-axis represents the relative number of tetramer and CD8 double positive cells. Data presented are from a single analysis of an independent experiment.

5.3.7 Gp120-aTexo-stimulated effector $CD8^+$ T cells have cytotoxic activity

To further analyze effector functions of the Gp120-specific $CD8^+$ T cells, an *in vivo* cytotoxicity assay was performed in above mice (used in section 5.3.5) as described previously (164). The data is presented as mean% ± 1 S.D (n=8) of Gp120-specific $CD8^+$ T cells out of the total $CD8^+$ T cell population in DC_{GP120} or Gp120-aTexo group: ** $p<0.05$ when compared with PBS or $CD8^+$ aT-injected groups. For statistical analysis, the values of both first and second experiments with four mice per group were used. Due to an efficient cytotoxic response, significant lysis of $CFSE_{high}$-labeled target cells was observed in Gp120-aTexo and DC_{Gp120}-immunized mice **(Figure 5.18).** An average of 25% $\pm^1$ 5.6 and 20% $\pm^1$ 4.7 of residual target cells were observed in A2-K^b mice immunized with Gp120-aTexo and $DC_{Gp120,}$ respectively. On the other hand, no such cytotoxic activity was observed in PBS- or $CD8^+$ aT-injected mice.

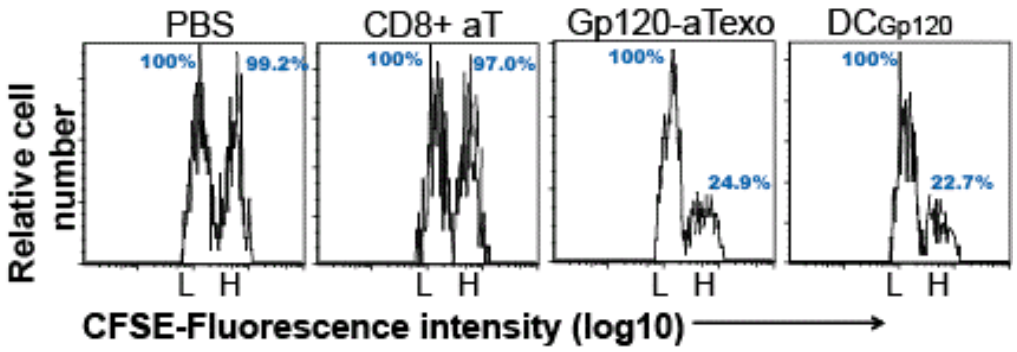

Figure 5.18 Gp120-aTexo vaccine stimulates $CD8^+$ T-cell differentiation into effector CTLs. Immunized mice were adoptively transferred on day 7 with 1:1 ratio of splenocytes labeled with high (3.0 M, $CFSE_{high}$) and low (0.6 M, $CFSE_{low}$) CFSE-pulsed with Gp120 and Mut1 peptide, respectively. After 16 hr, the residual $CFSE_{high}$ (target) and $CFSE_{low}$ (control) cells remaining in the spleens were determined in the immunized mice by flow cytometry. In each figure, X-axis represents histograms of fluorescence intensity (log_{10}) of $CFSE^{low}$ and $CFSE^{high}$ and Y-axis represents the relative number of labeled cells. An average of 1,000 labeled cells were analyzed by flow cytometry for each sample. The values in each figure represent the residual $CFSE^{high}$ and $CFSE^{low}$ cells remaining in the spleen. Data presented is from a single analysis of an independent experiment.

5.3.8 Gp120-aTexo vaccine stimulates an efficient Ag-specific memory response

In another experiment, the presence of Ag-specific memory cells was studied in Gp120-aTexo- and DC_{Gp120}-injected mice. On day 30 after immunization, peripheral blood samples from Gp120-aTexo- and DC_{Gp120}-immunized mice were analyzed using tetramer assay to determine the percentage of Gp120-specific $CD8^+$ T cells before tumor challenge. In the analysis, an average of 0.54% $\pm^1$ 0.08 and 0.81% $\pm^1$ 0.12 of tetramer-positive cells were observed in Gp120aTexo- and DC_{Gp120}-injected groups, respectively **(Figure 5.19A)**. These are T memory cells specific for Gp120 protein after immunization. To confirm whether tetramer-positive cells are memory cells, these cells were phenotypically characterized on day 30 for the expression of memory markers. The flow cytometry analyses showed the expression of memory markers, such as CD44, CD62L, CCR7 and IL-7Rα, in tetramer-positive cells **(Figure 5.19B),** suggesting that these cells are transformed long-lived T memory cells (183).

In whole blood samples, the lymphocyte population was gated and used for the analysis by flow cytometry. A total of 0.5 to 0.8 X 10^6 cells (events) were used for analysis in each sample. To see the expression of specific markers on proliferated Gp120-specific $CD8^+$ T cells, tetramer and CD8 double positive cells were gated to obtain histogram fluroscence on FL3 (ECD). Experiment was performed twice wherein blood from different animals of each group were pooled, stained for different markers and analyzed.

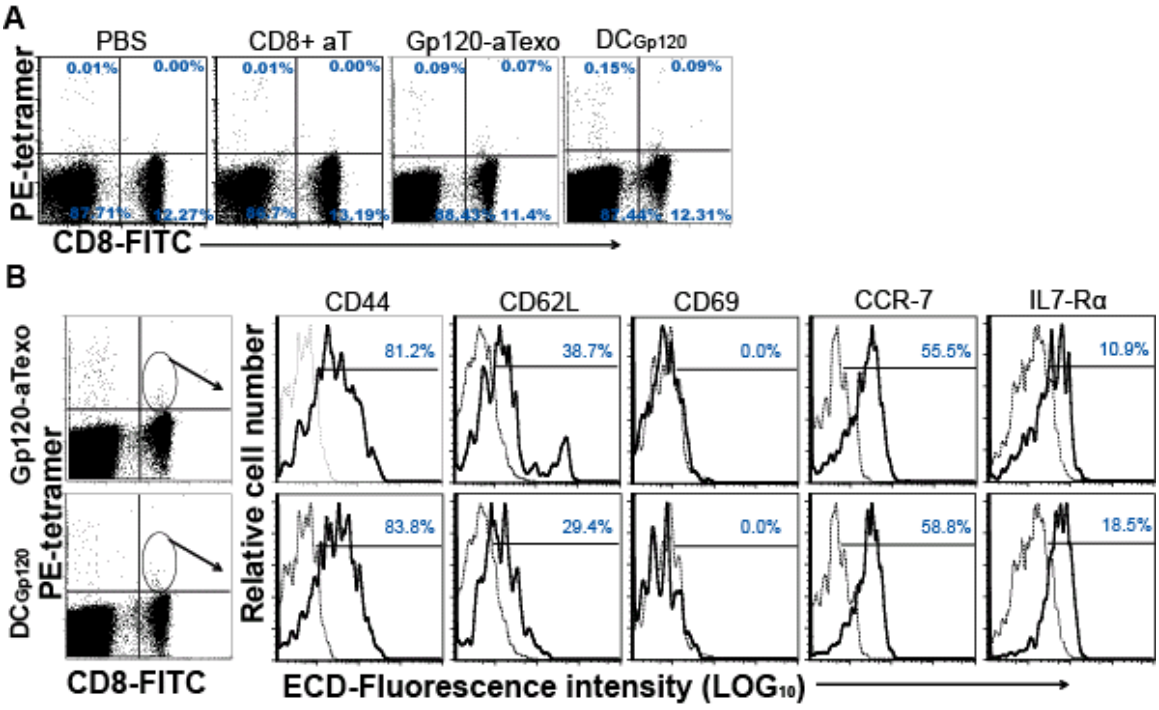

Figure 5.19 Phenotypic characterization of Ag-specific memory T cells. A) On day 30 after Gp120-aTexo or DC_{Gp120} injection, blood samples were collected and stained with PE-HLA-A2/$Gp120_{121-129}$ tetramer and FITC-CD8 Ab. The scatter-dot plots are derived from a representative mouse in each group on day 6 post-immunization. In flow cytometric analysis, a total of 0.5 to 0.8 X 10^6 cells in lymphocyte-gated population were used for analysis in each sample. In each dot-scatter plot, X-axis represents fluorescence intensity of FITC (CD8 molecule expression) and Y-axis represents fluorescence intensity of PE (Gp120-specific tetramer). The net percentage of labeled cells within the gated analysis region is presented in each figure. Data presented is from a single analysis of an independent experiment. B) Phenotypically characterized tetramer and CD8 double positive cells using a panel of biotin-labeled Abs specific for effector or memory markers, and streptavidin-PE-Texas Red (ECD) (solid thick lines). Tetramer and CD8 double positive cells stained with irrelevant isotype-matched Abs were used as controls

(dotted thin lines). In each figure, X-axis represents histograms of fluorescence intensity (log_{10}) of ECD (analyzed for CD44, CD62L, CD69, CCR7, and IL-7Rα expression) and Y-axis represents the relative number of tetramer and CD8 double positive cells. Data presented are from a single analysis of an independent experiment.

5.3.9 Gp120-aTexo vaccine induces efficient short- and long-term anti-tumor immunity

The efficacy of Gp120-aTexo vaccine in inducing functional effector and memory $CD8^+$ CTLs was studied using a tumor protection approach. A2-K^b mice were injected IV with DC_{Gp120}, Gp120-aTexo vaccine, $CD8^+$ aT cells or PBS, and challenged with BL6-10_{Gp120}/A2-K^b tumor cells on day 6 after immunization in experiment I, and on day 30 after immunization in experiment II **(Table 5.3)**. Before tumor challenge, BL6-10_{Gp120}/A2-K^b cell were cultured overnight in the presence of IFN-γ to enhance pMHC-I expression. All mice were sacrificed on day 24 after tumor challenge, and the lungs were observed for the black tumor colonies.

In both experiment-I and –II, results showed that the mice which received Gp120-aTexo or $DC2.4_{Gp120}$ cells were completely protected with no tumor colonies development for 24 days from tumor challenge, whereas PBS- or $CD8^+$ aT-injected mice showed development of black-pigmented tumor colonies in their lungs **(Figure 5.20; Table 5.3),** suggesting Gp120-aTexo vaccine can stimulate $CD8^+$ CTL responses capable of inducing anti-tumor immunity both during effector and memory stage. Experiment was performed twice each with 8 mice per group. After immunization, 4 mice in each group were used for the effector-stage anti-tumor immunity study, whereas another 4 mice were used for the memory-stage anti-tumor immunity.

Table 5.3 Gp120-aTexo vaccine protects A2-K^b mice against lung tumor metastases during effector and memory stage

Immunization	Tumor challenge	Visible tumor growth incidence	Median number of lung tumor colonies
Exp. I.			
Gp120-aTexo	BL6-10$_{Gp120}$/A2-K^b	0/8 (0)[a]	0
DC$_{Gp120}$	BL6-10$_{Gp120}$/A2-K^b	0/8 (0) [a]	0
CD8$^+$ aT	BL6-10$_{Gp120}$/A2-K^b	8/8 (100)[b]	>100
PBS	BL6-10$_{Gp120}$/A2-K^b	8/8 (100) [b]	>100
Exp. II			
Gp120-aTexo	BL6-10$_{Gp120}$/A2-K^b	0/8 (0) [a]	0
DC$_{Gp120}$	BL6-10$_{Gp120}$/A2-K^b	0/8 (0) [a]	0
CD8$^+$ aT	BL6-10$_{Gp120}$/A2-K^b	8/8 (100)[b]	>100
PBS	BL6-10$_{Gp120}$/A2-K^b	8/8 (100)[b]	>100

[a]: Immunized group, [b]: control group

A2-K^b mice were injected IV with DC$_{Gp120}$, Gp120-aTexo vaccine, CD8$^+$ aT cells or PBS, and challenged with BL6-10$_{Gp120}$/A2-K^b tumor cells on day 6 post-immunization in experiment I, and on day 30 post-immunization in experiment II. All mice were sacrificed on day 24 after tumor challenge, and the lungs were examined for the number of black tumor colonies. Values in the table are cumulative of two independent experiments with four mice per group.

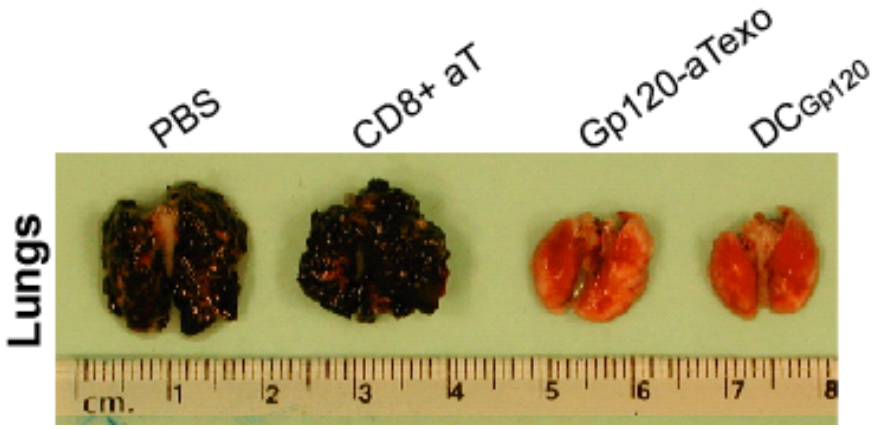

Figure 5.20 Gp120-aTexo vaccine induces both effector and memory anti-tumor immunity. Gp120-aTexo, $DC_{Gp120,}$ $CD8^+$ aT or PBS were injected IV into A2-K^b mice. The mice were later challenged with BL6-10_{Gp120}/A2-K^b tumor cells. The Gp120-aTexo- and DC_{Gp120}-immunized groups showed complete protection against lung tumor colonies formation. Lungs from one mouse/group in one of two independent experiments are shown.

PART D

5.4 Gp120-aTexo vaccine possesses a therapeutic effect when injected 3- or 6-day post challenge on the establishments of lung tumors in A2-K^b transgenic mice

This study examined the therapeutic efficacy of Gp120-aTexo vaccine in A2-K^b transgenic mouse model by employing a tumor challenge study (BL6-10_{Gp120}/A2-K^b). A2-K^b mice were challenged with BL6-10_{Gp120}/A2-K^b melanoma tumor cells, and immunized with Gp120-aTexo cells on 3 or 6 days after tumor challenge as presented in the **Table 5.4**. All mice were sacrificed on day 24 after tumor challenge, and the lungs were examined for the number of black-pigmented tumor colonies.

In the results, 100% (8/8) and 75% (2/8) of Gp120-aTexo-injection A2-K^b mice were protected from lung tumor metastases in experiment I and II, respectively. Mice injected with PBS showed 0% protection in both experiments **(Table 5.4).** These results indicate that Gp120-aTexo vaccine has the potential to eradicate tumor cells early after their engraftment, suggesting a possible therapeutic effect for the vaccine. Experiment was performed twice each with 8 mice per group. After tumor challenge, 4 mice in each group were used for immunization on day 3, whereas another 4 mice were used for immunization on day 6.

.

Table 5.4 Therapeutic efficacy of Gp120-aTexo vaccine in a melanoma tumor model

Animal groups	Tumor challenge	Injection IV	Tumor growth	Median number of
Exp. I. (Day -3)				
Test group	BL6-10_{Gp120}/ A2-K^b	Gp120-aTexo[a]	0% (0/8)	0
Control group	BL6-10_{Gp120}/ A2-K^b	PBS[b]	100% (8/8)	>100
Exp. II (Day -6)				
Test group	BL6-10_{Gp120}/A2-K^b	Gp120-aTexo[a]	25% (2/8)	19±6
Control group	BL6-10_{Gp120}/ A2-K^b	PBS[b]	100% (8/8)	>100

[a]: Immunized group, [b]: control group

In experiment-I and -II, mice were immunized with Gp120-aTexo vaccine 3 or 6 days after tumor challenge, respectively. Mice were sacrificed 24 days after tumor challenge and the number of lung tumor colonies was determined. Values in the table are cumulative of two independent experiments with four mice per group.

CHAPTER 6

DISCUSSION

Immuno-suppression is a hallmark of HIV-1 infection. Continuous replication of HIV-1 in $CD4^+$ T cells leads to the depletion of the $CD4^+$ T cell population in the body. DCs are also targets for this virus since the virus infects DCs through C-type lectin and DC-SIGN receptors gradually rendering these cells dysfunctional or tolerogenic. Continuous exposure of DCs to HIV-1 envelope proteins, particularly to Gp120, leads to the incomplete activation of DC. These incompletely activated DCs secrete more IFNs and indoleamine 2,3 dioxygenase, but less IL-12 (59, 60). Due to less DC-derived IL-12, $CD4^+$ T cells are not stimulated, resulting in a CD4-derived IL-2 signal deficiency. As a result, HIV-1-specific $CD8^+$ CTL activation and differentiation occurs less efficiently. Consequent to these negative effects, the affected individual's immune system becomes susceptible to many opportunistic diseases.

Currently available HIV-1 vaccines such as killed, attenuated or subunit, were failed to induce a therapeutic immune response to HIV-1. Live attenuated HIV-1 vaccines have been shown to revert to their pathogenic forms (95, 96). Inactivated HIV-1 vaccines fail to induce effective immune responses in primates, perhaps due to the of $CD4^+$ T cell deficiency (98).

In search of a novel therapeutic vaccine designed to stimulate immune cells compromised by HIV infection and in view of the limitations of existing therapeutic vaccine strategies, this study developed a T cell-based $CD8^+$aTexo vaccine. The $CD8^+$aTexo vaccine stimulates the immune response through acquired Ag-presenting molecules and co-stimulatory molecules (in a $CD4^+$ T cell-independent manner). The

$CD8^+$aTexo vaccine was assessed for its preventive and therapeutic efficacy in both wild type (C57BL/6) and humanized (A2-K^b) mouse models using a melanoma challenge model.

In this study, the DC2.4 cell line (184) was used as a substitute for BMDC since it is cost effective and time saving. Using this cell line reduces the costs associated with the use of cytokines, such as GM-CSF, IL-4 and TNF-α, and the time needed for generating mature BMDC, which generally takes 7 days. The DC2.4 cell line (immature status) does not express maturation markers; therefore, the maturation of this cell line was induced by culturing with IFN-γ. IFN-γ is known to up-regulate the expression of class-I and -II MHC, CD40, CD80 and CCR7 in this cell line (184).

To generate Gp120-aTexo several components were created and are detailed in the Results Section. DC cell line (DC2.4) and B16 melanoma cell line (BL6-10) were transfected with *Gp120* to generate $DC2.4_{Gp120}$ and $BL6\text{-}10_{Gp120}$, respectively. EXO-targeted T cell vaccines (OVA-aTexo or Gp120-aTexo) were prepared by incubating ConA $CD8^+$ aT cells with EXO_{OVA} or EXO_{Gp120}. Immunization of wild-type mice with OVA-aTexo resulted in the induction of OVA-specific $CD8^+$ T cell effector and memory responses. Gp120-aTexo vaccine was also able to provide both preventive and therapeutic efficacy against Gp120-expressing BL610 melanoma challenge in wild-type mice.

DC-derived exosomes appear to be the key factor behind the stimulatory power of the aTexo vaccine. EXOs may mediate the immune response *in vivo* by either or both of two potential pathways: a) up-take of EXO by immature DC; and b) up-take of EXO by activated T cells. These EXO molecule up-take pathways might stimulate $CD8^+$ T cell

responses (185). DC-secreted EXOs express Ag-presenting molecules and co-stimulatory molecules (156, 157) and in association with immune cell types, especially DCs and activated T cells, they stimulated effector and memory CTL responses capable of protecting host against tumor challenge (149, 186, 187). In a murine model, when tumor-derived EXOs expressing tumor-specific peptides on MHC-I molecules were loaded onto mature DCs and injected into mice, strong $CD8^+$ CTL responses leading to regression of tumor growth were observed (138). Recently, in one human clinical trial, EXOs purified from the ascites fluid of cancer patients were loaded on to mature DCs and reintroduced to the patients, resulting in regression of tumors in skin and lymph nodes (148).

Previously, Hoa et al. (150) demonstrated that a $CD4^+$aTexo vaccine was able to stimulate OVA-specific $CD8^+$ CTL responses and elicit antitumor immunity more efficiently as compared to EXO_{OVA} or DC_{OVA} alone (150). Furthermore, it was shown that such a stimulatory function is mediated through secretion of IL-2, CD40L and CD80 signaling, and acquired pMHC-I molecules (188). In support of this, $CD4^+$ T cells acquiring pMHC-I and CD80 and CD86 co-stimulatory molecules from DCs, in the process of DC Ag-presentation and stimulation of T cells, have been shown to induce Ag-specific T cell responses by up-regulating NF-kB and Stat5 signaling molecules (189). Perhaps due to these reasons, $CD4^+$aTexo vaccine induces OVA-specific $CD8^+$ T cell responses independent of $CD4^+$ T cell help (150, 165). T regulatory cells are a subpopulation of T cells which induce immuno-suppression or tolerance by suppressing immune activation to self Ags (190, 191). Interestingly, the $CD4^+$aTexo vaccine stimulated $CD8^+$ central memory CTL responses in the presence of $CD25^+$ T regulatory

cells (151), indicating this vaccine can break T regulatory cell-mediated immune tolerance.

In line with previous results, this thesis demonstrates that non-specific ConA $CD8^+$ aT cells can also take up DC_{OVA}-released EXOs and express exosomal derived immunologically important molecules (Ag-presenting machinery and co-stimulatory molecules) on their surfaces, leading to development of the OVA-aTexo vaccine (138). In support of my hypothesis, the OVA-aTexo vaccine was able to induce both short- and long-term Ag-specific $CD8^+$ T cell responses and anti-tumor immunity independent of host DC and $CD4^+$ T cell help (192). Furthermore, the present study demonstrated that the stimulatory power of OVA-aTexo vaccine was mainly mediated through acquired pMHC-I complexes, which might interact with Ag-specific naive $CD8^+$ T cell receptor (signal-1), CD40L co-stimulation (signal-2) and IL-2 cytokine signal (signal-3), which is known to provide survival signals or act as growth factor for the expansion of $CD8^+$ aT cells (150). From these results, it appears both $CD4^+$aTexo and $CD8^+$aTexo vaccines follow similar mechanisms to induce efficient $CD8^+$ T cell responses.

Macaque monkeys with SIV infection are considered to be an excellent non-human primate model for HIV-1 pathogenesis study. Both HIV and SIV are closely related at the molecular level, in pathology and viral replication. However, several limitations are associated with the SIV model, such as cost, accredited primate facilities and differences in the rate of disease progression. Mouse models were proposed for studying HIV infection and vaccine studies, as these are more appealing for many reasons, including low cost, quick reproduction, and easy manipulation and handling. HIV-1 is normally non-infectious for mice (193). Therefore, murine models for HIV-1 infection involve

mice reconstituted with a human immune system either partially or in whole. In the second part of this thesis research, AdV_{Gp120}-infected DCs were used to generate $EXO_{Gp120.}$ These EXO_{Gp120} were then co-cultured with spleen-derived ConA $CD8^+$ aT cells to prepare a Gp120-aTexo vaccine. Vaccine efficacy was tested in A2-K^b transgenic humanized mice, which express α1 and α2 domains of HLA-A2 (forms antigenic peptide binding cleft of human class-I MHC). These A2-K^b mice allow studies of adaptive cellular immunity (Class I Ag presentation and $CD8^+$ CTL responses) in the context of a human Ag presentation (194). In addition, the tetramer reagent is available for quantifying Gp120-specific $CD8^+$ CTLs in HLA-A2 background; therefore, the number of $CD8^+$ CTLs can be easily assessed after immunization of A2-K^b mice. It has been shown that the Gp120-specific $CD8^+$ T cells in A2-K^b mice are similar to those found in humans in terms of their epitope specificity (195).

Several factors could explain this stimulatory power of the Gp120-aTexo vaccine. AdVs are known to provide the strong toll like receptor signaling required for maturation of DC and expression of co-stimulatory molecules (134, 165). Previously, Rea et al. and Hirschowitz et al. (196, 197) showed that AdV infection of DCs activates and increases the expression of maturation markers (MHC class-II, CD54) and co-stimulatory molecules (CD40, CD80, CD86). Similarly, Miller et al. (198) reported that AdV infection of DCs up-regulated the expression of immuno-stimulatory molecules compared to immature DCs. It was also demonstrated that AdV induces maturation of DCs via P13-kinase and involved TNF-α mediated signaling pathways of NF-kB activation (199, 200). This evidence together suggests AdV-stimulated DCs express higher levels of maturation and co-stimulatory molecules, and secreted EXOs expressing increased levels of Ag-

presenting machinery. In the preparation of Gp120-aTexo vaccine, high concentration of EXOs was used (10 μg EXO/1 X 10^6 $CD8^+$ aT cells). This high concentration might result in the increased expression of Ag-presenting molecules on $CD8^+$ aT cells. Thus, the increased levels of Ag-presenting molecules on Gp120-aTexo cells might have contributed to the increased $CD8^+$ CTL responses after immunization.

Many studies have shown that administration of activated T cells can result in immuno-regulatory effects. Hong et al. (201) reported immuno-suppression after injection of irradiated T cells in patients with multiple sclerosis. Kishimoto et al. (202) showed suppression of experimental autoimmune disease in mice when they were injected with myelin-basic-protein-reactive autologous T cells. Two other important studies by Hao et al. (150, 151) contradicted, these T cell-related immuno-regulatory effects. These studies showed that $CD4^+$ aT cells, which acquired OVA-specific EXO induce Ag-specific immune responses. My thesis research also showed in two different animal models, that Gp120-aTexo vaccine can stimulate efficient immune responses to Gp120-HIV-1-specific protein. The discrepancy in the results of these studies could be due to the nature of the T cells and the immunogen used for vaccine preparation. It has been confirmed that irradiation induces considerable apoptosis of T cells, and the apoptotic bodies have been shown to induce immuno-suppression by activating T regulatory cells. On the other hand, in the present study, IL-2-secreting ConA $CD8^+$ aT cells and EXOs as immunogen were used in the vaccine preparation. The peptide form of Gp120 in the EXOs appeared to be safer than using whole Gp120, which has shown to have inhibitory effects on T cells, B cells and DCs function. Indeed, previously CD4-independent functional $CD8^+$ T cell responses were observed when an AdV-encoded

lymphocytic choriomeningitis virus-derived epitope was used rather than full-length protein to induce immune responses (203). Similarly, another study also showed the generation of $CD8^+$ CTL responses to tumor in the absence of $CD4^+$ T cells help by using a high-concentration of peptide-pulsed DCs for immunization (204). These studies could explain why aTexo vaccines induce CD4-independent CTL responses.

Many studies have already demonstrated the pivotal role of $CD8^+$ T cells in controlling established HIV-1 infection. Schmitz et al. (82) demonstrated the importance of $CD8^+$ T cells in controlling SIV infection in macaque monkeys. When $CD8^+$ T cells were depleted in chronically SIV-infected macaque monkeys, the viral burden increased. Reconstitution of $CD8^+$ T cells, which reappear later in the lymph nodes and peripheral blood, led to a decline in the viral load suggesting the importance of $CD8^+$ T cells in halting viral replication. A study on HIV-1 patients also suggested that $CD8^+$ T cell responses can reduce viral load in plasma for more than 20 years without HAART therapy (46). These studies emphasize the importance of therapeutic vaccines in the control of HIV-1 infection since these vaccines may delay patients' anti-retroviral therapy. Gp120-aTexo vaccine effectively eradicated the early- and late established lung tumor colonies in A2-K^b mice, suggesting its therapeutic utility. Chronic diseases such as HIV and cancers follow similar immunological responses. For instance, both of these disease types are known to induce immuno-suppression and T cell exhaustion. Hence, Gp120-aTexo vaccine could efficiently induce CTL responses even in chronic diseases such as HIV in the presence of tolerance and the absence of $CD4^+$ T cells.

Anti-retroviral drugs reduce HIV-1-related morbidity and mortality. Indeed, HAART preserves HIV-1-specific $CD4^+$ T cells by controlling HIV replication in the

early period of the treatment (205). However, this treatment has adverse effects on patients' health, which reduces their life quality (206). Previously, several therapeutic vaccines used on patients under HAART therapy have shown to decrease the dose of the drug administration and prolonged their lives (207, 208). Based on these results, it is possible that Gp120-aTexo vaccine can act as an excellent adjunct to HAART therapy, especially during established infections. Current and previous evidence on aTexo vaccine studies suggest Gp120-aTexo vaccine might induce $CD8^+$ T cell responses in HIV patients without $CD4^+$ T cells and DCs help. Therefore, Gp120-aTexo vaccine could be useful at any stage of the infection.

It is clearly understood that development of a protective vaccine, which induces neutralizing Ab production, is difficult during HIV-1 infection. Consequently, newer approaches that induce T cell responses are being evaluated or are under development. The rationale is that the cellular immune response can control HIV-1 replication through destruction of infected host cells thereby controlling disease progression. Collectively, although further in depth study and characterization is required to consider their use in humans, the present results suggest that the Gp120-aTexo vaccine may be an attractive candidate for the treatment of HIV-1 patients who suffer from $CD4^+$ T cell deficiency.

CHAPTER 7

FUTURE DIRECTIONS

The development of efficient HIV-1 therapeutic vaccines is partly hindered by the lack of suitable animal models to test vaccine efficacy. It has been already shown that the $Rag2^{-/-}\gamma C^{-/-}$ double knockout model, which lacks B cells and NK cells (209, 210), is an excellent model for testing the immunotherapeutic effect of HIV vaccines (211, 212). The low dose irradiation (400 cGy) of newborn $Rag2^{-/-}\gamma C^{-/-}$ DKO mice can enhance human-transgraft survival (213). Therefore, these mice can be reconstituted with human cord ($CD34^{+}$) blood-derived hematopoietic stem cells (hHSC), which ultimately leads to the development of human B cells, T cells, monocytes, macrophage, and different DC subtypes (214). These cells together develop structures like lymphoid follicles in lymph nodes. $CD4^{+}$ T cells present in the blood, spleen and bone marrow express both CCR5 and CXCR4 chemokine receptors, which help to maintain viremia for longer period after introduction of HIV-1 infection. HIV-1 infection in $Rag2^{-/-}\gamma C^{-/-}$ DKO mice appears to follow a similar pathogenesis as in human patients.

Gp120-aTexo vaccine can be further characterized efficiently in this model, where these DKO-hHSC-HIV mice produce active HIV-1 replication and virus-specific immune responses. These mice will be vaccinated with Gp120-aTexo prepared from A2-K^{b-} derived $CD8^{+}$ T cells to assess Gp120-specific effector and memory $CD8^{+}$ T cell responses. Furthermore, the clearance of HIV-1 in the sera and different organs can be determined.

Hepatitis C virus primarily causes liver infection. The chronic infection by this virus is associated with T-cell dysfunction. Currently, antiviral drugs are being used to

control hepatitis C virus disease progression. However, this therapy causes significant reduction in $CD4^+$ T cell counts (210). Immunization of hepatitis C virus-specific $CD8^+$aTexo vaccine in infected individuals' could induce virus specific immune responses independent of $CD4^+$ T cell but through acquired exosomal molecules. Hence, $CD8^+$aTexo vaccine may be used in adjunction with antiviral therapy to induce hepatitis C virus-specific $CD8^+$ CTL responses to control virus replication or disease progression.

CHAPTER 8

REFERENCES

1. Vidal, N., M. Peeters, C. Mulanga-Kabeya, N. Nzilambi, D. Robertson, W. Ilunga, H. Sema, K. Tshimanga, B. Bongo, and E. Delaporte. 2000. Unprecedented degree of human immunodeficiency virus type 1 (HIV-1) group M genetic diversity in the Democratic Republic of Congo suggests that the HIV-1 pandemic originated in Central Africa. J Virol 74:10498-10507.
2. Barre-Sinoussi, F., J. C. Chermann, F. Rey, M. T. Nugeyre, S. Chamaret, J. Gruest, C. Dauguet, C. Axler-Blin, F. Vezinet-Brun, C. Rouzioux, W. Rozenbaum, and L. Montagnier. 1983. Isolation of a T-lymphotropic retrovirus from a patient at risk for acquired immune deficiency syndrome (AIDS). Science 220:868-871.
3. Tindall, B., L. Evans, P. Cunningham, P. McQueen, L. Hurren, E. Vasak, J. Mooney, and D. A. Cooper. 1992. Identification of HIV-1 in semen following primary HIV-1 infection. AIDS 6:949-952.
4. Mens, H., M. Kearney, A. Wiegand, W. Shao, K. Schonning, J. Gerstoft, N. Obel, F. Maldarelli, J. W. Mellors, T. Benfield, and J. M. Coffin. HIV-1 continues to replicate and evolve in patients with natural control of HIV infection. J Virol 84:12971-12981.
5. Dalgleish, A. G., P. C. Beverley, P. R. Clapham, D. H. Crawford, M. F. Greaves, and R. A. Weiss. 1984. The CD4 (T4) antigen is an essential component of the receptor for the AIDS retrovirus. Nature 312:763-767.
6. Knight, S. C., S. E. Macatonia, and S. Patterson. 1990. HIV I infection of dendritic cells. Int Rev Immunol 6:163-175.
7. Palella, F. J., Jr., K. M. Delaney, A. C. Moorman, M. O. Loveless, J. Fuhrer, G. A. Satten, D. J. Aschman, and S. D. Holmberg. 1998. Declining morbidity and mortality among patients with advanced human immunodeficiency virus infection. HIV Outpatient Study Investigators. N Engl J Med 338:853-860.
8. Malhotra, U., M. M. Berrey, Y. Huang, J. Markee, D. J. Brown, S. Ap, L. Musey, T. Schacker, L. Corey, and M. J. McElrath. 2000. Effect of combination antiretroviral therapy on T-cell immunity in acute human immunodeficiency virus type 1 infection. J Infect Dis 181:121-131.
9. Oxenius, A., D. A. Price, P. J. Easterbrook, C. A. O'Callaghan, A. D. Kelleher, J. A. Whelan, G. Sontag, A. K. Sewell, and R. E. Phillips. 2000. Early highly active antiretroviral therapy for acute HIV-1 infection preserves immune function of CD8+ and CD4+ T lymphocytes. Proc Natl Acad Sci U S A 97:3382-3387.
10. Harshyne, L. A., S. C. Watkins, A. Gambotto, and S. M. Barratt-Boyes. 2001. Dendritic cells acquire antigens from live cells for cross-presentation to CTL. J Immunol 166:3717-3723.
11. Briggs, J. A., T. Wilk, R. Welker, H. G. Krausslich, and S. D. Fuller. 2003. Structural organization of authentic, mature HIV-1 virions and cores. EMBO J 22:1707-1715.

12. Ratner, L., W. Haseltine, R. Patarca, K. J. Livak, B. Starcich, S. F. Josephs, E. R. Doran, J. A. Rafalski, E. A. Whitehorn, K. Baumeister, and et al. 1985. Complete nucleotide sequence of the AIDS virus, HTLV-III. Nature 313:277-284.
13. Jouvenet, N., S. M. Simon, and P. D. Bieniasz. 2009. Imaging the interaction of HIV-1 genomes and Gag during assembly of individual viral particles. Proc Natl Acad Sci U S A 106:19114-19119.
14. Dowbenko, D., G. Nakamura, C. Fennie, C. Shimasaki, L. Riddle, R. Harris, T. Gregory, and L. Lasky. 1988. Epitope mapping of the human immunodeficiency virus type 1 gp120 with monoclonal antibodies. J Virol 62:4703-4711.
15. Dayton, A. I., J. G. Sodroski, C. A. Rosen, W. C. Goh, and W. A. Haseltine. 1986. The trans-activator gene of the human T cell lymphotropic virus type III is required for replication. Cell 44:941-947.
16. Stevceva, L., V. Yoon, D. Anastasiades, and M. C. Poznansky. 2007. Immune responses to HIV Gp120 that facilitate viral escape. Curr HIV Res 5:47-54.
17. Farzan, M., H. Choe, E. Desjardins, Y. Sun, J. Kuhn, J. Cao, D. Archambault, P. Kolchinsky, M. Koch, R. Wyatt, and J. Sodroski. 1998. Stabilization of human immunodeficiency virus type 1 envelope glycoprotein trimers by disulfide bonds introduced into the gp41 glycoprotein ectodomain. J Virol 72:7620-7625.
18. Allan, J. S., J. E. Coligan, F. Barin, M. F. McLane, J. G. Sodroski, C. A. Rosen, W. A. Haseltine, T. H. Lee, and M. Essex. 1985. Major glycoprotein antigens that induce antibodies in AIDS patients are encoded by HTLV-III. Science 228:1091-1094.
19. Robey, W. G., B. Safai, S. Oroszlan, L. O. Arthur, M. A. Gonda, R. C. Gallo, and P. J. Fischinger. 1985. Characterization of envelope and core structural gene products of HTLV-III with sera from AIDS patients. Science 228:593-595.
20. Wu, L., N. P. Gerard, R. Wyatt, H. Choe, C. Parolin, N. Ruffing, A. Borsetti, A. A. Cardoso, E. Desjardin, W. Newman, C. Gerard, and J. Sodroski. 1996. CD4-induced interaction of primary HIV-1 gp120 glycoproteins with the chemokine receptor CCR-5. Nature 384:179-183.
21. Doranz, B. J., J. Rucker, Y. Yi, R. J. Smyth, M. Samson, S. C. Peiper, M. Parmentier, R. G. Collman, and R. W. Doms. 1996. A dual-tropic primary HIV-1 isolate that uses fusin and the beta-chemokine receptors CKR-5, CKR-3, and CKR-2b as fusion cofactors. Cell 85:1149-1158.
22. Alkhatib, G., C. Combadiere, C. C. Broder, Y. Feng, P. E. Kennedy, P. M. Murphy, and E. A. Berger. 1996. CC CKR5: a RANTES, MIP-1alpha, MIP-1beta receptor as a fusion cofactor for macrophage-tropic HIV-1. Science 272:1955-1958.
23. Preston, B. D., B. J. Poiesz, and L. A. Loeb. 1988. Fidelity of HIV-1 reverse transcriptase. Science 242:1168-1171.
24. Bebenek, K., J. Abbotts, S. H. Wilson, and T. A. Kunkel. 1993. Error-prone polymerization by HIV-1 reverse transcriptase. Contribution of template-primer misalignment, miscoding, and termination probability to mutational hot spots. J Biol Chem 268:10324-10334.
25. Jordan, A., P. Defechereux, and E. Verdin. 2001. The site of HIV-1 integration in the human genome determines basal transcriptional activity and response to Tat transactivation. EMBO J 20:1726-1738.

26. Triques, K., A. Bourgeois, N. Vidal, E. Mpoudi-Ngole, C. Mulanga-Kabeya, N. Nzilambi, N. Torimiro, E. Saman, E. Delaporte, and M. Peeters. 2000. Near-full-length genome sequencing of divergent African HIV type 1 subtype F viruses leads to the identification of a new HIV type 1 subtype designated K. AIDS Res Hum Retroviruses 16:139-151.
27. Ayouba, A., S. Souquieres, B. Njinku, P. M. Martin, M. C. Muller-Trutwin, P. Roques, F. Barre-Sinoussi, P. Mauclere, F. Simon, and E. Nerrienet. 2000. HIV-1 group N among HIV-1-seropositive individuals in Cameroon. Aids 14:2623-2625.
28. Balzarini, J., B. Degreve, and E. De Clercq. 1998. Improving AZT efficacy. Nat Med 4:132.
29. Simon, F., P. Mauclere, P. Roques, I. Loussert-Ajaka, M. C. Muller-Trutwin, S. Saragosti, M. C. Georges-Courbot, F. Barre-Sinoussi, and F. Brun-Vezinet. 1998. Identification of a new human immunodeficiency virus type 1 distinct from group M and group O. Nat Med 4:1032-1037.
30. Van Heuverswyn, F., Y. Li, C. Neel, E. Bailes, B. F. Keele, W. Liu, S. Loul, C. Butel, F. Liegeois, Y. Bienvenue, E. M. Ngolle, P. M. Sharp, G. M. Shaw, E. Delaporte, B. H. Hahn, and M. Peeters. 2006. Human immunodeficiency viruses: SIV infection in wild gorillas. Nature 444:164.
31. Yamaguchi, J., R. Coffey, A. Vallari, C. Ngansop, D. Mbanya, N. Ndembi, L. Kaptue, L. G. Gurtler, P. Bodelle, G. Schochetman, S. G. Devare, and C. A. Brennan. 2006. Identification of HIV type 1 group N infections in a husband and wife in Cameroon: viral genome sequences provide evidence for horizontal transmission. AIDS Res Hum Retroviruses 22:83-92.
32. Gray, R. H., M. J. Wawer, R. Brookmeyer, N. K. Sewankambo, D. Serwadda, F. Wabwire-Mangen, T. Lutalo, X. Li, T. vanCott, and T. C. Quinn. 2001. Probability of HIV-1 transmission per coital act in monogamous, heterosexual, HIV-1-discordant couples in Rakai, Uganda. Lancet 357:1149-1153.
33. Vittinghoff, E., J. Douglas, F. Judson, D. McKirnan, K. MacQueen, and S. P. Buchbinder. 1999. Per-contact risk of human immunodeficiency virus transmission between male sexual partners. Am J Epidemiol 150:306-311.
34. Sanders, R. W., E. C. de Jong, C. E. Baldwin, J. H. Schuitemaker, M. L. Kapsenberg, and B. Berkhout. 2002. Differential transmission of human immunodeficiency virus type 1 by distinct subsets of effector dendritic cells. J Virol 76:7812-7821.
35. Fong, L., M. Mengozzi, N. W. Abbey, B. G. Herndier, and E. G. Engleman. 2002. Productive infection of plasmacytoid dendritic cells with human immunodeficiency virus type 1 is triggered by CD40 ligation. J Virol 76:11033-11041.
36. Barrera, A., B. Guerra, H. Lee, and R. E. Lanford. 2004. Analysis of host range phenotypes of primate hepadnaviruses by in vitro infections of hepatitis D virus pseudotypes. J Virol 78:5233-5243.
37. Geijtenbeek, T. B., D. S. Kwon, R. Torensma, S. J. van Vliet, G. C. van Duijnhoven, J. Middel, I. L. Cornelissen, H. S. Nottet, V. N. KewalRamani, D. R. Littman, C. G. Figdor, and Y. van Kooyk. 2000. DC-SIGN, a dendritic cell-specific HIV-1-binding protein that enhances trans-infection of T cells. Cell 100:587-597.

38. Kwon, D. S., G. Gregorio, N. Bitton, W. A. Hendrickson, and D. R. Littman. 2002. DC-SIGN-mediated internalization of HIV is required for trans-enhancement of T cell infection. Immunity 16:135-144.
39. Rodriguez, B., A. K. Sethi, V. K. Cheruvu, W. Mackay, R. J. Bosch, M. Kitahata, S. L. Boswell, W. C. Mathews, D. R. Bangsberg, J. Martin, C. C. Whalen, S. Sieg, S. Yadavalli, S. G. Deeks, and M. M. Lederman. 2006. Predictive value of plasma HIV RNA level on rate of CD4 T-cell decline in untreated HIV infection. JAMA 296:1498-1506.
40. Pope, M., M. G. Betjes, N. Romani, H. Hirmand, P. U. Cameron, L. Hoffman, S. Gezelter, G. Schuler, and R. M. Steinman. 1994. Conjugates of dendritic cells and memory T lymphocytes from skin facilitate productive infection with HIV-1. Cell 78:389-398.
41. Mattapallil, J. J., D. C. Douek, B. Hill, Y. Nishimura, M. Martin, and M. Roederer. 2005. Massive infection and loss of memory CD4+ T cells in multiple tissues during acute SIV infection. Nature 434:1093-1097.
42. Phillips, A. N. 1996. Reduction of HIV concentration during acute infection: independence from a specific immune response. Science 271:497-499.
43. Borrow, P., H. Lewicki, B. H. Hahn, G. M. Shaw, and M. B. Oldstone. 1994. Virus-specific CD8+ cytotoxic T-lymphocyte activity associated with control of viremia in primary human immunodeficiency virus type 1 infection. J Virol 68:6103-6110.
44. Safrit, J. T., C. A. Andrews, T. Zhu, D. D. Ho, and R. A. Koup. 1994. Characterization of human immunodeficiency virus type 1-specific cytotoxic T lymphocyte clones isolated during acute seroconversion: recognition of autologous virus sequences within a conserved immunodominant epitope. J Exp Med 179:463-472.
45. Ioannidis, J. P., P. G. McQueen, J. J. Goedert, and R. A. Kaslow. 1998. Use of neural networks to model complex immunogenetic associations of disease: human leukocyte antigen impact on the progression of human immunodeficiency virus infection. Am J Epidemiol 147:464-471.
46. Rinaldo, C., X. L. Huang, Z. F. Fan, M. Ding, L. Beltz, A. Logar, D. Panicali, G. Mazzara, J. Liebmann, M. Cottrill, and et al. 1995. High levels of anti-human immunodeficiency virus type 1 (HIV-1) memory cytotoxic T-lymphocyte activity and low viral load are associated with lack of disease in HIV-1-infected long-term nonprogressors. J Virol 69:5838-5842.
47. Carmichael, A., X. Jin, P. Sissons, and L. Borysiewicz. 1993. Quantitative analysis of the human immunodeficiency virus type 1 (HIV-1)-specific cytotoxic T lymphocyte (CTL) response at different stages of HIV-1 infection: differential CTL responses to HIV-1 and Epstein-Barr virus in late disease. J Exp Med 177:249-256.
48. Matloubian, M., R. J. Concepcion, and R. Ahmed. 1994. CD4+ T cells are required to sustain CD8+ cytotoxic T-cell responses during chronic viral infection. J Virol 68:8056-8063.
49. Nichols, L., K. Balogh, and M. Silverman. 1989. Bacterial infections in the acquired immune deficiency syndrome. Clinicopathologic correlations in a series of autopsy cases. Am J Clin Pathol 92:787-790.

50. Boshoff, C., and R. Weiss. 2002. AIDS-related malignancies. Nat Rev Cancer 2:373-382.
51. Yarchoan, R., G. Tosato, and R. F. Little. 2005. Therapy insight: AIDS-related malignancies--the influence of antiviral therapy on pathogenesis and management. Nat Clin Pract Oncol 2:406-415; quiz 423.
52. Alter, G., N. Teigen, R. Ahern, H. Streeck, A. Meier, E. S. Rosenberg, and M. Altfeld. 2007. Evolution of innate and adaptive effector cell functions during acute HIV-1 infection. J Infect Dis 195:1452-1460.
53. Stacey, A. R., P. J. Norris, L. Qin, E. A. Haygreen, E. Taylor, J. Heitman, M. Lebedeva, A. DeCamp, D. Li, D. Grove, S. G. Self, and P. Borrow. 2009. Induction of a striking systemic cytokine cascade prior to peak viremia in acute human immunodeficiency virus type 1 infection, in contrast to more modest and delayed responses in acute hepatitis B and C virus infections. J Virol 83:3719-3733.
54. Mueller, Y. M., D. H. Do, S. R. Altork, C. M. Artlett, E. J. Gracely, C. D. Katsetos, A. Legido, F. Villinger, J. D. Altman, C. R. Brown, M. G. Lewis, and P. D. Katsikis. 2008. IL-15 treatment during acute simian immunodeficiency virus (SIV) infection increases viral set point and accelerates disease progression despite the induction of stronger SIV-specific CD8+ T cell responses. J Immunol 180:350-360.
55. Michaelsson, J., B. R. Long, C. P. Loo, L. L. Lanier, G. Spotts, F. M. Hecht, and D. F. Nixon. 2008. Immune reconstitution of CD56(dim) NK cells in individuals with primary HIV-1 infection treated with interleukin-2. J Infect Dis 197:117-125.
56. Welsch, S., O. T. Keppler, A. Habermann, I. Allespach, J. Krijnse-Locker, and H. G. Krausslich. 2007. HIV-1 buds predominantly at the plasma membrane of primary human macrophages. PLoS Pathog 3:e36.
57. Groot, F., S. Welsch, and Q. J. Sattentau. 2008. Efficient HIV-1 transmission from macrophages to T cells across transient virological synapses. Blood 111:4660-4663.
58. Killian, M. S., S. H. Fujimura, F. M. Hecht, and J. A. Levy. 2006. Similar changes in plasmacytoid dendritic cell and CD4 T-cell counts during primary HIV-1 infection and treatment. Aids 20:1247-1252.
59. Boasso, A., J. P. Herbeuval, A. W. Hardy, S. A. Anderson, M. J. Dolan, D. Fuchs, and G. M. Shearer. 2007. HIV inhibits CD4+ T-cell proliferation by inducing indoleamine 2,3-dioxygenase in plasmacytoid dendritic cells. Blood 109:3351-3359.
60. Manches, O., D. Munn, A. Fallahi, J. Lifson, L. Chaperot, J. Plumas, and N. Bhardwaj. 2008. HIV-activated human plasmacytoid DCs induce Tregs through an indoleamine 2,3-dioxygenase-dependent mechanism. J Clin Invest 118:3431-3439.
61. Granelli-Piperno, A., V. Finkel, E. Delgado, and R. M. Steinman. 1999. Virus replication begins in dendritic cells during the transmission of HIV-1 from mature dendritic cells to T cells. Curr Biol 9:21-29.
62. Wu, L., and V. N. KewalRamani. 2006. Dendritic-cell interactions with HIV: infection and viral dissemination. Nat Rev Immunol 6:859-868.

63. Hogervorst, E., S. Jurriaans, F. de Wolf, A. van Wijk, A. Wiersma, M. Valk, M. Roos, B. van Gemen, R. Coutinho, F. Miedema, and et al. 1995. Predictors for non- and slow progression in human immunodeficiency virus (HIV) type 1 infection: low viral RNA copy numbers in serum and maintenance of high HIV-1 p24-specific but not V3-specific antibody levels. J Infect Dis 171:811-821.
64. Chargelegue, D., C. M. Stanley, C. M. O'Toole, B. T. Colvin, and M. W. Steward. 1995. The affinity of IgG antibodies to gag p24 and p17 in HIV-1-infected patients correlates with disease progression. Clin Exp Immunol 99:175-181.
65. Shibata, R., T. Igarashi, N. Haigwood, A. Buckler-White, R. Ogert, W. Ross, R. Willey, M. W. Cho, and M. A. Martin. 1999. Neutralizing antibody directed against the HIV-1 envelope glycoprotein can completely block HIV-1/SIV chimeric virus infections of macaque monkeys. Nat Med 5:204-210.
66. Li, M., F. Gao, J. R. Mascola, L. Stamatatos, V. R. Polonis, M. Koutsoukos, G. Voss, P. Goepfert, P. Gilbert, K. M. Greene, M. Bilska, D. L. Kothe, J. F. Salazar-Gonzalez, X. Wei, J. M. Decker, B. H. Hahn, and D. C. Montefiori. 2005. Human immunodeficiency virus type 1 env clones from acute and early subtype B infections for standardized assessments of vaccine-elicited neutralizing antibodies. J Virol 79:10108-10125.
67. Mikell, I., D. N. Sather, S. A. Kalams, M. Altfeld, G. Alter, and L. Stamatatos. Characteristics of the earliest cross-neutralizing antibody response to HIV-1. PLoS Pathog 7:e1001251.
68. Ho, J., S. Moir, A. Malaspina, M. L. Howell, W. Wang, A. C. DiPoto, M. A. O'Shea, G. A. Roby, R. Kwan, J. M. Mican, T. W. Chun, and A. S. Fauci. 2006. Two overrepresented B cell populations in HIV-infected individuals undergo apoptosis by different mechanisms. Proc Natl Acad Sci U S A 103:19436-19441.
69. McCaffrey, R. A., C. Saunders, M. Hensel, and L. Stamatatos. 2004. N-linked glycosylation of the V3 loop and the immunologically silent face of gp120 protects human immunodeficiency virus type 1 SF162 from neutralization by anti-gp120 and anti-gp41 antibodies. J Virol 78:3279-3295.
70. Doranz, B. J., S. S. Baik, and R. W. Doms. 1999. Use of a gp120 binding assay to dissect the requirements and kinetics of human immunodeficiency virus fusion events. J Virol 73:10346-10358.
71. Gandhi, R. T., B. K. Chen, S. E. Straus, J. K. Dale, M. J. Lenardo, and D. Baltimore. 1998. HIV-1 directly kills CD4+ T cells by a Fas-independent mechanism. J Exp Med 187:1113-1122.
72. Hickman, H. D., A. D. Luis, W. Bardet, R. Buchli, C. L. Battson, M. H. Shearer, K. W. Jackson, R. C. Kennedy, and W. H. Hildebrand. 2003. Cutting edge: class I presentation of host peptides following HIV infection. J Immunol 171:22-26.
73. Le Borgne, S., M. Fevrier, C. Callebaut, S. P. Lee, and Y. Riviere. 2000. CD8(+)-Cell antiviral factor activity is not restricted to human immunodeficiency virus (HIV)-specific T cells and can block HIV replication after initiation of reverse transcription. J Virol 74:4456-4464.
74. Li, Q., L. Duan, J. D. Estes, Z. M. Ma, T. Rourke, Y. Wang, C. Reilly, J. Carlis, C. J. Miller, and A. T. Haase. 2005. Peak SIV replication in resting memory CD4+ T cells depletes gut lamina propria CD4+ T cells. Nature 434:1148-1152.

75. Gloster, S. E., P. Newton, D. Cornforth, J. D. Lifson, I. Williams, G. M. Shaw, and P. Borrow. 2004. Association of strong virus-specific CD4 T cell responses with efficient natural control of primary HIV-1 infection. Aids 18:749-755.
76. Kelleher, A. D., C. Long, E. C. Holmes, R. L. Allen, J. Wilson, C. Conlon, C. Workman, S. Shaunak, K. Olson, P. Goulder, C. Brander, G. Ogg, J. S. Sullivan, W. Dyer, I. Jones, A. J. McMichael, S. Rowland-Jones, and R. E. Phillips. 2001. Clustered mutations in HIV-1 gag are consistently required for escape from HLA-B27-restricted cytotoxic T lymphocyte responses. J Exp Med 193:375-386.
77. Boissonnas, A., O. Bonduelle, A. Antzack, Y. C. Lone, C. Gache, P. Debre, B. Autran, and B. Combadiere. 2002. In vivo priming of HIV-specific CTLs determines selective cross-reactive immune responses against poorly immunogenic HIV-natural variants. J Immunol 169:3694-3699.
78. Milicic, A., D. A. Price, P. Zimbwa, B. L. Booth, H. L. Brown, P. J. Easterbrook, K. Olsen, N. Robinson, U. Gileadi, A. K. Sewell, V. Cerundolo, and R. E. Phillips. 2005. CD8+ T cell epitope-flanking mutations disrupt proteasomal processing of HIV-1 Nef. J Immunol 175:4618-4626.
79. Del Val, M., H. J. Schlicht, T. Ruppert, M. J. Reddehase, and U. H. Koszinowski. 1991. Efficient processing of an antigenic sequence for presentation by MHC class I molecules depends on its neighboring residues in the protein. Cell 66:1145-1153.
80. Said, E. A., F. P. Dupuy, L. Trautmann, Y. Zhang, Y. Shi, M. El-Far, B. J. Hill, A. Noto, P. Ancuta, Y. Peretz, S. G. Fonseca, J. Van Grevenynghe, M. R. Boulassel, J. Bruneau, N. H. Shoukry, J. P. Routy, D. C. Douek, E. K. Haddad, and R. P. Sekaly. Programmed death-1-induced interleukin-10 production by monocytes impairs CD4+ T cell activation during HIV infection. Nat Med 16:452-459.
81. Amara, R. R., F. Villinger, J. D. Altman, S. L. Lydy, S. P. O'Neil, S. I. Staprans, D. C. Montefiori, Y. Xu, J. G. Herndon, L. S. Wyatt, M. A. Candido, N. L. Kozyr, P. L. Earl, J. M. Smith, H. L. Ma, B. D. Grimm, M. L. Hulsey, J. Miller, H. M. McClure, J. M. McNicholl, B. Moss, and H. L. Robinson. 2001. Control of a mucosal challenge and prevention of AIDS by a multiprotein DNA/MVA vaccine. Science 292:69-74.
82. Schmitz, J. E., M. J. Kuroda, S. Santra, V. G. Sasseville, M. A. Simon, M. A. Lifton, P. Racz, K. Tenner-Racz, M. Dalesandro, B. J. Scallon, J. Ghrayeb, M. A. Forman, D. C. Montefiori, E. P. Rieber, N. L. Letvin, and K. A. Reimann. 1999. Control of viremia in simian immunodeficiency virus infection by CD8+ lymphocytes. Science 283:857-860.
83. Dong, T., G. Stewart-Jones, N. Chen, P. Easterbrook, X. Xu, L. Papagno, V. Appay, M. Weekes, C. Conlon, C. Spina, S. Little, G. Screaton, A. van der Merwe, D. D. Richman, A. J. McMichael, E. Y. Jones, and S. L. Rowland-Jones. 2004. HIV-specific cytotoxic T cells from long-term survivors select a unique T cell receptor. J Exp Med 200:1547-1557.
84. Turnbull, E. L., A. R. Lopes, N. A. Jones, D. Cornforth, P. Newton, D. Aldam, P. Pellegrino, J. Turner, I. Williams, C. M. Wilson, P. A. Goepfert, M. K. Maini, and P. Borrow. 2006. HIV-1 epitope-specific CD8+ T cell responses strongly

associated with delayed disease progression cross-recognize epitope variants efficiently. J Immunol 176:6130-6146.
85. Chen, B., E. M. Vogan, H. Gong, J. J. Skehel, D. C. Wiley, and S. C. Harrison. 2005. Structure of an unliganded simian immunodeficiency virus gp120 core. Nature 433:834-841.
86. Wyatt, R., P. D. Kwong, E. Desjardins, R. W. Sweet, J. Robinson, W. A. Hendrickson, and J. G. Sodroski. 1998. The antigenic structure of the HIV gp120 envelope glycoprotein. Nature 393:705-711.
87. Shirai, A., M. Cosentino, S. F. Leitman-Klinman, and D. M. Klinman. 1992. Human immunodeficiency virus infection induces both polyclonal and virus-specific B cell activation. J Clin Invest 89:561-566.
88. Scheid, J. F., H. Mouquet, N. Feldhahn, M. S. Seaman, K. Velinzon, J. Pietzsch, R. G. Ott, R. M. Anthony, H. Zebroski, A. Hurley, A. Phogat, B. Chakrabarti, Y. Li, M. Connors, F. Pereyra, B. D. Walker, H. Wardemann, D. Ho, R. T. Wyatt, J. R. Mascola, J. V. Ravetch, and M. C. Nussenzweig. 2009. Broad diversity of neutralizing antibodies isolated from memory B cells in HIV-infected individuals. Nature 458:636-640.
89. Mascola, J. R., P. D'Souza, P. Gilbert, B. H. Hahn, N. L. Haigwood, L. Morris, C. J. Petropoulos, V. R. Polonis, M. Sarzotti, and D. C. Montefiori. 2005. Recommendations for the design and use of standard virus panels to assess neutralizing antibody responses elicited by candidate human immunodeficiency virus type 1 vaccines. J Virol 79:10103-10107.
90. Li, Y., K. Svehla, M. K. Louder, D. Wycuff, S. Phogat, M. Tang, S. A. Migueles, X. Wu, A. Phogat, G. M. Shaw, M. Connors, J. Hoxie, J. R. Mascola, and R. Wyatt. 2009. Analysis of neutralization specificities in polyclonal sera derived from human immunodeficiency virus type 1-infected individuals. J Virol 83:1045-1059.
91. McElrath, M. J., and B. F. Haynes. Induction of immunity to human immunodeficiency virus type-1 by vaccination. Immunity 33:542-554.
92. Cheng-Mayer, C., A. Brown, J. Harouse, P. A. Luciw, and A. J. Mayer. 1999. Selection for neutralization resistance of the simian/human immunodeficiency virus SHIVSF33A variant in vivo by virtue of sequence changes in the extracellular envelope glycoprotein that modify N-linked glycosylation. J Virol 73:5294-5300.
93. Berberian, L., L. Goodglick, T. J. Kipps, and J. Braun. 1993. Immunoglobulin VH3 gene products: natural ligands for HIV gp120. Science 261:1588-1591.
94. Pruenster, M., D. Wilflingseder, Z. Banki, C. G. Ammann, B. Muellauer, M. Meyer, C. Speth, M. P. Dierich, and H. Stoiber. 2005. C-type lectin-independent interaction of complement opsonized HIV with monocyte-derived dendritic cells. Eur J Immunol 35:2691-2698.
95. Barouch, D. H., J. Kunstman, M. J. Kuroda, J. E. Schmitz, S. Santra, F. W. Peyerl, G. R. Krivulka, K. Beaudry, M. A. Lifton, D. A. Gorgone, D. C. Montefiori, M. G. Lewis, S. M. Wolinsky, and N. L. Letvin. 2002. Eventual AIDS vaccine failure in a rhesus monkey by viral escape from cytotoxic T lymphocytes. Nature 415:335-339.

96. Maecker, H. T., A. Rinfret, P. D'Souza, J. Darden, E. Roig, C. Landry, P. Hayes, J. Birungi, O. Anzala, M. Garcia, A. Harari, I. Frank, R. Baydo, M. Baker, J. Holbrook, J. Ottinger, L. Lamoreaux, C. L. Epling, E. Sinclair, M. A. Suni, K. Punt, S. Calarota, S. El-Bahi, G. Alter, H. Maila, E. Kuta, J. Cox, C. Gray, M. Altfeld, N. Nougarede, J. Boyer, L. Tussey, T. Tobery, B. Bredt, M. Roederer, R. Koup, V. C. Maino, K. Weinhold, G. Pantaleo, J. Gilmour, H. Horton, and R. P. Sekaly. 2005. Standardization of cytokine flow cytometry assays. BMC Immunol 6:13.
97. Berkhout, B., K. Verhoef, J. L. van Wamel, and N. K. Back. 1999. Genetic instability of live, attenuated human immunodeficiency virus type 1 vaccine strains. J Virol 73:1138-1145.
98. Edupuganti, S., D. Weber, and C. Poole. 2004. Cytotoxic T-lymphocyte responses to canarypox vector-based HIV vaccines in HIV-seronegative individuals: a meta-analysis of published studies. HIV Clin Trials 5:259-268.
99. Sumida, S. M., D. M. Truitt, A. A. Lemckert, R. Vogels, J. H. Custers, M. M. Addo, S. Lockman, T. Peter, F. W. Peyerl, M. G. Kishko, S. S. Jackson, D. A. Gorgone, M. A. Lifton, M. Essex, B. D. Walker, J. Goudsmit, M. J. Havenga, and D. H. Barouch. 2005. Neutralizing antibodies to adenovirus serotype 5 vaccine vectors are directed primarily against the adenovirus hexon protein. J Immunol 174:7179-7185.
100. Dreesman, G. R., F. B. Hollinger, Y. Sanchez, P. Oefinger, and J. L. Melnick. 1981. Immunization of chimpanzees with hepatitis B virus-derived polypeptides. Infect Immun 32:62-67.
101. Purcell, R. H., and J. L. Gerin. 1975. Hepatitis B subunit vaccine: a preliminary report of safety and efficacy tests in chimpanzees. Am J Med Sci 270:395-399.
102. Flynn, N. M., D. N. Forthal, C. D. Harro, F. N. Judson, K. H. Mayer, and M. F. Para. 2005. Placebo-controlled phase 3 trial of a recombinant glycoprotein 120 vaccine to prevent HIV-1 infection. J Infect Dis 191:654-665.
103. Watkins, D. I., D. R. Burton, E. G. Kallas, J. P. Moore, and W. C. Koff. 2008. Nonhuman primate models and the failure of the Merck HIV-1 vaccine in humans. Nat Med 14:617-621.
104. Leslie, A., D. Kavanagh, I. Honeyborne, K. Pfafferott, C. Edwards, T. Pillay, L. Hilton, C. Thobakgale, D. Ramduth, R. Draenert, S. Le Gall, G. Luzzi, A. Edwards, C. Brander, A. K. Sewell, S. Moore, J. Mullins, C. Moore, S. Mallal, N. Bhardwaj, K. Yusim, R. Phillips, P. Klenerman, B. Korber, P. Kiepiela, B. Walker, and P. Goulder. 2005. Transmission and accumulation of CTL escape variants drive negative associations between HIV polymorphisms and HLA. J Exp Med 201:891-902.
105. Peyerl, F. W., H. S. Bazick, M. H. Newberg, D. H. Barouch, J. Sodroski, and N. L. Letvin. 2004. Fitness costs limit viral escape from cytotoxic T lymphocytes at a structurally constrained epitope. J Virol 78:13901-13910.
106. Huang, X., B. Lu, W. Yu, Q. Fang, L. Liu, K. Zhuang, T. Shen, H. Wang, P. Tian, L. Zhang, and Z. Chen. 2009. A novel replication-competent vaccinia vector MVTT is superior to MVA for inducing high levels of neutralizing antibody via mucosal vaccination. PLoS One 4:e4180.

107. McShane, H., A. A. Pathan, C. R. Sander, S. M. Keating, S. C. Gilbert, K. Huygen, H. A. Fletcher, and A. V. Hill. 2004. Recombinant modified vaccinia virus Ankara expressing antigen 85A boosts BCG-primed and naturally acquired antimycobacterial immunity in humans. Nat Med 10:1240-1244.
108. Horton, H., T. U. Vogel, D. K. Carter, K. Vielhuber, D. H. Fuller, T. Shipley, J. T. Fuller, K. J. Kunstman, G. Sutter, D. C. Montefiori, V. Erfle, R. C. Desrosiers, N. Wilson, L. J. Picker, S. M. Wolinsky, C. Wang, D. B. Allison, and D. I. Watkins. 2002. Immunization of rhesus macaques with a DNA prime/modified vaccinia virus Ankara boost regimen induces broad simian immunodeficiency virus (SIV)-specific T-cell responses and reduces initial viral replication but does not prevent disease progression following challenge with pathogenic SIVmac239. J Virol 76:7187-7202.
109. O'Brien, K. L., J. Liu, S. L. King, Y. H. Sun, J. E. Schmitz, M. A. Lifton, N. A. Hutnick, M. R. Betts, S. A. Dubey, J. Goudsmit, J. W. Shiver, M. N. Robertson, D. R. Casimiro, and D. H. Barouch. 2009. Adenovirus-specific immunity after immunization with an Ad5 HIV-1 vaccine candidate in humans. Nat Med 15:873-875.
110. Moodie, Z., A. J. Rossini, M. G. Hudgens, P. B. Gilbert, S. G. Self, and N. D. Russell. 2006. Statistical evaluation of HIV vaccines in early clinical trials. Contemp Clin Trials 27:147-160.
111. Lu, W., L. C. Arraes, W. T. Ferreira, and J. M. Andrieu. 2004. Therapeutic dendritic-cell vaccine for chronic HIV-1 infection. Nat Med 10:1359-1365.
112. Robinson, C. M., G. Singh, C. Henquell, M. P. Walsh, H. Peigue-Lafeuille, D. Seto, M. S. Jones, D. W. Dyer, and J. Chodosh. Computational analysis and identification of an emergent human adenovirus pathogen implicated in a respiratory fatality. Virology 409:141-147.
113. Xiao, X., J. Li, and R. J. Samulski. 1996. Efficient long-term gene transfer into muscle tissue of immunocompetent mice by adeno-associated virus vector. J Virol 70:8098-8108.
114. Rauschhuber, C., A. Wolf, and A. Ehrhardt. Transcriptional activity of inverted terminal repeats of various human adenovirus serotypes. J Gen Virol 92:669-674.
115. Mack, C. A., W. R. Song, H. Carpenter, T. J. Wickham, I. Kovesdi, B. G. Harvey, C. J. Magovern, O. W. Isom, T. Rosengart, E. Falck-Pedersen, N. R. Hackett, R. G. Crystal, and A. Mastrangeli. 1997. Circumvention of anti-adenovirus neutralizing immunity by administration of an adenoviral vector of an alternate serotype. Hum Gene Ther 8:99-109.
116. Tsai, V., D. E. Johnson, A. Rahman, S. F. Wen, D. LaFace, J. Philopena, J. Nery, M. Zepeda, D. C. Maneval, G. W. Demers, and R. Ralston. 2004. Impact of human neutralizing antibodies on antitumor efficacy of an oncolytic adenovirus in a murine model. Clin Cancer Res 10:7199-7206.
117. Kirby, I., E. Davison, A. J. Beavil, C. P. Soh, T. J. Wickham, P. W. Roelvink, I. Kovesdi, B. J. Sutton, and G. Santis. 2000. Identification of contact residues and definition of the CAR-binding site of adenovirus type 5 fiber protein. J Virol 74:2804-2813.
118. Bergelson, J. M., J. A. Cunningham, G. Droguett, E. A. Kurt-Jones, A. Krithivas, J. S. Hong, M. S. Horwitz, R. L. Crowell, and R. W. Finberg. 1997. Isolation of a

common receptor for Coxsackie B viruses and adenoviruses 2 and 5. Science 275:1320-1323.
119. Tillman, B. W., T. D. de Gruijl, S. A. Luykx-de Bakker, R. J. Scheper, H. M. Pinedo, T. J. Curiel, W. R. Gerritsen, and D. T. Curiel. 1999. Maturation of dendritic cells accompanies high-efficiency gene transfer by a CD40-targeted adenoviral vector. J Immunol 162:6378-6383.
120. Okada, N., Y. Masunaga, Y. Okada, S. Iiyama, N. Mori, T. Tsuda, A. Matsubara, H. Mizuguchi, T. Hayakawa, T. Fujita, and A. Yamamoto. 2003. Gene transduction efficiency and maturation status in mouse bone marrow-derived dendritic cells infected with conventional or RGD fiber-mutant adenovirus vectors. Cancer Gene Ther 10:421-431.
121. Wickham, T. J., P. Mathias, D. A. Cheresh, and G. R. Nemerow. 1993. Integrins alpha v beta 3 and alpha v beta 5 promote adenovirus internalization but not virus attachment. Cell 73:309-319.
122. Russell, W. C. 2000. Update on adenovirus and its vectors. J Gen Virol 81:2573-2604.
123. Volpers, C., and S. Kochanek. 2004. Adenoviral vectors for gene transfer and therapy. J Gene Med 6 Suppl 1:S164-171.
124. Freimuth, P., K. Springer, C. Berard, J. Hainfeld, M. Bewley, and J. Flanagan. 1999. Coxsackievirus and adenovirus receptor amino-terminal immunoglobulin V-related domain binds adenovirus type 2 and fiber knob from adenovirus type 12. J Virol 73:1392-1398.
125. Sas, S., T. Chan, A. Sami, A. El-Gayed, and J. Xiang. 2008. Vaccination of fiber-modified adenovirus-transfected dendritic cells to express HER-2/neu stimulates efficient HER-2/neu-specific humoral and CTL responses and reduces breast carcinogenesis in transgenic mice. Cancer Gene Ther 15:655-666.
126. De Smedt, T., B. Pajak, E. Muraille, L. Lespagnard, E. Heinen, P. De Baetselier, J. Urbain, O. Leo, and M. Moser. 1996. Regulation of dendritic cell numbers and maturation by lipopolysaccharide in vivo. J Exp Med 184:1413-1424.
127. Tassaneetrithep, B., T. H. Burgess, A. Granelli-Piperno, C. Trumpfheller, J. Finke, W. Sun, M. A. Eller, K. Pattanapanyasat, S. Sarasombath, D. L. Birx, R. M. Steinman, S. Schlesinger, and M. A. Marovich. 2003. DC-SIGN (CD209) mediates dengue virus infection of human dendritic cells. J Exp Med 197:823-829.
128. West, M. A., R. P. Wallin, S. P. Matthews, H. G. Svensson, R. Zaru, H. G. Ljunggren, A. R. Prescott, and C. Watts. 2004. Enhanced dendritic cell antigen capture via toll-like receptor-induced actin remodeling. Science 305:1153-1157.
129. Mackensen, A., B. Herbst, J. L. Chen, G. Kohler, C. Noppen, W. Herr, G. C. Spagnoli, V. Cerundolo, and A. Lindemann. 2000. Phase I study in melanoma patients of a vaccine with peptide-pulsed dendritic cells generated in vitro from CD34(+) hematopoietic progenitor cells. Int J Cancer 86:385-392.
130. Heiser, A., D. Coleman, J. Dannull, D. Yancey, M. A. Maurice, C. D. Lallas, P. Dahm, D. Niedzwiecki, E. Gilboa, and J. Vieweg. 2002. Autologous dendritic cells transfected with prostate-specific antigen RNA stimulate CTL responses against metastatic prostate tumors. J Clin Invest 109:409-417.

131. Steinman, R. M., and M. C. Nussenzweig. 2002. Avoiding horror autotoxicus: the importance of dendritic cells in peripheral T cell tolerance. Proc Natl Acad Sci U S A 99:351-358.
132. Collins, S. A., B. A. Guinn, P. T. Harrison, M. F. Scallan, G. C. O'Sullivan, and M. Tangney. 2008. Viral vectors in cancer immunotherapy: which vector for which strategy? Curr Gene Ther 8:66-78.
133. Xia, D., T. Moyana, and J. Xiang. 2006. Combinational adenovirus-mediated gene therapy and dendritic cell vaccine in combating well-established tumors. Cell Res 16:241-259.
134. Molinier-Frenkel, V., A. Prevost-Blondel, S. S. Hong, R. Lengagne, S. Boudaly, M. K. Magnusson, P. Boulanger, and J. G. Guillet. 2003. The maturation of murine dendritic cells induced by human adenovirus is mediated by the fiber knob domain. J Biol Chem 278:37175-37182.
135. Figdor, C. G., I. J. de Vries, W. J. Lesterhuis, and C. J. Melief. 2004. Dendritic cell immunotherapy: mapping the way. Nat Med 10:475-480.
136. Thery, C., M. Boussac, P. Veron, P. Ricciardi-Castagnoli, G. Raposo, J. Garin, and S. Amigorena. 2001. Proteomic analysis of dendritic cell-derived exosomes: a secreted subcellular compartment distinct from apoptotic vesicles. J Immunol 166:7309-7318.
137. Guermonprez, P., L. Saveanu, M. Kleijmeer, J. Davoust, P. Van Endert, and S. Amigorena. 2003. ER-phagosome fusion defines an MHC class I cross-presentation compartment in dendritic cells. Nature 425:397-402.
138. Zitvogel, L., A. Regnault, A. Lozier, J. Wolfers, C. Flament, D. Tenza, P. Ricciardi-Castagnoli, G. Raposo, and S. Amigorena. 1998. Eradication of established murine tumors using a novel cell-free vaccine: dendritic cell-derived exosomes. Nat Med 4:594-600.
139. Whiteside, T. L. 2005. Tumour-derived exosomes or microvesicles: another mechanism of tumour escape from the host immune system? Br J Cancer 92:209-211.
140. Wubbolts, R., R. S. Leckie, P. T. Veenhuizen, G. Schwarzmann, W. Mobius, J. Hoernschemeyer, J. W. Slot, H. J. Geuze, and W. Stoorvogel. 2003. Proteomic and biochemical analyses of human B cell-derived exosomes. Potential implications for their function and multivesicular body formation. J Biol Chem 278:10963-10972.
141. Babst, M., G. Odorizzi, E. J. Estepa, and S. D. Emr. 2000. Mammalian tumor susceptibility gene 101 (TSG101) and the yeast homologue, Vps23p, both function in late endosomal trafficking. Traffic 1:248-258.
142. Wolfers, J., A. Lozier, G. Raposo, A. Regnault, C. Thery, C. Masurier, C. Flament, S. Pouzieux, F. Faure, T. Tursz, E. Angevin, S. Amigorena, and L. Zitvogel. 2001. Tumor-derived exosomes are a source of shared tumor rejection antigens for CTL cross-priming. Nat Med 7:297-303.
143. Raposo, G., H. W. Nijman, W. Stoorvogel, R. Liejendekker, C. V. Harding, C. J. Melief, and H. J. Geuze. 1996. B lymphocytes secrete antigen-presenting vesicles. J Exp Med 183:1161-1172.

144. Denzer, K., M. J. Kleijmeer, H. F. Heijnen, W. Stoorvogel, and H. J. Geuze. 2000. Exosome: from internal vesicle of the multivesicular body to intercellular signaling device. J Cell Sci 113 Pt 19:3365-3374.
145. Clayton, A., J. Court, H. Navabi, M. Adams, M. D. Mason, J. A. Hobot, G. R. Newman, and B. Jasani. 2001. Analysis of antigen presenting cell derived exosomes, based on immuno-magnetic isolation and flow cytometry. J Immunol Methods 247:163-174.
146. Thery, C., A. Regnault, J. Garin, J. Wolfers, L. Zitvogel, P. Ricciardi-Castagnoli, G. Raposo, and S. Amigorena. 1999. Molecular characterization of dendritic cell-derived exosomes. Selective accumulation of the heat shock protein hsc73. J Cell Biol 147:599-610.
147. Escudier, B., T. Dorval, N. Chaput, F. Andre, M. P. Caby, S. Novault, C. Flament, C. Leboulaire, C. Borg, S. Amigorena, C. Boccaccio, C. Bonnerot, O. Dhellin, M. Movassagh, S. Piperno, C. Robert, V. Serra, N. Valente, J. B. Le Pecq, A. Spatz, O. Lantz, T. Tursz, E. Angevin, and L. Zitvogel. 2005. Vaccination of metastatic melanoma patients with autologous dendritic cell (DC) derived-exosomes: results of thefirst phase I clinical trial. J Transl Med 3:10.
148. Morse, M. A., J. Garst, T. Osada, S. Khan, A. Hobeika, T. M. Clay, N. Valente, R. Shreeniwas, M. A. Sutton, A. Delcayre, D. H. Hsu, J. B. Le Pecq, and H. K. Lyerly. 2005. A phase I study of dexosome immunotherapy in patients with advanced non-small cell lung cancer. J Transl Med 3:9.
149. Chaput, N., N. E. Schartz, F. Andre, J. Taieb, S. Novault, P. Bonnaventure, N. Aubert, J. Bernard, F. Lemonnier, M. Merad, G. Adema, M. Adams, M. Ferrantini, A. F. Carpentier, B. Escudier, T. Tursz, E. Angevin, and L. Zitvogel. 2004. Exosomes as potent cell-free peptide-based vaccine. II. Exosomes in CpG adjuvants efficiently prime naive Tc1 lymphocytes leading to tumor rejection. J Immunol 172:2137-2146.
150. Hao, S., J. Yuan, and J. Xiang. 2007. Nonspecific CD4(+) T cells with uptake of antigen-specific dendritic cell-released exosomes stimulate antigen-specific CD8(+) CTL responses and long-term T cell memory. J Leukoc Biol 82:829-838.
151. Hao, S., Y. Liu, J. Yuan, X. Zhang, T. He, X. Wu, Y. Wei, D. Sun, and J. Xiang. 2007. Novel exosome-targeted CD4+ T cell vaccine counteracting CD4+25+ regulatory T cell-mediated immune suppression and stimulating efficient central memory CD8+ CTL responses. J Immunol 179:2731-2740.
152. Patel, D. M., and M. D. Mannie. 2001. Intercellular exchange of class II major histocompatibility complex/peptide complexes is a conserved process that requires activation of T cells but is constitutive in other types of antigen presenting cell. Cell Immunol 214:165-172.
153. Carlin, L. M., K. Eleme, F. E. McCann, and D. M. Davis. 2001. Intercellular transfer and supramolecular organization of human leukocyte antigen C at inhibitory natural killer cell immune synapses. J Exp Med 194:1507-1517.
154. Tabiasco, J., E. Espinosa, D. Hudrisier, E. Joly, J. J. Fournie, and A. Vercellone. 2002. Active trans-synaptic capture of membrane fragments by natural killer cells. Eur J Immunol 32:1502-1508.

155. Stinchcombe, J. C., G. Bossi, S. Booth, and G. M. Griffiths. 2001. The immunological synapse of CTL contains a secretory domain and membrane bridges. Immunity 15:751-761.
156. Thery, C., L. Zitvogel, and S. Amigorena. 2002. Exosomes: composition, biogenesis and function. Nat Rev Immunol 2:569-579.
157. Patel, D. M., R. W. Dudek, and M. D. Mannie. 2001. Intercellular exchange of class II MHC complexes: ultrastructural localization and functional presentation of adsorbed I-A/peptide complexes. Cell Immunol 214:21-34.
158. Grakoui, A., S. K. Bromley, C. Sumen, M. M. Davis, A. S. Shaw, P. M. Allen, and M. L. Dustin. 1999. The immunological synapse: a molecular machine controlling T cell activation. Science 285:221-227.
159. Viola, A., S. Schroeder, Y. Sakakibara, and A. Lanzavecchia. 1999. T lymphocyte costimulation mediated by reorganization of membrane microdomains. Science 283:680-682.
160. Hwang, I., J. F. Huang, H. Kishimoto, A. Brunmark, P. A. Peterson, M. R. Jackson, C. D. Surh, Z. Cai, and J. Sprent. 2000. T cells can use either T cell receptor or CD28 receptors to absorb and internalize cell surface molecules derived from antigen-presenting cells. J Exp Med 191:1137-1148.
161. Huang, J. F., Y. Yang, H. Sepulveda, W. Shi, I. Hwang, P. A. Peterson, M. R. Jackson, J. Sprent, and Z. Cai. 1999. TCR-Mediated internalization of peptide-MHC complexes acquired by T cells. Science 286:952-954.
162. Xiang, J., H. Huang, and Y. Liu. 2005. A new dynamic model of CD8+ T effector cell responses via CD4+ T helper-antigen-presenting cells. J Immunol 174:7497-7505.
163. He, T., S. Zong, X. Wu, Y. Wei, and J. Xiang. 2007. CD4+ T cell acquisition of the bystander pMHC I colocalizing in the same immunological synapse comprising pMHC II and costimulatory CD40, CD54, CD80, OX40L, and 41BBL. Biochem Biophys Res Commun 362:822-828.
164. Umeshappa, C. S., H. Huang, Y. Xie, Y. Wei, S. J. Mulligan, Y. Deng, and J. Xiang. 2009. CD4+ Th-APC with acquired peptide/MHC class I and II complexes stimulate type 1 helper CD4+ and central memory CD8+ T cell responses. J Immunol 182:193-206.
165. Xia, D., S. Hao, and J. Xiang. 2006. CD8+ cytotoxic T-APC stimulate central memory CD8+ T cell responses via acquired peptide-MHC class I complexes and CD80 costimulation, and IL-2 secretion. J Immunol 177:2976-2984.
166. Li, M., G. M. Davey, R. M. Sutherland, C. Kurts, A. M. Lew, C. Hirst, F. R. Carbone, and W. R. Heath. 2001. Cell-associated ovalbumin is cross-presented much more efficiently than soluble ovalbumin in vivo. J Immunol 166:6099-6103.
167. Dupuis, M., S. K. Kundu, and T. C. Merigan. 1995. Characterization of HLA-A 0201-restricted cytotoxic T cell epitopes in conserved regions of the HIV type 1 gp160 protein. J Immunol 155:2232-2239.
168. Woodberry, T., J. Gardner, L. Mateo, D. Eisen, J. Medveczky, I. A. Ramshaw, S. A. Thomson, R. A. Ffrench, S. L. Elliott, H. Firat, F. A. Lemonnier, and A. Suhrbier. 1999. Immunogenicity of a human immunodeficiency virus (HIV) polytope vaccine containing multiple HLA A2 HIV CD8(+) cytotoxic T-cell epitopes. J Virol 73:5320-5325.

169. He, T. C., S. Zhou, L. T. da Costa, J. Yu, K. W. Kinzler, and B. Vogelstein. 1998. A simplified system for generating recombinant adenoviruses. Proc Natl Acad Sci U S A 95:2509-2514.
170. Luo, J., Z. L. Deng, X. Luo, N. Tang, W. X. Song, J. Chen, K. A. Sharff, H. H. Luu, R. C. Haydon, K. W. Kinzler, B. Vogelstein, and T. C. He. 2007. A protocol for rapid generation of recombinant adenoviruses using the AdEasy system. Nat Protoc 2:1236-1247.
171. Xiang, J., and J. Wu. 2003. Genetic engineering of dendritic cells by adenovirus-mediated TNF-alpha gene transfer. Methods Mol Biol 215:213-225.
172. Ye, Z., K. A. Ahmed, J. Huang, Y. Xie, M. A. Munegowda, and J. Xiang. 2008. T cell precursor frequency differentially affects CTL responses under different immune conditions. Biochem Biophys Res Commun 367:427-434.
173. Thery, C., S. Amigorena, G. Raposo, and A. Clayton. 2006. Isolation and characterization of exosomes from cell culture supernatants and biological fluids. Curr Protoc Cell Biol Chapter 3:Unit 3 22.
174. Shedlock, D. J., J. K. Whitmire, J. Tan, A. S. MacDonald, R. Ahmed, and H. Shen. 2003. Role of CD4 T cell help and costimulation in CD8 T cell responses during Listeria monocytogenes infection. J Immunol 170:2053-2063.
175. Boehm, U., T. Klamp, M. Groot, and J. C. Howard. 1997. Cellular responses to interferon-gamma. Annu Rev Immunol 15:749-795.
176. Shirayoshi, Y., P. A. Burke, E. Appella, and K. Ozato. 1988. Interferon-induced transcription of a major histocompatibility class I gene accompanies binding of inducible nuclear factors to the interferon consensus sequence. Proc Natl Acad Sci U S A 85:5884-5888.
177. Gallez-Hawkins, G., M. C. Villacres, X. Li, M. C. Sanborn, N. A. Lomeli, and J. A. Zaia. 2003. Use of transgenic HLA A*0201/Kb and HHD II mice to evaluate frequency of cytomegalovirus IE1-derived peptide usage in eliciting human CD8 cytokine response. J Virol 77:4457-4462.
178. Zhou, H., Y. Luo, M. Mizutani, N. Mizutani, J. C. Becker, F. J. Primus, R. Xiang, and R. A. Reisfeld. 2004. A novel transgenic mouse model for immunological evaluation of carcinoembryonic antigen-based DNA minigene vaccines. J Clin Invest 113:1792-1798.
179. Engelhard, V. H., E. Lacy, and J. P. Ridge. 1991. Influenza A-specific, HLA-A2.1-restricted cytotoxic T lymphocytes from HLA-A2.1 transgenic mice recognize fragments of the M1 protein. J Immunol 146:1226-1232.
180. Newberg, M. H., J. P. Ridge, D. R. Vining, R. D. Salter, and V. H. Engelhard. 1992. Species specificity in the interaction of CD8 with the alpha 3 domain of MHC class I molecules. J Immunol 149:136-142.
181. Vitiello, A., D. Marchesini, J. Furze, L. A. Sherman, and R. W. Chesnut. 1991. Analysis of the HLA-restricted influenza-specific cytotoxic T lymphocyte response in transgenic mice carrying a chimeric human-mouse class I major histocompatibility complex. J Exp Med 173:1007-1015.
182. Bolesta, E., A. Kowalczyk, A. Wierzbicki, C. Eppolito, Y. Kaneko, M. Takiguchi, L. Stamatatos, P. A. Shrikant, and D. Kozbor. 2006. Increased level and longevity of protective immune responses induced by DNA vaccine expressing the HIV-1

Env glycoprotein when combined with IL-21 and IL-15 gene delivery. J Immunol 177:177-191.
183. Dutton, R. W., L. M. Bradley, and S. L. Swain. 1998. T cell memory. Annu Rev Immunol 16:201-223.
184. He, T., C. Tang, S. Xu, T. Moyana, and J. Xiang. 2007. Interferon gamma stimulates cellular maturation of dendritic cell line DC2.4 leading to induction of efficient cytotoxic T cell responses and antitumor immunity. Cell Mol Immunol 4:105-111.
185. Kennedy, R., A. H. Undale, W. C. Kieper, M. S. Block, L. R. Pease, and E. Celis. 2005. Direct cross-priming by th lymphocytes generates memory cytotoxic T cell responses. J Immunol 174:3967-3977.
186. Andre, F., N. E. Schartz, M. Movassagh, C. Flament, P. Pautier, P. Morice, C. Pomel, C. Lhomme, B. Escudier, T. Le Chevalier, T. Tursz, S. Amigorena, G. Raposo, E. Angevin, and L. Zitvogel. 2002. Malignant effusions and immunogenic tumour-derived exosomes. Lancet 360:295-305.
187. Hsu, D. H., P. Paz, G. Villaflor, A. Rivas, A. Mehta-Damani, E. Angevin, L. Zitvogel, and J. B. Le Pecq. 2003. Exosomes as a tumor vaccine: enhancing potency through direct loading of antigenic peptides. J Immunother 26:440-450.
188. Behrens, G. M., M. Li, G. M. Davey, J. Allison, R. A. Flavell, F. R. Carbone, and W. R. Heath. 2004. Helper requirements for generation of effector CTL to islet beta cell antigens. J Immunol 172:5420-5426.
189. Zhou, J., Y. Tagaya, R. Tolouei-Semnani, J. Schlom, and H. Sabzevari. 2005. Physiological relevance of antigen presentasome (APS), an acquired MHC/costimulatory complex, in the sustained activation of CD4+ T cells in the absence of APCs. Blood 105:3238-3246.
190. Levings, M. K., R. Sangregorio, and M. G. Roncarolo. 2001. Human cd25(+)cd4(+) t regulatory cells suppress naive and memory T cell proliferation and can be expanded in vitro without loss of function. J Exp Med 193:1295-1302.
191. Martin, B., A. Banz, B. Bienvenu, C. Cordier, N. Dautigny, C. Becourt, and B. Lucas. 2004. Suppression of CD4+ T lymphocyte effector functions by CD4+CD25+ cells in vivo. J Immunol 172:3391-3398.
192. Nanjundappa, R. H., R. Wang, Y. Xie, C. S. Umeshappa, R. Chibbar, Y. Wei, Q. Liu, and J. Xiang. GP120-specific exosome-targeted T cell-based vaccine capable of stimulating DC- and CD4(+) T-independent CTL responses. Vaccine 29:3538-3547.
193. Lu, S., J. C. Santoro, D. H. Fuller, J. R. Haynes, and H. L. Robinson. 1995. Use of DNAs expressing HIV-1 Env and noninfectious HIV-1 particles to raise antibody responses in mice. Virology 209:147-154.
194. Bernhard, E. J., A. X. Le, J. A. Barbosa, E. Lacy, and V. H. Engelhard. 1988. Cytotoxic T lymphocytes from HLA-A2 transgenic mice specific for HLA-A2 expressed on human cells. J Exp Med 168:1157-1162.
195. Kiszka, I., D. Kmieciak, J. Gzyl, T. Naito, E. Bolesta, A. Sieron, S. P. Singh, A. Srinivasan, G. Trinchieri, Y. Kaneko, and D. Kozbor. 2002. Effect of the V3 loop deletion of envelope glycoprotein on cellular responses and protection against challenge with recombinant vaccinia virus expressing gp160 of primary human immunodeficiency virus type 1 isolates. J Virol 76:4222-4232.

196. Rea, D., F. H. Schagen, R. C. Hoeben, M. Mehtali, M. J. Havenga, R. E. Toes, C. J. Melief, and R. Offringa. 1999. Adenoviruses activate human dendritic cells without polarization toward a T-helper type 1-inducing subset. J Virol 73:10245-10253.
197. Hirschowitz, E. A., J. D. Weaver, G. E. Hidalgo, and D. E. Doherty. 2000. Murine dendritic cells infected with adenovirus vectors show signs of activation. Gene Ther 7:1112-1120.
198. Miller, G., S. Lahrs, V. G. Pillarisetty, A. B. Shah, and R. P. DeMatteo. 2002. Adenovirus infection enhances dendritic cell immunostimulatory properties and induces natural killer and T-cell-mediated tumor protection. Cancer Res 62:5260-5266.
199. Morelli, A. E., A. T. Larregina, R. W. Ganster, A. F. Zahorchak, J. M. Plowey, T. Takayama, A. J. Logar, P. D. Robbins, L. D. Falo, and A. W. Thomson. 2000. Recombinant adenovirus induces maturation of dendritic cells via an NF-kappaB-dependent pathway. J Virol 74:9617-9628.
200. Philpott, N. J., M. Nociari, K. B. Elkon, and E. Falck-Pedersen. 2004. Adenovirus-induced maturation of dendritic cells through a PI3 kinase-mediated TNF-alpha induction pathway. Proc Natl Acad Sci U S A 101:6200-6205.
201. Hong, J., Y. C. Zang, H. Nie, and J. Z. Zhang. 2006. CD4+ regulatory T cell responses induced by T cell vaccination in patients with multiple sclerosis. Proc Natl Acad Sci U S A 103:5024-5029.
202. Kishimoto, C., H. Takada, Y. Hiraoka, H. Shinohara, and M. Kitazawa. 2000. Protection against murine coxsackievirus B3 myocarditis by T cell vaccination. J Mol Cell Cardiol 32:2269-2277.
203. Holst, P. J., C. Bartholdy, A. Stryhn, A. R. Thomsen, and J. P. Christensen. 2007. Rapid and sustained CD4(+) T-cell-independent immunity from adenovirus-encoded vaccine antigens. J Gen Virol 88:1708-1716.
204. Wang, B., C. C. Norbury, R. Greenwood, J. R. Bennink, J. W. Yewdell, and J. A. Frelinger. 2001. Multiple paths for activation of naive CD8+ T cells: CD4-independent help. J Immunol 167:1283-1289.
205. Autran, B., G. Carcelain, T. S. Li, C. Blanc, D. Mathez, R. Tubiana, C. Katlama, P. Debre, and J. Leibowitch. 1997. Positive effects of combined antiretroviral therapy on CD4+ T cell homeostasis and function in advanced HIV disease. Science 277:112-116.
206. Brinkman, K., J. A. Smeitink, J. A. Romijn, and P. Reiss. 1999. Mitochondrial toxicity induced by nucleoside-analogue reverse-transcriptase inhibitors is a key factor in the pathogenesis of antiretroviral-therapy-related lipodystrophy. Lancet 354:1112-1115.
207. Rosenberg, E. S., J. M. Billingsley, A. M. Caliendo, S. L. Boswell, P. E. Sax, S. A. Kalams, and B. D. Walker. 1997. Vigorous HIV-1-specific CD4+ T cell responses associated with control of viremia. Science 278:1447-1450.
208. Lyles, R. H., A. Munoz, T. E. Yamashita, H. Bazmi, R. Detels, C. R. Rinaldo, J. B. Margolick, J. P. Phair, and J. W. Mellors. 2000. Natural history of human immunodeficiency virus type 1 viremia after seroconversion and proximal to AIDS in a large cohort of homosexual men. Multicenter AIDS Cohort Study. J Infect Dis 181:872-880.

209. Goldman, J. P., M. P. Blundell, L. Lopes, C. Kinnon, J. P. Di Santo, and A. J. Thrasher. 1998. Enhanced human cell engraftment in mice deficient in RAG2 and the common cytokine receptor gamma chain. Br J Haematol 103:335-342.
210. Mazurier, F., A. Fontanellas, S. Salesse, L. Taine, S. Landriau, F. Moreau-Gaudry, J. Reiffers, B. Peault, J. P. Di Santo, and H. de Verneuil. 1999. A novel immunodeficient mouse model--RAG2 x common cytokine receptor gamma chain double mutants--requiring exogenous cytokine administration for human hematopoietic stem cell engraftment. J Interferon Cytokine Res 19:533-541.
211. Choudhary, S. K., N. L. Rezk, W. L. Ince, M. Cheema, L. Zhang, L. Su, R. Swanstrom, A. D. Kashuba, and D. M. Margolis. 2009. Suppression of human immunodeficiency virus type 1 (HIV-1) viremia with reverse transcriptase and integrase inhibitors, CD4+ T-cell recovery, and viral rebound upon interruption of therapy in a new model for HIV treatment in the humanized Rag2-/-{gamma}c-/- mouse. J Virol 83:8254-8258.
212. Koo, G. C., A. Hasan, and R. J. O'Reilly. 2009. Use of humanized severe combined immunodeficient mice for human vaccine development. Expert Rev Vaccines 8:113-120.
213. Gorantla, S., H. Sneller, L. Walters, J. G. Sharp, S. J. Pirruccello, J. T. West, C. Wood, S. Dewhurst, H. E. Gendelman, and L. Poluektova. 2007. Human immunodeficiency virus type 1 pathobiology studied in humanized BALB/c-Rag2-/-gammac-/- mice. J Virol 81:2700-2712.
214. Baenziger, S., R. Tussiwand, E. Schlaepfer, L. Mazzucchelli, M. Heikenwalder, M. O. Kurrer, S. Behnke, J. Frey, A. Oxenius, H. Joller, A. Aguzzi, M. G. Manz, and R. F. Speck. 2006. Disseminated and sustained HIV infection in CD34+ cord blood cell-transplanted Rag2-/-gamma c-/- mice. Proc Natl Acad Sci U S A 103:15951-15956.
215. Sambrook, J., Fritsch, E. and Maniatis, T. (1989). Molecular Cloning: a laboratory manual. Cold Spring Harbor, Cold Spring Harbor Laboratory Press.
216. Sambrook, J. and Russell, D. (2001). Molecular Cloning: A Laboratory Manual. Cold Spring Harbor, Cold Spring Harbor Laboratory Press.